TECHNISCHE
UNIVERSITÄT
WIEN
Vienna University of Technology

Diplomarbeit

Towards Life originating de-novo: Strategies how Compartmentalization could be induced by a synthetic Self-Replicator

Ausgeführt zum Zwecke der Erlangung des akademischen Grades der

Diplom-Ingeneurin

(Dipl.-Ing.)

im Rahmen des Studiums Technische Chemie unter der Leitung von

Univ.Prof. Dipl.-Ing. Dr. (tech) Johannes Fröhlich
Institut für Angewandte Synthesechemie
Technische Universität Wien

und

Prof. Dr. Sijbren Otto
Stratingh Institut für Systemchemie
Universität Groningen

Eingereicht an der Technischen Universität Wien
Institut für Angewandte Synthesechemie

von

Anna-Patricia Wolf, BSc.

1302118

Wien, am 23. April 2020

Unterschrift Verfasserin

"Der Mensch braucht ein Ziel!"

- Heinz Tauscher

DECLARATION ON OATH

STATUTORY DECLARATION

I declare that I have written this thesis independently, that I have not used other than the declared sources or resources, and that I have explicitly marked all material, which has been quoted either literally or by content from the used sources.

EIDESSTATTLICHE ERKLÄRUNG

Ich erkläre an Eides statt, dass ich die vorliegende Arbeit selbstständig verfasst, andere als die angegebenen Quellen oder Hilfsmittel nicht benutzt und die den benutzten Quellen wörtlich und inhaltlich entnommenen Stellen als solche kenntlich gemacht habe.

ABSTRACT

Mankind has always speculated about the origin of life and sought to understand its own existence. Searching for our origin is a natural thrive of human beings. This leads us to one of the biggest questions in science: how can life emerge from simple molecules and, even more interestingly, how can we achieve this process in the lab starting from inanimate matter?

The research group of *Prof. Sijbren Otto* at the Stratingh Institute for Systems Chemistry at the University of Groningen is driven by unmasking the mystery of the origin of life. This research group aims to build up life-like systems by the bottom up approach using the tools of dynamic combinatoral chemistry based on reversible disulfide chemistry, being already successful in creating self-replicating molecules. According to a common definition, life is defined by the combination of the three fundamental functions reproduction, metabolism and compartmentalization. The *Otto* group was able to combine self-replication and a primitive metabolism by extending the replicator's catalytic capability from autocatalysis to the Fmoc deprotection of Fmoc-glycine.

This thesis initially aims to address the combination of all three fundamental functions of life in a conceptional way. Specific focus of the present project was to catalyze reactions that will lead to the formation of compartments and hence the combination of self-replication, a primitive metabolism and compartmentalization in a conceptual way. This objective was approached by making use of the known as well as expansion of catalytic activities of the replicator.

Via the capped surfactant approach, protected head groups of surfactants were successfully deprotected by the self-replicator, which led to the exploration of the replicator's substrate scope to primary amines until dodecylamine. The new protecting group dSmoc, a double sulfonated analogon of the Fmoc-group, was successfully synthesized, which should increase the water solubility of protected amines finally aiming a further exploration of the substrate scope.

The catalytic capabilities of the self-replicator were investigated towards carbon-carbon bond formations, including the Aldol and Knoevenagel reaction, which could potentially be used for the synthesis of surfactants. This work shows that the self-replicator might be able to catalyze the Knoevenagel condensation in water.

The introduction of a cascade reaction system including the deprotection of a Smoc-protected organocatalyst by the self-replicator led to new knowledge about reactivities and interactions in such complex mixtures, which expanded the pool of ideas and possibilities for the self-replicator induced compartmentalization.

After all, the present project sets a basic fundament for the combination of all three fundamental functions of life in a conceptional way by the exploration of the knowledge about the deprotection kinetics and catalytic capabilities of the self-replicator.

KURZFASSUNG

Seit jeher philosophiert die Menschheit über den Ursprung des Lebens und versucht ihre eigene Existenz zu verstehen. Die Suche nach unserem Ursprung ist ein natürlicher Trieb des Menschen. Dies führt uns zu einer der größten Fragen der Wissenschaft: Wie kann Leben aus einfachen Molekülen entstehen? Wobei sich die noch interessanterere Frage stellt: Wie können wir diesen Prozess im Labor ausgehend von unbelebter Materie erreichen?

Die Forschungsgruppe von Prof. Sijbren Otto am Stratingh Institut für Systemchemie an der Universität Groningen wird durch das Mysterium über den Ursprung des Lebens getrieben. Diese Forschungsgruppe hat sich zum Ziel gesetzt, lebensähnliche Systeme durch einen Bottom-up-Ansatz mit den Werkzeugen der dynamischen kombinatorischen Chemie auf der Grundlage der Chemie der reversiblen Disulfide aufzubauen. Dadurch gelang es bereits dieser Arbeitsgruppe selbstreplizierende Moleküle zu schaffen. Einer gängigen Definition zufolge wird Leben über die Kombination der drei grundlegenden Funktionen Reproduktion, Metabolismus und die Formierung von Kompartimenten definiert. Die Otto-Gruppe konnte bereits die beiden Funktionen Selbstreplikation und einen primitiven Metabolismus kombinieren, indem sie die katalytische Fähigkeit des Replikators von der Autokatalyse auf die Fmoc-Entschützung von Fmoc-Glycin ausdehnte.

Ziel dieser Arbeit war zunächst die Kombination aller drei Grundfunktionen auf konzeptionelle Weise. In diesem Projekt wurden die katalytischen Fähigkeiten eines Replikators über die Autokatalyse hinaus erweitert. Insbesondere wurde die Fähigkeit eines peptidbasierten Selbstreplikators, welcher zuvor in der Forschungsgruppe von Sijbren Otto entwickelt wurde, erweitert, um verschiedene Reaktionen zu katalysieren. Ein besonderer Schwerpunkt des vorliegenden Projekts lag auf der Katalyse von Reaktionen, welche schlussendlich zur Bildung von Kompartimenten führen und damit zur Kombination der drei Grundfunktionen auf eine konzeptuelle Weise. Dieses Ziel wurde durch die Nutzung der bekannten sowie der Erweiterung der katalytischen Fähigkeiten des Replikators erreicht.

Über den Ansatz der gekappten Tenside wurden geschützte Kopfgruppen von Amphiphilen erfolgreich durch den Selbstreplikator entschützt. Dadurch wurde der Substratumfang des Replikators auf primäre Amine bis hin zu Dodecylamin erweitert. Die neue Schutzgruppe dSmoc, das doppelt sulfonierte Analogon der Fmoc-Gruppe, wurde erfolgreich synthetisiert, was die Wasserlöslichkeit von geschützten Aminen erhöhen soll und schließlich zu einer erneuten Erweiterung des Substratumfangs führen könnte.

Die katalytischen Kapazitäten des Selbstreplikators wurden hinsichtlich Kohlenstoff-Kohlenstoff Bindungsformationen untersucht, mit besonderem Hinblick auf die Aldol- und Knoevenagel-Reaktion, welche schlussendlich für die Synthese von Tensiden durch den Replikator verwendet werden können. Diese Arbeit zeigt, dass der Selbstreplikator in der Lage sein könnte, die Knoevenagel-Kondensation in Wasser zu katalysieren.

Die Implementierung eines Kaskadenreaktionssystems, welches die Entschützung eines Organokatalysators durch den Selbstreplikaor beinhält, führte zu neuen Erkenntnissen über Reaktivitäten und Wechselwirkungen in solch komplexen Mischungen,

welche Möglichkeiten zur Selbstreplikator induzierten Formierung von Kompartimenten maßgeblich erweitern.

Das vorliegende Projekt liefert einen wichtigen Grundstein für die Kombination aller drei fundamentalen Funktionen des Lebens in konzeptionelle Weise durch die Erweiterung des Wissens über die Reaktionskinetik und die katalytischen Fähigkeiten des Selbstreplikators.

ACRONYMS

a.u. Absorption unit

ACN Acetonitrile

BRIJ30 Polyoxythylene(4) lauryl ether

CAC Critical aggregation concentration

$CDCl_3$ Deuterated chloroform

CMC Critical micelle concentration

CTAB Cetyltrimethylammoniumbromid

DBF Dibenzofulvene

DCM Dichloromethane

ddH_2O Doubly distilled water

D_2O Deuterated water

DNA Desoxyribonucleicacid

G Glycine

L Leucine

K Lysine

F Phenylalanine

HCl Hydrochloric acid

HEPES 2-(4-(2-Hydroxyethyl)-1-piperazinyl)-ethanesulfuric acid

Fmoc Fluorenylmethoxycarbonyl

Fmoc-Cl 9-Fluorenylmethyloxycarbonylchloride

FmocGly Fmoc-Glycine

EA Ethylacetate

EtOH Ethanol

EWG Electron-withdrawing group

KCl Potassium chloride

MeOH Methanol

Mg_2SO_4 Magnesium sulfate

NaCl Sodium chloride

Na_2CO_3 Sodium carbonate

PAA Polyacrylic acid

PBS Phosphor buffered saline

RP Reversed phase

SDBS Sodiumdodecylbenzenesulfate

SDBF Sulfo-dibenzofulvene

dSmoc-Cl 9-(x,x-disulfo)fluorenylmethyloxycarbonylchloride

dSmocGly dSmoc-glycine

Smoc 9-(2-Sulfo)fluorenylmethoxycarbonyl

Smoc-Cl 9-(2-Sulfo)fluorenylmethyloxycarbonylchloride

SmocGly Smoc-glycine

SmocProl Smoc-L-proline

SmocPyr Smoc-pyrrolidine

TEM Transmission electron microscopy

TLC Thin layer chromatography

UPLC Ultrahigh pressure liquid chromatography

UPLC-MS Ultrahigh pressure liquid chromatography coupled to mass spectrometry

UV Ultra violet

CONTENTS

1 INTRODUCTION

Mankind's probably most mysterious questions discussed in community, science, philosophy, ethics, religion and even politics are: what is life? When does life start? And how did life emerge? This thrive for our roots defines today's prebiotic research starting from life as we know it today tracing it back to early microorganisms finally ending up with the molecules from which life could have emerged. This includes the long-standing philosophical as well as scientific problem about the definition of life. We will not be able to overcome the problem about the definition of life until there is a general theory about the nature of living systems. However, the synthesis of living systems in the laboratory will help us to earn a better understanding about the nature of life.

1.1 THE FUNDAMENTAL FUNCTIONS OF LIFE

Nowadays living organisms as we know them are built up from molecules which are per se not alive, hence these living organisms must possess properties that distinguish them from non-living systems. No matter what kind of collisions may occur between definitions about what is life, all living systems collectively possess three main functions.[1–3] One of these functions is reproduction, meaning the ability to transfer information through the process of self-replication.[4] Furthermore, living systems must posses the ability to sustain themselves by staying out of the thermodynamical equilibrium through metabolism, meaning a series of reactions that are characterized by energy consumption and the renewal of metabolites.[4] These reactions need to take place in a locally restricted area thus boundaries between environment and the system are needed, referred as compartmentalization.[4] The three fundamental functions reproduction, metabolism and compartmentalization are present in all living systems that we know and hence these properties are a good starting point for unmasking the roots of how life has emerged.

The top-down approach, which is often referred as the biologists approach, is using biological molecules like desoxyribonucleicacid (DNA), proteins and lipids for the creation of protocells.[5] However, the bottom-up approach is based on chemical and physical interactions between non-living molecules as building blocks for the creation of life-like systems without the use of biological molecules.[5] The bottom-up approach, which is often referred as the chemists approach, will be treated in this work for achieving a better understanding of how life could have emerged from simple molecules.

1.1.1 *Self-Replication*

Meanwhile, information in living systems is transferred through copies of information-rich molecules such as DNA, using a complex protein machinery referred as the term self-replication, meaning the transfer of information.[2,6–8] Research in these areas has mainly focused on biomolecules that are crucial to current life or on the bottom-up approach of constructing chemical systems which mimic the essential characteristics of life.[2,6,9] However, it is assumed that in the prebiotic world these processes must have occurred through much simpler systems.[2,8]

Living systems function by a complex interplay of covalent bond formation and non-covalent assembly processes. The introduction of dynamic covalent chemistry made the development of regimes that feature concurrent covalent and non-covalent interactions.[10] Systems, which are made from different building blocks capable of undergoing reversible covalent bonds, show a tendency to result in diverse mixtures of products, which continuously undergo an exchange of building blocks via reversible covalent bond formation.[10] Non-covalent interactions, which lead to certain assemblies and hence are energetically more favored, shift the equilibrium towards a specific product. This is a very important behavior for the question about the origin of life. Such building block libraries result in spontaneous and in some cases even in autocatalytic emergence of specific molecules that had gained information and are able to pass this information on the next generation during self-replication.[5,11]

Over the last decades, pioneering works about synthetic replicators by the groups of Chiemlewsky,[12] Ghadiri,[13] Ashkenasy[14] and Otto[15–18] use the fields of systems chemistry and dynamic combinatoral chemistry focusing largely on autocatalysis whereby a molecule is able to catalyze its own formation from a set of precursors.[9,19]

Synthetic peptide-based Self-Replicators

The research group of Sijbren Otto at the University of Groningen is largely focused on the development of molecules that are capable of promoting their own formation with simultaneous assembly into supramolecular structures by using the tools of dynamic combinatoral chemistry.[19] By mixing building blocks, which can react with each other through the formation of reversible covalent bonds, a dynamic combinatoral library is created leading to a mixture of products which are all in equilibrium. If a formed product is able to stabilize its own species through non-covalent interactions the equilibrium is shifted towards the formation of this particular product at the expense of all other products in this library.

A specific building block that has been intensively investigated in the Otto group is shown in Figure 1. This synthetic building block consists out of an aromatic core bearing two thiol groups in meta position as well as a peptide chain out of the five α-amino acids glycine (G), leucine (L), lysine (K), phenylalanine (F) and again lysine (K). Such peptide structures that feature alternating polarity are known for a high tendency to assemble into β-sheets.[21] Through oxidation of the thiol groups on the aromatic core reversible covalent disulfide bonds are formed between the precursor molecules. These molecules can undergo exchange reactions leading to a mixture of different sizes of macrocycles that are in equilibrium with each other. It has been shown that the hexamer species shows the most favored non-covalent interactions resulting in the assembly of hexamers into fibers. This supramolecular structure shifts the equilibrium towards the hexamer at the expense to the other macrocycles. It has been shown that the assembled stacks grow from the fibre ends via a nucleation/growth mechanism. When the library is stirred, mechanical forces cause breakage of the fibers, which results in an exponential growth via elongation/breakage mechanism, in the end achieving self-replication hence the information transfer of the ring size is managed through a template effect to the next generation.[17,19]

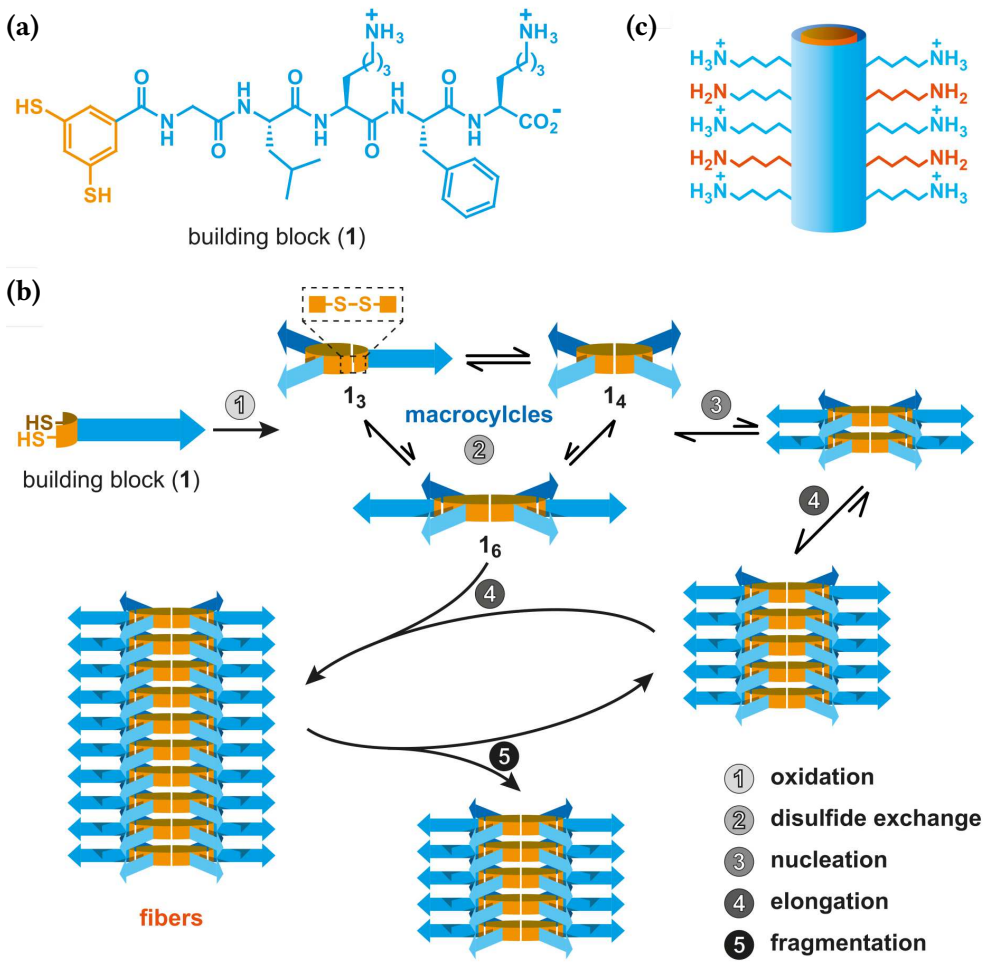

Figure 1: Formation of disulfide linkages result in different sizes of macrocycles through oxidation between two aromatic thiol groups of a building block which bears a peptide chain with five amino acids in alternating polarity which favor non-covalent interactions between each other in a way that leads to β-sheet formation resulting in stacks of nano fibres. These non-covalent interactions seem to be most favored for hexamers and hence the equilibrium of different sizes of macrocycles is driven towards hexamers. Growth of the stacks happens at the fibre ends. External mechanical sheer forces break the stacks which leads to an exponential growth via an elongation/breakage mechanism resulting in self-replication.[20]

1.1.2 *Metabolism*

Self-replication is a necessary but not a sufficient functionality in order for life to emerge. One of the central features of living systems is that they operate out of equilibrium meaning a continuous supply of energy. Equilibrium means death since living systems need thermodynamic openness for a constant flow of energy to power reaction networks.[22]

Early Stages of combining Self-Replication and a primitive Metabolism

Recently the Otto group has demonstrated that the assembly into fibres as driving force for self-replication introduces catalytic abilities as a new function which is another important purpose for life. Emergence experiments showed an autocat-

alytic reproduction of catalytic capabilities.[24] It was shown that the stacked fibre conformation is able to catalyze the retro aldol reaction of methodol to 6-methoxy-2-naphthaldehyde and acetone. This reaction includes the imine formation between the carbonyl group of methodol and the deprotonated lysine residues of the fibres, which is shown in Figure 2 (b). Another reaction, which can be catalyzed by the self-replicator, is the deprotection of Fluorenylmethoxycarbonyl (Fmoc) protected glycine. This reaction can be catalyzed by the replicator due to the placement of its lysine residues into a microenvironment that activates ϵ-amines for catalysis upon the formation of a fibre shown in Figure 2 (a). The coulomb interaction in this close proximity changes the pK_a of some ϵ-amines contained in the lysine side chain, thus increasing their nucleophilicity.[24] This phenomenon can be compared to the non-covalent assembly of protein complexes which affects the protein's ability to catalyze chemical reactions.

Protecting groups are used in chemical synthesis as a tool for preventing a functional group from unwanted reactions. If a molecule contains such a vulnerable functional group, as a given example an amine group, it can be coupled to the so called Fmoc protecting group in order to prevent the amine functionality to undergo a reaction. The Fmoc group can be removed under basic conditions due to the acidity of the proton in position 9. The removal of this specific proton is usually carried out with amine bases like piperidine or pyrrolidine. Due to the perturbed pK_a in the lysine side chains also the replicator is capable to deprotonate the proton in position 9 which is followed by a β-elimination leading to the release of the free amine as well as carbon dioxide acting as the driving force and DBF.[23]

Another essential feature is a phenomenon referred as feedback which is a control element that controls auto-inhibition denoted as negative feedback and

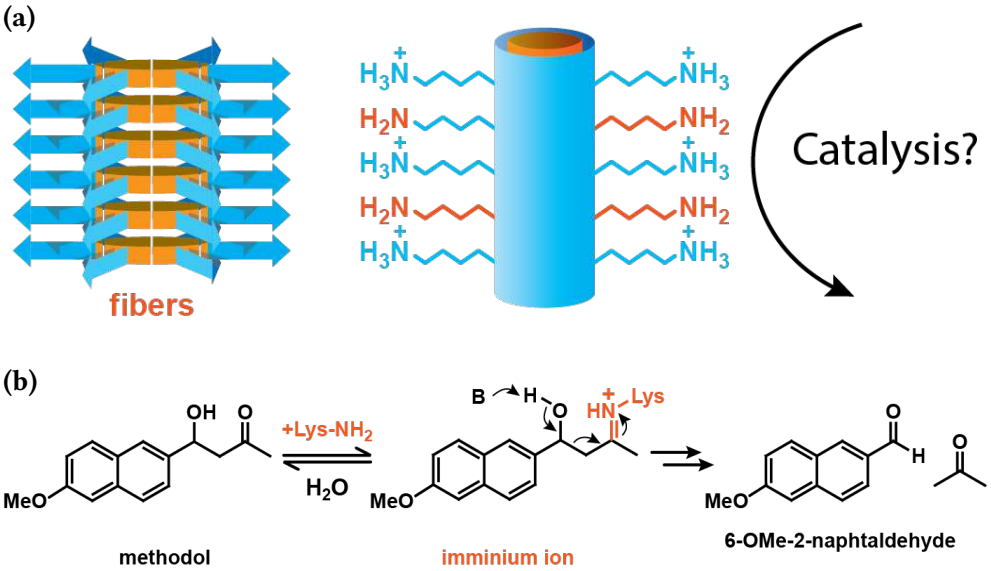

Figure 2: The assembly into fibres **(a)** places the amino groups from the lysine side chains into microenvironments that activates ϵ-amines for catalysis upon the formation of a fibre through lowering the amine's pK_a of about 3 units. The amino groups in the stacked conformation are due to their perturbed pK_a now capable of catalyzing reactions. Scheme **(b)** shows the retro aldol reaction of methodol to 6-methoxy-2-naphthaldehyde and acetone which happens via an intermediate iminium formation between the carbonyl group of methodol and the ϵ-amine of the replicator.

auto-amplification called positive feedback. The latter provides the basis for self-replication.[22]

Recently, the Otto group has shown emerging catalytic properties that create a positive feedback loop which is reminiscent to a primordial anabolism.[24] It was shown that the side product DBF resulting from the Fmoc deprotection speeds up thiol oxidation hence it creates a positive feedback on the replication mechanism. It is suspected that super-oxide radicals, working as reactive oxygen species, play a central role during the oxidation of the building block thiols, resulting in a one electron oxidation of thiolates to thiyl radicals. Furthermore, through oxidative addition of the reactive oxygen species to the released side product DBF, the super-oxide radicals

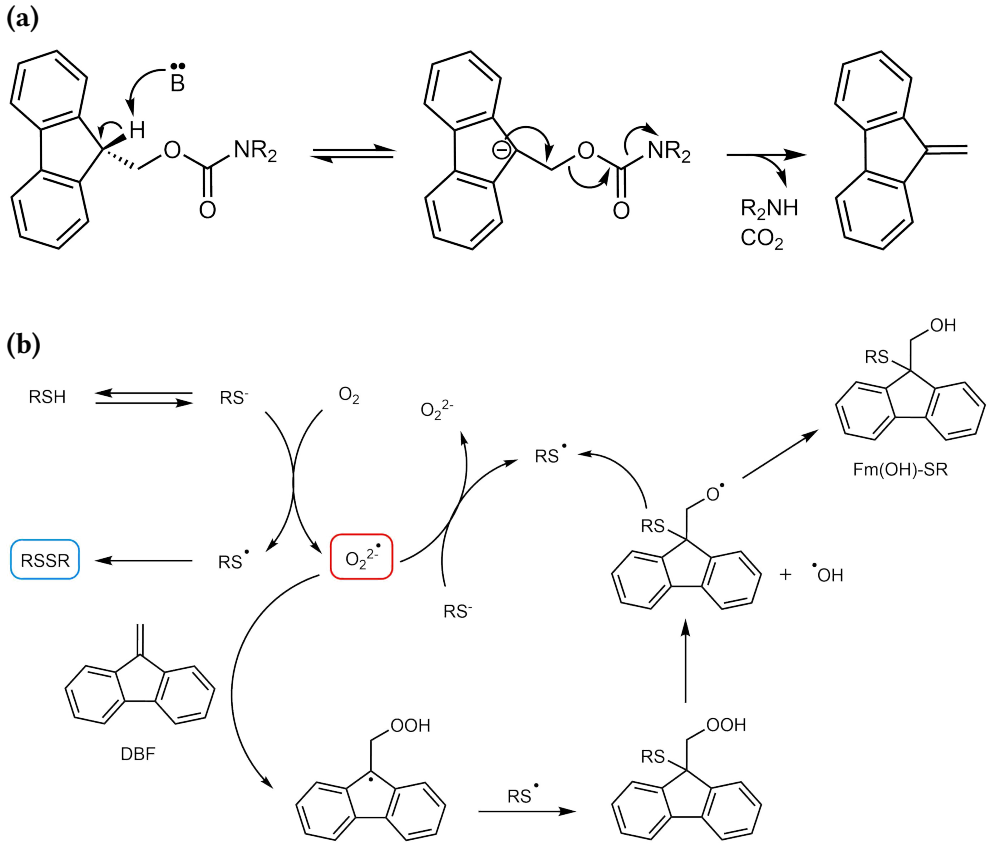

Figure 3: Mechanism of **(a)** the Fmoc deprotection. The proton that has to be removed in position 9 shows a pK_a of about 25[23] since its conjugate base is an aromatic cyclopentadienyl anion also stabilized by the two phenyl rings leading to a stable 14 electron aromatic system. Via an E_1cB mechanism the elimination is usually carried out by a secondary amine like piperidine as the base with following loss of CO_2 as the driving force finally resulting in the elimination of the free amine as well as dibenzofulvene (DBF)[23] which **(b)** speeds up thiol oxidation through oxidative addition of the reactive oxygen species to the C=C double bond stabilizing super-oxide radicals. The following decomposition generates even more radicals which oxidize the thiolates of the building block creating a radical avalanche resulting in a positive feedback on the replication mechanism.[24] Due to solubility issues of the apolar Fmoc group the water soluble sulfonated analogon **(c)** 9-(2-Sulfo)fluorenylmethoxycarbonyl (Smoc), first established by *Merrifield et al.*[25], was successfully tested in the Otto group to be deprotected by the self-replicator.

are stabilized and the following decomposition generates even more radicals, which oxidize the thiolates of the building block creating a radical avalanche.[24]

Recent Catalysis Expansions of a peptide-based Self-Replicator

The substrate scope has also been explored to the sulfonated analogon of the Fmoc group, the water soluble Smoc protecting group first established by *Merrifield et al.* in the 1970s.[25] The deprotection rate of Smoc-glycine (SmocGly) is even faster compared to the Fmoc analogon. This could be due to higher coulomb attraction between the negatively charged sulfonate group on the substrate and the positively charged lysine residues of the replicator, probably causing a tighter and more favored arrangement between substrate and replicator leading to a faster deprotection. Furthermore, the released side product sulfo-dibenzofulvene (SDBF) seems to have a higher impact on the positive feedback loop resulting in a faster thiol oxidation compared to DBF.[26]

With the Fmoc- and Smoc-deprotection of glycine a first step towards creating metabolic-type pathways was accomplished. This achievement combines two necessary functions for life which is self-replication and a primitive metabolism.

1.1.3 *Compartmentalization*

Another necessary requirement for a living system is the local restriction of self-replication and metabolism to a confined environment meaning defined boundary between "inside" and "outside" by compartments.[27] Without local restriction a cell would not be able for the transfer of mass and information and would rather be a mixed-reactor with having potential interactions and reactions between all components.[22]

Surfactants, also denoted as amphiphiles, consist out of a hydrophilic moiety referred as head group as well as a hydrophobic moiety, which is often denoted

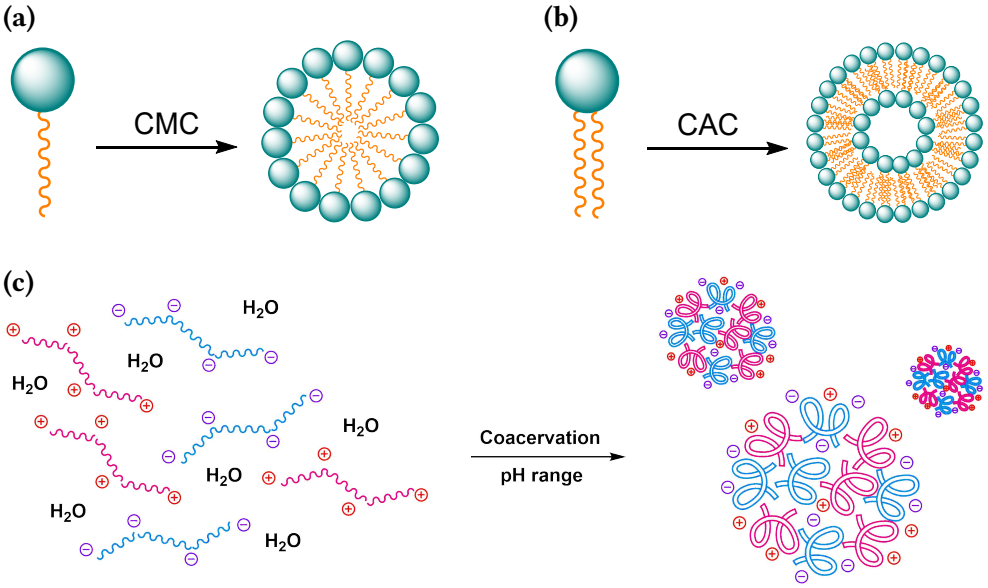

Figure 4: Different forms of compartmentalization **(a)** mizellation through the supramolecular assembly of single tail amiphiphiles when above the critical micelle concentration (CMC) **(b)** formation of vesicles from double tailed surfactants when above the critical aggregation concentration (CAC) and **(c)** coacervation through equilibration of opposite charges carried by polymers in a certain pH range.

as tail and usually corresponds to an alkyl chain. In aqueous systems amphiphiles start to assemble into compartments above a certain concentration with having the hydrophobic tails on the inside and the polar headgroup on the outside. With the formation of compartments, hydrophobic attraction between the hydrocarbon chains in aqueous media and repulsive forces caused by steric and electrostatic interactions between the neighboring hydrophilic head groups become relevant. The driving force for these supramolecular assemblies is the tendency of the hydrophobic part of the surfactant to minimize its contact with water, which is denoted as the hydrophobic effect. This is achieved by bunching together the apolar alkyl chains forming the core of the compartment. The hydrophilic head groups remain on the surface of the compartment, which further reduces the contact between the hydrophobic chains and water.[28]

In most cases single tailed amphiphiles self-assemble in aqueous systems into micelles, when above the so called CMC. In micelles the hydrophobic chains come in close contact and form an oily core which is surrounded by polar head groups. Due to the hydrophobic core, micelles are important to solubilize water-insoluble compounds.[29]

Amphiphiles that bear two hydrophobic tails and a hydrophilic head group are mostly able to self-assemble into hollow closed bilayers denoted as vesicles. They have drawn much attention due to the structural similarities to biological cell membranes but also because of their capacity to entrap active compounds in their insides.[29,30] When above the CAC, which is usually lower than the CMC, vesicles are often spherical but can also have other shapes in a uni- or multilamellar arrangement. An important difference between vesicles and micelles is, that the former is able to enclose some of the aqueous phase due to the hollow hydrophilic inner structure, which can be used to entrap active compounds.[29]

Another form of compartmentalization is coacervation which is shown in Figure 4 (c).[31] *"IUPAC defines coacervation as the separation into two liquid phases in colloidal systems (the phase more concentrated in colloid component is the coacervate, and the other phase is the equilibrium solution). The phenomenon can be divided into "simple" and "complex" coacervation"*[31] *p.*1313 Systems which contain only one colloidal solute are denoted as simple coacervation, while the complex phenomenum usually involves more than one colloid. The latter process has been found to be pH dependent and has been discovered in systems containing two dispersed colloids showing opposite electrical charge. The optimum condition for complex coacervation is achieved at a certain pH where equivalent amounts of oppositely charges of the two colloids are present, since the greatest number of salt bonds is formed at this point. These compartments can be used for micro encapsulation and thus also for entrapping active molecules like the self-replicator.

Recent Developments of Self-Replication in Compartments

Recent developments in the Otto group showed the entrapment of a synthetic self-replicator in coacervates.[32] Further works dealed with the entrapment of the self-replicator bearing the peptide chain -GLKFK in vesicles formed by phospholipides in order to investigate the behavior of the replicator in presence of liposomes.[33] However, none of these compartmentalizations were directly induced by the self-replicator, which will be treated in this thesis by applying three different main strategies.

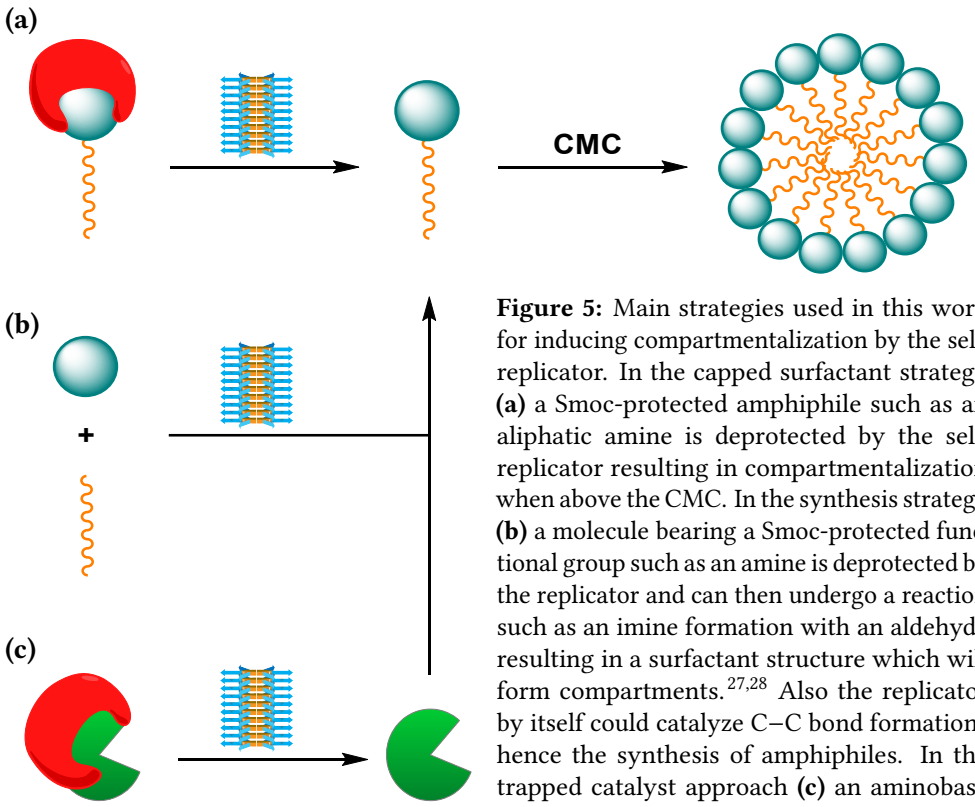

Figure 5: Main strategies used in this work for inducing compartmentalization by the self-replicator. In the capped surfactant strategy **(a)** a Smoc-protected amphiphile such as an aliphatic amine is deprotected by the self-replicator resulting in compartmentalization when above the CMC. In the synthesis strategy **(b)** a molecule bearing a Smoc-protected functional group such as an amine is deprotected by the replicator and can then undergo a reaction such as an imine formation with an aldehyde resulting in a surfactant structure which will form compartments.[27,28] Also the replicator by itself could catalyze C–C bond formations hence the synthesis of amphiphiles. In the trapped catalyst approach **(c)** an aminobase such as pyrrolidine, which is able to catalyze C–C bond formations, is protected with the Smoc-group. When it is deprotected by the self-replicator the amino base is released and can catalyze the synthesis of a surfactant. The mentioned strategies can be expanded to double tailed surfactants resulting in vesicle formation.

1.2 MAIN RESEARCH STRATEGIES ELABORATED IN THIS THESIS

Connecting the three fundamental functions of life self-replication, a primitive metabolsim and compartmentalization in a conceptual way is a crucial step for a better understanding about how life could have emerged. In order to achieve this, three different main strategies were applied in this work: the deprotection of amiphiphiles, deprotection of "active" molecules which then undergo a reaction leading to surfactants, and the synthesis of surfactants through a cascade reaction by an organocatalyst which needs to be deprotected by the self-replicator at first.

1.2.1 *Deprotection of Surfactants*

The deprotection of compartment forming molecules by the synthetic self-replicator should lead on the one hand to compartmentalization and hence to the combination of self-replication, a primitive metabolism and formation of compartments in a conceptual way as well as on the other hand to knew knowledge about substrate dependence.

As described in Figure 5 (a), a Smoc potected surfactant such as a primary amine, is deprotected by the self-replicator and when the concentration of the released amphiphile becomes higher than the CMC, compartmentalization is induced. However, during the work for this thesis, solubility issues with the non-polar Fmoc protecting group occurred, which led to a switch to the Smoc group, the water soluble analogon of Fmoc. Although Smoc protected amines already show a surfactant structure, it

is assumed that due to the heavy negatively charged sulfonate group, the CMC is higher compared to the free aliphatic amine and hence compartmentalization still can be induced through deprotection.

1.2.2 *Synthesis of Surfactants induced by the Self-Replicator*

It was reported by *Šegota*[28] and *Seoane*[27] that the formation of vesicles was achieved by imine formation between a phospholipid bearing an amine group and an aliphatic aldehyde. As described in Figure 5 (b), the deprotection of a molecule featuring an amine moiety which can undergo imine formation with an aliphatic aldehyde after its release should lead to the formation of amphiphiles followed compartmentalization when above the CAC.

Furthermore, it could be that the self-replicator is not just able to catalyze the Fmoc/Smoc deprotection or methodol retro aldol reaction, but also other aminobase catalyzed reactions like the Knoevenagel condensation between a CH-active methylene compound and an aldehyde. By choosing the substrates and reaction media wisely it could be that even the self-replicator is able to be the catalyst and synthesize amphiphiles by itself leading to compartmentalization.

1.2.3 *Synthesis of surfactants through a reaction cascade*

Various aldol reactions and Knoevenagel condensations catalyzed by aminobases in water are reported in literature, among others by *Jiang*[34] and *Gomes*[35]. In nature, biochemical reaction cascades involving a series of chemical reactions such as signaling cascades causing cell responses, are very common and essential for keeping the biochemical machinery alive.[36] A reaction cascade involving the deprotection of a Smoc protected organocatalyst, which can then catalyze a reaction leading to a surfactant, finally forming compartments, is used as one of the strategies in this work and is described in Figure 5 (c).

1.3 AIM AND OUTLINE

The aim of this thesis is to connect the three fundamental functions of life self-replication as transfer of information, a primitive metabolism for a constant supply of energy and compartmentalization for a local restriction and prevention from unwanted side reactions.

During the course of this master project the long-term goals for each of the treated projects remained constant. However, as research uncovered new data and contradicted expectations, the strategies and milestones for achieving these goals changed often. The pursuit of the main research lines also opened new ones, which were only marginally treated (if at all) due to limited time available during the course of this master project.

Despite understanding that the main focus should be on finished projects, the author believes that this master thesis would not be complete without describing those initial ideas and possible chances of the treated research lines. For this reason, some chapters include an "Outlook"-section.

The reminder of this thesis is organized as follows: Chapter 2 is giving an introduction to the behavior of the self-replicator in presence of compartment forming molecules and the exploration of its substrate scope, Chapter 3 deals with the intro-

duction of a reaction cascade induced by the replicator followed by the synthesis of amphiphiles by a released organocatalyst which should lead to the formation of compartments and Chapter 4 is dealing with the synthesis of surfactants induced by the replicator. The whole analysis data can be found in the appendix.

2 TOWARDS COMPARTMENTALIZATION IN PRESENCE OF A SYNTHETIC SELF-REPLICATOR

Previous works in the Otto group have shown that the synthetic self-replicator featuring the peptide chain -GLKFK is capable of deprotecting Fmoc- and Smoc-glycine. In order to use this reaction to catalyze the formation of compartments, we first need to address if the replicator remains stable and catalytically active in presence of relevant compartment-forming molecules. Furthermore, the substrate scope should be expanded to protected surfactants in order to achieve compartmentalization by the capped surfactant approach.

2.1 STABILITY AND CATALYTIC ACTIVITY OF A PEPTIDE-BASED SELF-REPLICATOR IN PRESENCE OF DIFFERENT TYPES OF SURFACTANTS

To answer the question about the replicator's stability and catalytic activity in presence of surfactants, transmission electron microscopy (TEM) was used to visualize the fibres and ultra violett (UV) measurements to confirm that the fibres are still catalytically active in presence of compartment-forming molecules.

2.1.1 *Proof of Stability by TEM Measurements*

In order to investigate if surfactants destroy the fibres or inhibit the emergence of hexamer, non-ionic (polyoxythylene(4) lauryl ether (BRIJ30)), cationic (cetyltrimethylammoniumbromid (CTAB)) and anionic (sodiumdodecylbenzenesulfate (SDBS)) surfactants were each mixed with hexamer and monomer in borate buffer (50 mM, pH 8.2) and stirred with 1200 rpm at ambient temperature for 10 days. Negative stain TEM was then performed for all six samples (Figure 6, (a) - (f)). Additionally, oleic acid was mixed with monomer in borate buffer (50 mM, pH 8.2) and stirred with 1200 rpm at ambient temperature for 2 days. With this sample cryo-TEM was performed (Figure 6, (g)). In all experiments, the concentration of the surfactant was chosen to be above the critical micelle concentration (CMC).[37–40]

Since the TEM images (a) - (c) in Figure 6 show that the fibres are still present when mixed with the different surfactant types, it can be assumed that the tested surfactants do not significantly destroy the fibres. Furthermore due to the presence of fibres in (d) and (e) it can be assumed that the emergence of hexamer and its assembly to fibres is not significantly hindered by the non-ionic BRIJ30 or cationic CTAB. Since it seems that no fibres are present in (f) it could be that the anionic surfactant SDBS inhibits the emergence of hexamer and its assembly to fibres due to an electrostatic attraction between the positive charge of the lysine residues present in the monomer and the negatively charged head group of SDBS. The structures in (f) appear to be dried membranous structures of SDBS. However, it could also be that the fibres are aggregated to the surfactant or covered up by the dried membraneous structures due to an electrostatic attraction. In order to confirm the latter, cryo TEM needs to be performed (not in this thesis). Interestingly, the cryo TEM picture of monomer mixed with oleic acid in (g) shows fibre-like structures with a diameter of about 25 nm whereas hexamer fibres show dimension of about 3 nm.[8] It could be

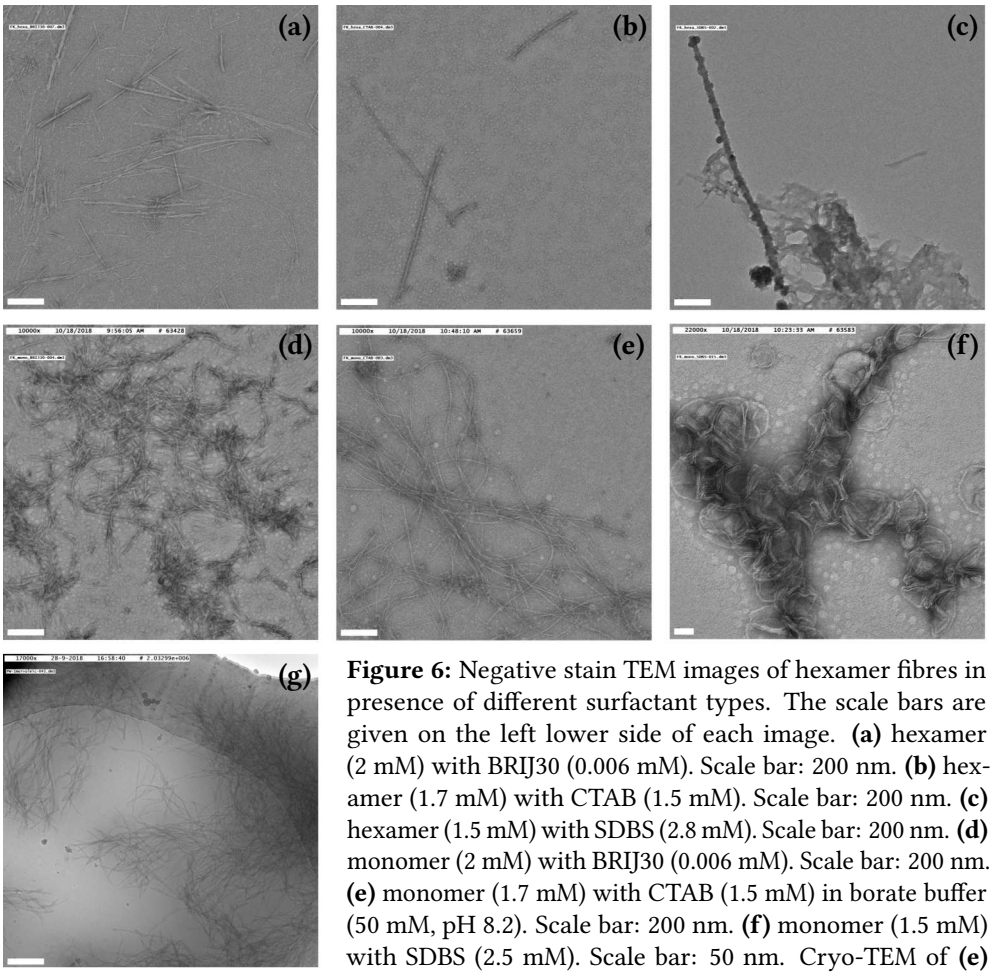

Figure 6: Negative stain TEM images of hexamer fibres in presence of different surfactant types. The scale bars are given on the left lower side of each image. **(a)** hexamer (2 mM) with BRIJ30 (0.006 mM). Scale bar: 200 nm. **(b)** hexamer (1.7 mM) with CTAB (1.5 mM). Scale bar: 200 nm. **(c)** hexamer (1.5 mM) with SDBS (2.8 mM). Scale bar: 200 nm. **(d)** monomer (2 mM) with BRIJ30 (0.006 mM). Scale bar: 200 nm. **(e)** monomer (1.7 mM) with CTAB (1.5 mM) in borate buffer (50 mM, pH 8.2). Scale bar: 200 nm. **(f)** monomer (1.5 mM) with SDBS (2.5 mM). Scale bar: 50 nm. Cryo-TEM of **(e)** monomer (0.5 mM) with oleic acid (3 mM) in borate buffer (50 mM, pH 8.2). Scale bar: 200 nm.

that the structures in (g) are intertwined hexamer fibres but this was not confirmed in this work.

2.1.2 *Proof of Catalytic Activity by UV Measurements*

As shown in the section before, in presence of different surfactant types the fibres seem to be stable. However, TEM images do not give any indication of their catalytic activity. In order to probe catalytic activity the deprotection of the standard substrate Smoc-glycine (SmocGly) by the replicator in presence of different surfactant types was monitored by UV measurements where the absorption of the released side product sulfo-dibenzofulvene (SDBF) from the deprotection is measured at its absorption maximum of 308 nm. The catalytic rates are given in Abs/min since the absorption coefficient of SDBF is difficult to measure due to various side reactions that SDBF can undergo in water. These side reactions include polymerization, water addition to the double bond and recent results from the *Otto* group show that the self-replicator forms addition products with SDBF as well. These side reactions could cause a shift of the absorption maximum which makes the measurement of its absorption coefficient difficult. Nevertheless, in this measurement set up the evolution of absorbance over time gives an indication of the rate of deprotection.

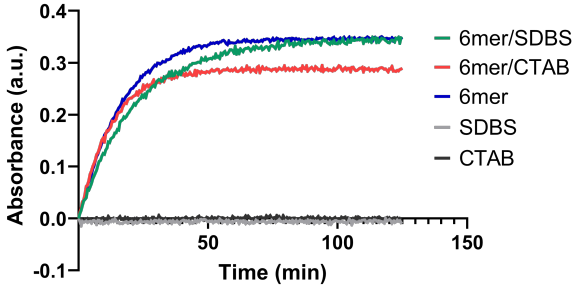

	Catalytic rate $*10^{-5}$ [Abs/min]
6mer/SDBS	1410 ± 4
6mer/CTAB	1880 ± 3
6mer	1760 ± 2
SDBS	-19 ± 5
CTAB	-80 ± 2

Figure 7: Results of SmocGly deprotection by the self-replicator in presence of different surfactant types. The UV measurements were performed without stirring in 50 mM borate buffer pH 8.2 at 25°C using 308 nm as the detection wavelength for SDBF. The concentration for the substrate SmocGly was 50 µM, the replicator 20 µM, SDBS 20 µM and CTAB 20 µM. The catalytic rates are given in $*10^{-5}$ Abs/min in the table to the right beside the UV graph.

Figure 7 shows that the fibres are still capable of deprotecting SmocGly in presence of surfactants. The blank measurements were performed with just the substrate and surfactant without replicator in order to exclude a possible background reaction. The results for the catalytic rates are given in Table 1. Since the slopes of both blanks are negative, which does not make sense in this measurement set up, the background reaction is treated as 0 Abs/min. The control measurement included just the replicator and standard substrate SmocGly without adding any surfactants. It shows a catalytic rate of $1760*10^{-5}$ Abs/min.

The deprotection rate in presence of the positively charged surfactant CTAB is slightly higher than the control measurement which could result from possible pipetting mistakes. The positively charged surfactant does not hinder the replicator to be catalytic active. However, it is interesting that in presence of the cationic surfactant not the same plateau in absorption unit (a.u.) is reached compared to the control. A reason for this could be, that an electrostatic attraction between the anionic sulfonate group of SmocGly and the positively charged head group of CTAB traps the substrate, which results in an incomplete conversion of the substrate. It could also be that an electrostatic attraction between the cationic surfactant and the sulfonate group of the released side product SDBF causes a shift of the absorption maximum of SDBF and hence cannot be detected by the UV machine which measures just at the wave length of 308 nm. In presence of the negatively charged surfactant SDBS the deprotection rate is slowed down to $1410*10^{-5}$ Abs/min compared to the control measurement. However, the same plateau in a.u. as in the control was reached.

In order to confirm the phenomena, if the deprotection rate is indeed significantly slowed down by an anionic surfactant and enhanced by a cationic one, if the substrate is trapped by a positively charged surfactant or if the differences compared to the control result from pipetting mistakes, multiple measurements should be carried out (not in this thesis). However, the important conclusion from this section is that the replicator is still catalytic active in presence of surfactants.

2.2 DEPROTECTION OF COMPARTMENT FORMING MOLECULES MEDIATED BY A SYNTHETIC SELF-REPLICATOR

It was shown in the previous section that the synthetic self-replicator is indeed capable of deprotecting the standard substrate SmocGly in presence of different surfactant types. In order to combine self-replication and a primitive metabolism

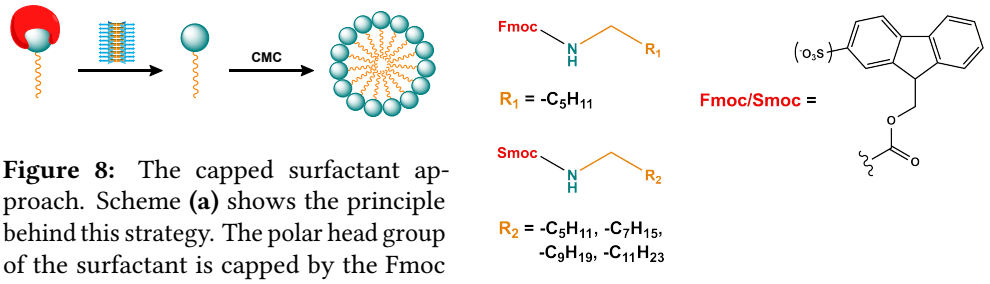

Figure 8: The capped surfactant approach. Scheme **(a)** shows the principle behind this strategy. The polar head group of the surfactant is capped by the Fmoc group and prevents compartmentalization. The self-replicator uncaps the protecting group so that the free surfactant forms compartments above the CMC. Scheme **(b)** shows the substrate scope of aliphatic single tail amines that was synthesized and tested.

with compartmentalization in a conceptual way the substrate scope will be explored to protected compartment-forming molecules (Figure 8).

2.2.1 *Deprotection of aliphatic primary amines*

Previous works in the *Otto* group have shown that this particular synthetic self-replicator is able to deprotect the substrate Fmoc-Glycine (FmocGly). Primary amines form micelles in water when their concentration is above the CMC. As a given example, hexylamine shows a CMC of $4*10^{-3}$ M in water at 25°C.[41]

As a first starting point, hexylamine was protected with the Fmoc group. The UV measurements in Figure 9 (a) show that the self-replicator is not able to do the Fmoc deprotection with hexylamine. The negative absorption results from solubility issues of the Fmoc group which already appeared with the standard substrate FmocGly (not in this thesis) but become even more crucial with Fmoc-hexylamine due to the hydrophobic aliphatic chain of the amine. Hence, in order to prevent solubility issues the experiment was repeated with the Smoc-protected hexylamine. Figure 9 (b) shows that the replicator is able to deprotect Smoc-hexylamine with a catalytic rate of $334*10^{-5}$ Abs/min.

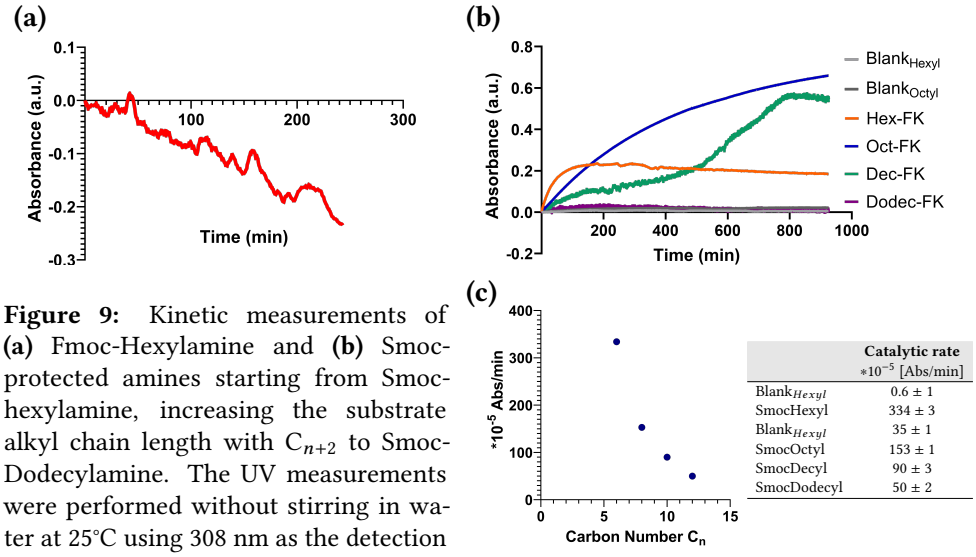

	Catalytic rate $*10^{-5}$ [Abs/min]
$Blank_{Hexyl}$	0.6 ± 1
SmocHexyl	334 ± 3
$Blank_{Hexyl}$	35 ± 1
SmocOctyl	153 ± 1
SmocDecyl	90 ± 3
SmocDodecyl	50 ± 2

Figure 9: Kinetic measurements of **(a)** Fmoc-Hexylamine and **(b)** Smoc-protected amines starting from Smoc-hexylamine, increasing the substrate alkyl chain length with C_{n+2} to Smoc-Dodecylamine. The UV measurements were performed without stirring in water at 25°C using 308 nm as the detection wavelength for SDBF. The concentration for each substrate was 100 µM and the replicator 40 µM. Panel **(c)** shows the correlation between aliphatic chain length of the substrate and catalytic rate. The catalytic rates are given in the table beside **(c)**.

In order to explore what is the longest amine that the replicator can deprotect before aggregation starts playing an important role, the experiments were continued with C_{n+2} Smoc-protected primary amines. In Figure 9 (b) it is shown that the replicator is able to deprotect Smoc-amines until dodecylamine.

Graphs (b) and (c) in Figure 9 clearly show the longer the alkyl chain is the lower is the catalytic rate. Thus, it seems to be that the deprotection rate correlates with hydrophibicity. It could be the hydrophobicity of the alkyl chains that makes the accessibility of the Smoc-protecting group harder for the hydrophilic replicator. The longer the alkyl chain is, the higher is the hydrophibicity and the lower the interaction becomes between the aliphatic amine and the self-replicator. At a certain chain length the hydrophobicity of the substrate is too high, so that the replicator cannot access the Smoc group anymore. In order to confirm if the correlation between catalytic rate and substrate hydrophobicity is linear, parabolic or exponential, as it looks like in graph (c), multiple measurements of each Smoc-amine should be carried out (not in this thesis).

2.2.2 *Deprotection Kinetics of Smoc-protected aliphatic primary Amines*

To study the effects of temperature, reaction medium and hydrophobicity on the catalytic rate, kinetic measurements of the Smoc-hexylamine as well as Smoc-octylamine deprotection were performed at different temperatures in various reaction media. The only structural difference between these two compounds is the additional $-C_2H_5$ group of octylamine which is ideal to study how the hydrophobicity and tendency for aggregation of the substrate changes the deprotection kinetics.

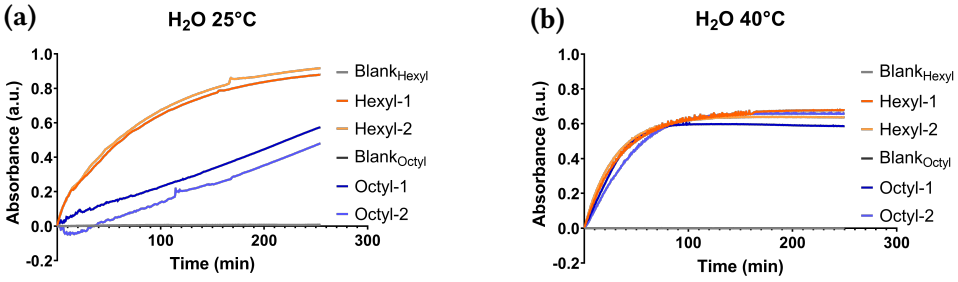

	25°C	40°C
	Catalytic rate $*10^{-5}$ [Abs/min]	**Catalytic rate** $*10^{-5}$ [Abs/min]
$Blank_{Hexyl}$	10 ± 1	3 ± 1
Hexyl-1	2150 ± 40	1800 ± 20
Hexyl-2	2240 ± 50	2060 ± 1
Mean	**2200** ± 100	**1900** ± 200
$Blank_{Octyl}$	6 ± 1	-3 ± 1
Octyl-1	198 ± 8	1360 ± 60
Octyl-2	150 ± 20	850 ± 20
Mean	**180** ± 30	**1100** ± 400

Figure 10: Kinetic UV measurements of Smoc-hexylamine and Smoc-octylamine deprotection by the self-replicator in water. The measurements were performed without stirring at 25°C **(a)** as well as 40°C **(b)** using 308 nm as the detection wavelength for SDBF. Each blank was the Smoc protected amine in water. The catalytic rates ($*10^{-5}$ Abs/min) are given in the table below the graphs.

In water (Figure 10) there is no significant background reaction for the Smoc-protected amines neither at 25°C nor at 40°C. Since the slope of the Smoc-octylamine blank at 40°C is negative, which does not make sense in this measurement set up, the background reaction is considered to be 0 Abs/min.

At 25°C a remarkable difference in the catalytic rate between the deprotection of Smoc-hexylamine and Smoc-octylamine occurs which shows that the length of the alkyl chain clearly influences the catalytic rate since Smoc-hexylamine is faster deprotected than Smoc-octylamine. Interestingly at 40°C there is not a significant difference for the deprotection rate of Smoc-hexylamine compared to the rate at 25°C while for Smoc-octylamine the deprotection rate at 40°C is almost 6 times increased.

Since Smoc-hexylamine carries a shorter alkyl chain it could be that at 25°C aggregation effects play a minor role for the accessibility to the replicator compared to Smoc-octylamine. The CMC increases with temperature, which is due to increased molecular motion. Hence a higher temperature could have more impact on the enhancement of the Smoc-octylamine deprotection rate, because more aggregates are broken and the substrate is suddenly way more accessible to the replicator compared to 25°C and thus is faster deprotected. Smoc-hexylamine is better accessible to the replicator at 25°C and it could be, that the increased temperature hence does not influence the deprotection rate by the same factor as it does with Smoc-octylamine because less aggregates need to be broken.

Another reason that the deprotection rate for Smoc-hexylamine shows not a significant difference between 25°C and 40°C could be that at higher temperatures the released side product SDBF undergoes faster addition reactions with water and the replicator so that SDBF could not be accurately detected which makes the rate appear to be not significantly affected by temperature. Furthermore a pipetting mistake could have happened as well, so that there was less substrate available compared to 25°C. However, when comparing the shapes of the curves at 25°C and 40°C of Smoc-hexylamine it appears to be that at higher temperature the curve is steeper than at 25°C.

After all, reaction rates tend to increase with temperature. Due to the fact that reactants must collide with one another with enough energy, and temperature increases the average kinetic energy of reactants the catalytic rate should actually be increased for Smoc-hexylamine as well.

Another interesting aspect is that at 25°C in case of Smoc-hexylamine the plateau is reached at almost 1 a.u. while at 40°C the plateau is reached at 0.7 a.u. Since in all UV measurements the same substrate concentration was used and the absorption maximum of 308 nm of the released sideproduct SDBF was measured, the decreased plateau at 40°C could either mean an incomplete conversion of the substrate or a shift of the absorption maximum due to various side reactions that SDBF can undergo. One of these side reactions is the polymerization at the double bond. It could be that SDBF polymerizes faster at higher temperatures compared to 25°C and the resulting multiple negatively charged polymer sticks to the replicator which carries positive charges and hinders it from further catalysis thus causes an incomplete conversion or the absorption maximum of the polymer is shifted so that the released SDBF which polymerized was not measured. An enhanced polymerization at higher temperatures could explain the fact that at 40°C a lower plateau in a.u. is reached than at 25°C. Furthermore, it is possible that an addition reaction of the replicator to the double bond of SDBF happens. It could be that either the deprotonated lysine residues form the adduct with SDBF or the more nucleophilic thiols which leads to the destruction of the self-replicator by opening the disulfide bonds. Both cases could

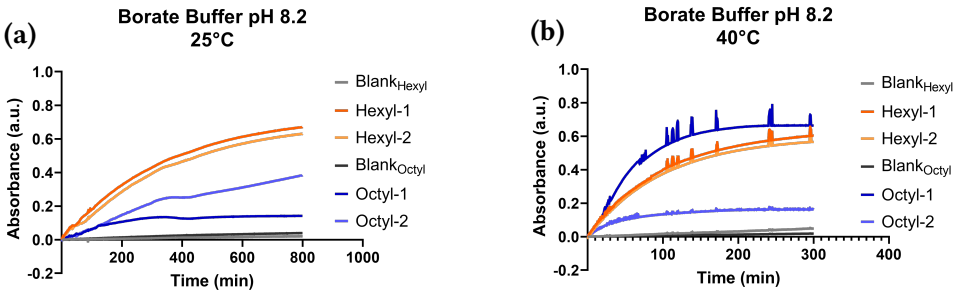

	25°C	40°C
	Catalytic rate $*10^{-5}$ [Abs/min]	**Catalytic rate** $*10^{-5}$ [Abs/min]
Blank$_{Hexyl}$	-1 ± 3	14 ± 1
Hexyl-1	250 ± 5	652 ± 6
Hexyl-2	228 ± 6	552 ± 3
Mean	**240** ± 20	**600** ± 70
Blank$_{Octyl}$	2 ± 1	10 ± 1
Octyl-1	30 ± 10	581 ± 7
Octyl-2	91 ± 3	329 ± 4
Mean	**60** ± 40	**460** ± 180

Figure 11: Kinetic UV measurements of Smoc-hexylamine and Smoc-octylamine deprotection by the self-replicator in 50 mM borate buffer pH 8.2. The measurements were performed without stirring at 25°C **(a)** as well as 40°C **(b)** using 308 nm as the detection wavelength for SDBF. Each blank was the Smoc protected amine in buffer. The catalytic rates ($*10^{-5}$ Abs/min) are given in the table below the graphs.

cause an incomplete conversion or a shift of the absorption maximum. The addition of water to the double bond is another possible side reaction that could also explain a lower plateau in a.u. resulting from the absorption maximum shift. Furthermore the mentioned explanations for a lower plateau in a.u. could also explain the issues in determining the absorption coefficient of the released SDBF.

In 50 mM borate buffer pH 8.2 (Figure 11) there is no significant background reaction for the Smoc-protected amines neither at 25°C nor at 40°C. The negative slope in the Smoc-hexylamine blank at 25°C is considered as 0 Abs/min.

At 25°C the catalytic rate for Smoc-hexylamine is almost 4 times faster compared to Smoc-octylamine. The significant difference in catalytic rate between the single measurements of Smoc-octylamine could be explained by possible aggregation effects. The Smoc-protected amines are surfactants and the longer the alkyl chain length is the lower is the aggregation concentration which could cause inhomogenities in the different measurements.

At 40°C the catalytic rate for Smoc-hexylamine is more than twice as fast as the deprotection at 25°C. For Smoc-octylamine the catalytic rate at 40°C is about 7 times faster compared to the deprotection at 25°C. Temperature seems to have more influence on the catalytic rate of the Smoc-octylamine deprotection which could explained by aggregation which plays a bigger role for Smoc-octylamine than for Smoc-hexylamine. Since reaction rates tend to be increased with temperature also the Smoc-hexyl deprotection is enhanced at 40°C.

Interestingly, the Smoc-hexylamine measurements reach the same plateau in a.u. at both temperatures while the Smoc-octylamine show significant differences of more than 0.2 a.u. at 25°C and 0.4 a.u. at 40°C. This could also be explained by

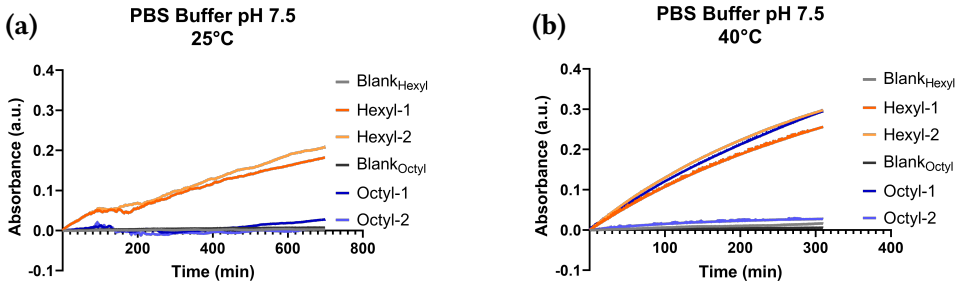

	25°C	40°C
	Catalytic rate $*10^{-5}$ [Abs/min]	**Catalytic rate** $*10^{-5}$ [Abs/min]
Blank$_{Hexyl}$	10 ± 1	-3 ± 1
Hexyl-1	89 ± 1	128 ± 6
Hexyl-2	81 ± 1	146 ± 2
Mean	**86** ± 4	**140** ± 10
Blank$_{Octyl}$	6 ± 1	4 ± 1
Octyl-1	7 ± 1	159 ± 8
Octyl-2	9 ± 1	20 ± 1
Mean	**8** ± 2	**90** ± 100

Figure 12: Kinetic UV measurements of Smoc-hexylamine and Smoc-octylamine deprotection by the self-replicator in 50 mM phosphor buffered saline (PBS) buffer pH 7.5. The measurements were performed without stirring at 25°C **(a)** as well as 40°C **(b)** using 308 nm as the detection wavelength for SDBF. Each blank was the Smoc protected amine in buffer. The catalytic rates ($*10^{-5}$ Abs/min) are given in the table below the graphs.

inhomogenities between the single measurements due to aggregation which could make the Smoc-protected octylamine less accessible for the replicator.

In 118 mM PBS buffer pH 7.5 (Figure 12) there is no significant background reaction neither at 25°C nor at 40°C. The negative slope in the Smoc-hexylamine blank at 40°C is considered as 0 Abs/min.

At 25°C Smoc-hexylamine can be deprotected by the self-replicator while the rate for Smoc-octylamine is comparable with its blank. At 40°C the catalytic rate for Smoc-hexylamine is increased by a factor of approximately 1.5 while the deprotection of Smoc-octylamine is increased by a factor of 11. Thus at higher temperature it can be deprotected by the self-replicator while at 25°C this is not the case. However, the single Smoc-octylamine deprotection measurements show a huge difference in the catalytic rate. One measurement (Octyl-1) shows a deprotection rate of $159*10^{-5}$ Abs/min which is in the magnitude of the Smoc-hexylamine deprotection rate but the second one (Octyl-2) shows almost no deprotection. Hence the error is bigger than the average which makes this result unreliable. It is very likely that a pipetting mistake happened. Either in the Octyl-1 measurement Smoc-hexylamine was used as substrate instead since the catalytic rate is very similar to the Smoc-hexylamine deprotection or the substrate was forgotten in the Octyl-2 measurement since there is almost no deprotection. In order to exclude a pipetting mistake the measurement should be repeated (not in this thesis).

In 50 mM HEPES buffer pH 7.5 (Figure 13) there is a significant background reaction for Smoc-hexylamine at both temperatures as well as for Smoc-octylamine at 40°C which could also be an indication that aggregation effects play a bigger role

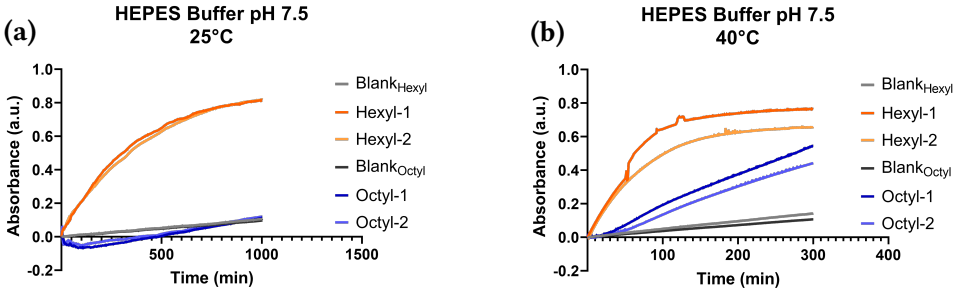

	25°C	40°C
	Catalytic rate $*10^{-5}$ [Abs/min]	**Catalytic rate** $*10^{-5}$ [Abs/min]
Blank$_{Hexyl}$	17 ± 2	42 ± 1
Hexyl-1	760 ± 20	1400 ± 100
Hexyl-2	660 ± 10	920 ± 10
Mean	**710** ± 70	**1200** ± 300
Blank$_{Octyl}$	9 ± 1	27 ± 2
Octyl-1	8 ± 0.008	250 ± 10
Octyl-2	9 ± 0.006	196 ± 3
Mean	**8.0** ± 0.4	**220** ± 40

Figure 13: Kinetic UV measurements of Smoc-hexylamine and Smoc-octylamine deprotection by the self-replicator in 50 mM 2-(4-(2-Hydroxyethyl)-1-piperazinyl)-ethanesulfuric acid (HEPES) buffer pH 7.5. The measurements were performed without stirring at 25°C **(a)** as well as 40°C **(b)** using 308 nm as the detection wavelength for SDBF. Each blank was the Smoc protected amine in buffer. The catalytic rates ($*10^{-5}$ Abs/min) are given in the table below the graphs.

for Smoc-octylamine which shows almost no background reaction at 25°C but a significant one at 40°C.

At 25°C Smoc-hexylamine can be deprotected by the self-replicator while the rate for Smoc-octylamine is comparable with its blank of $8*10^{-5}$ Abs/min. At 40°C the catalytic rate for Smoc-hexylamine is increased by a factor of approximately 1.7 while the deprotection of Smoc-octylamine is increased by a factor of 28 hence at higher temperature it can be deprotected by the self-replicator while at 25°C this is not the case. Interestingly, Figure 13 **(b)** shows that between the Smoc-hexylamine measurements there is a difference of around 0.2 a.u. of the reached plateau. It could be that in these measurements inhomogenities due to aggregation effects played a role.

Another interesting aspect is that the reaction medium has a remarkable influence on the catalytic rate. Table 5 shows a summary of all catalytic rates mentioned in this section for a better overview. At 25°C the order from highest to lowest catalytic rate for Smoc-hexylamine is water, HEPES pH 7.5, borate pH 8.2 and PBS pH 7.5 buffer. Smoc-octylamine showed a different order of water, borate pH 7.5 and almost no deprotection in HEPES pH 7.5 and PBS pH 7.5 buffer. Hence with both substrates the highest catalytic rates were achieved in water. At 40°C for Smoc-hexylamine the order from highest to lowest catalytic rates is water, HEPES pH 7.5, borate pH 8.2 and PBS pH 7.5 buffer. Smoc-octylamine shows a different order of water, borate pH 7.5, HEPES pH 7.5 and PBS[i] pH 7.5 buffer. Again, with both substrates

[i]Note that the error is bigger than the mean due to a possible pipetting mistake.

	H_2O	Borate	PBS	HEPES
	Catalytic rate $*10^{-5}$ [Abs/min]	**Catalytic rate** $*10^{-5}$ [Abs/min]	**Catalytic rate** $*10^{-5}$ [Abs/min]	**Catalytic rate** $*10^{-5}$ [Abs/min]
$Hexyl_{25C}$	2200 ± 70	240 ± 20	86 ± 4	710 ± 70
$Hexyl_{40C}$	1900 ± 200	600 ± 70	140 ± 10	1200 ± 300
$Octyl_{25C}$	180 ± 30	60 ± 40	8 ± 2	8.0 ± 0.4
$Octyl_{40C}$	1100 ± 400	560 ± 180	90 ± 100	220 ± 40

Table 5: Summary of the mean values of the deprotection rates of Smoc-hexylamine and Smoc-octylamine received by the kinetic UV measurements at 25°C and 40°C in different reaction media.

the highest catalytic rates were achieved in water. To find a possible explanation for the order of reaction media, one has to take a closer look at the properties of the reaction media. Boric acid shows pK_a values of ~ 9.2, 12.4 and 13.3 and phosphoric acid ~ 2.2, 7.2 and 12.3. HEPES is a zwitterionic compound bearing one sulfonate group that is completely dissociated over almost the whole pH range and a piperazine moiety with two nitrogens, showing a pK_a of ~ 3.0 and ~ 7.6, respectively. HEPES has its isoelectronic point pI at ~ 5.0. At pH 7.5 the sulfonate group and one nitrogen are completely deprotonated and the other one partially protonated at this pH. Hence a possible explanation for the order of reaction media could be that the buffered solutions contain a certain amount of charged molecules depending on the dissociation grade which is linked to the pK_a of the buffer molecules. Negatively charged salts and molecules could have an inhibition effect to the positively charged replicator. Furthermore, the sulfonate group of the substrate could be blocked by positively charged buffer salts and therefore the substrate and replicator do not attract each other which could hinder the arrangement of substrate and replicator into a suitable conformation for a faster deprotection.

An important aspect regarding the influence of the reaction medium on the catalytic rate could be the ionic strength which is according to *Allen et al.* defined as a dimensionless parameter that provides a measure of concentration and charge of ions influencing the properties of a solution containing ions. It is determined by all ions in the solution and hence given by the sum of the product of the molality and charge of all ions.[ii] *Palladino et al.* showed ionic strength effects on the CMC drawing the conclusion that an increasing ionic strength decreases the CMC. The order of reaction media after the catalytic rates could be explained by their ionic strength. Compared to the other reaction media that were used, water shows the lowest ionic strength hence according to *Palladino et al.* the highest CMC for Smoc-hexylamine as well as Smoc-octylamine. The 118 mM PBS buffer with the additional salts sodium chloride (NaCl) and potassium chloride (KCl) shows the highest ionic strength, thus the lowest CMC, which possibly explains why Smoc-hexylamine is at 25°C very slowly deprotected and Smoc-octylamine not at all.This is due to more aggregation in the PBS buffer.

According to the ionic strength explanation the order of reaction media from highest to lowest catalytic rate should be water - borate pH 8.2 - HEPES pH 7.5 - PBS pH 7.5 which fits for Smoc-octylamine but not exactly for Smoc-hexylamine. The latter shows a significant higher catalytic rate in HEPES pH 7.5 compared to borate pH 8.2. Furthermore, at 25°C Smoc-hexylamine shows a significant background reaction in HEPES buffer in contrast to Smoc-octylamine. The background reaction in HEPES buffer could be caused by the piperazine moiety, which seems to have more impact on Smoc-hexylamine than on Smoc-octylamine. This can also be explained by

[ii]Note that there exist different definitions for the term ionic strength with different units.

the lower aggregation effects of Smoc-hexylamine and therefore is more accessible for the deprotection compared to Smoc-octylamine, not just for the replicator but for the buffer as well. However, wether the order of reaction media results from inhibition of the replicator by charged buffer molecules, or from aggregation effects by different CMCs depending on ionic strength, or if it is a combination of both effects, kinetic UV measurements should be carried out with substrates that do not form aggregates which will be discussed in Chapter 3.

Another important aspect is the temperature, which seems to have more impact on the catalytic rate for the Smoc-octylamine deprotection than for Smoc-hexylamine. As with all equilibrium constants, K_a is a function of temperature since it is related to the Gibbs free energy of reaction. The pK_a decreases with increasing temperature. Hence at 40°C the pK_a and pH values are lower than at 25°C which could also affect the reaction rate. At lower pH values a larger amount of lysines of the self-replicator are protonated hence it should be less efficient as a catalyst for the Smoc deprotection. However, the reaction rates increase at higher temperatures due to higher average kinetic energies as well as broken aggregates as already discussed. The last two aspects might play a bigger role so that they overrule decreased pK_a values and higher temperatures speed up the deprotection.

2.2.3 *Deprotection of Coacervate forming Molecules*

Another approach for compartment formation is coacervation (Figure 14 **(a)**). Previous works in the *Otto* group have shown that synthetic peptide based self-replicators can be trapped inside coacervates. The tetraamine spermine forms in combination with PAA in the ratio 1:4 in water within the pH range 7,4 - 7,9 coacervates. In this section the approach is to protect all four nitrogens of spermine with the Smoc-group and test if the replicator is able to deprotect the tetraamine and finally induces coacervation (Figure 14 **(a)**).

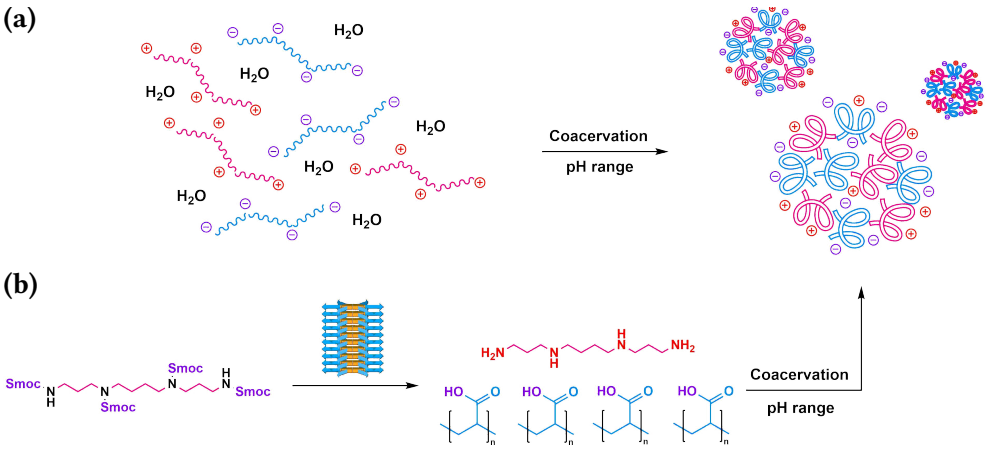

Figure 14: Coacervation is also a form of compartmentalization. Scheme **(a)** shows the principle behind coacervation. Scheme **(b)** shows the idea of combining self-replication with coacervation. The polyamine spermine is protected with the Smoc-group hence the positive charge of the amines is capped and no coacervation happens. The self-replicator cuts off the protection groups and in a 1:4 ratio of spermine and polyacrylic acid (PAA) at pH 7.6 coacervates are formed.

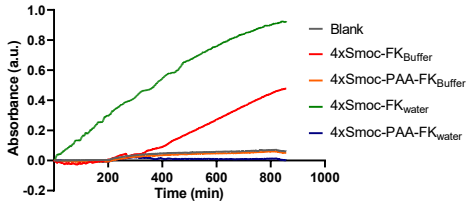

	Catalytic rate $*10^{-5}$ [Abs/min]
Blank$_{Buffer}$	-9 ± 4
4xSmocSpermine/FK$_{Buffer}$	84 ± 4
4xSmocSpermine/PAA/FK$_{Buffer}$	18 ± 3
4xSmocSpermine/FK$_{water}$	260 ± 9
4xSmocSpermine/PAA/FK$_{water}$	-33 ± 4

Figure 15 & Table 6: Kinetic measurements of 4xSmocSpermine in water and 50 mM borate buffer pH 7.7 at 25°C using 308 nm as the detection wavelength for SDBF without stirring. The concentration for the substrate was 100 µM, for PAA 40 µM and the replicator 40 µM. The results for the catalytic rates are given in the table beside the graph.

After the synthesis of the protected tetraamine 4xSmocSpermine, UV measurements were performed to see if the self-replicator is capable of deprotecting it in general but also under the conditions which are necessary for coacervation.

The graph in Figure 15 shows that in general the replicator is able to deptrotect 4xSmocSpermine in water. Borate buffer with a pH of 7.7 slows the deprotection down which could be caused on the one hand by buffer salts and on the other hand by the pH of 7.7 where more lysines are protonated and hence the replicator becomes less efficient deprotecting the Smoc-group. However, 4xSmocSpermine cannot be deprotected in presence of PAA, neither in water nor in borate buffer. The reason for that is most likely that the negatively charged PAA is electrostatically attracted to the positive lysine residues of the replicator and hinders therby the deprotection of the tetraamine.

2.2.4 *Outlook*

A possible solution to the inhibition of the replicator by the negatively charged polymer could be the addition of PAA after 4xSmocSpermine was deprotected so that the lysine residues are not blocked by the negatively charged polymer but this was not done in this thesis.

Another possible solution to continue this project could be the idea of a destructing self-replicator. It should be tested if 4xSmocSpermine which is four times negatively charged forms coacervates with the four times positively charged spermine in a 1:1 ratio. If coacervation happens the self-replicator could destroy the compartments through deprotection of the negatively charged component 4xSmocSpermine.

2.3 INTRODUCTION OF A NEW PROTECTING GROUP

The *Otto* group has explored the substrate scope, that the self-replicator is capable to deprotect, from the Fmoc protecting group starting with the substrate FmocGly to the mono sulfonated pendant Smoc using SmocGly as the analogon to FmocGly. To continue this sequence of Fmoc analoga for further exploring the replicator's substrate scope, the double sulfonated pendant dSmoc is introduced in this thesis.

Figure 9 (a) shows that the replicator is not able to deprotect Fmoc-hexylamine probably due to solubility issues of the substrate whereas (b) shows that the replicator is capable to deprotect the mono sulfonated analogon Smoc-hexylamine. The substrate scope was expanded until Smoc-dodecylamine, where possibly solubility issues and aggregation hindered the replicator to access the substrate for carrying out the deprotection. It is assumed in this thesis that the introduction of the dSmoc

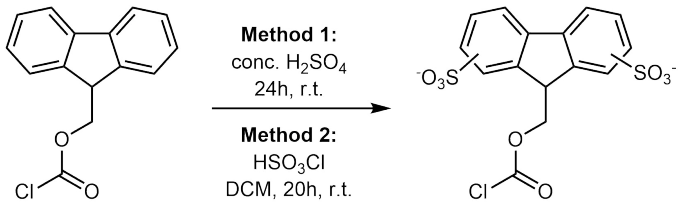

Figure 16: Synthesis of a di-sulfonated Fmoc protecting group via two methods. Method 1 was performed according to a patent of *Knauer et al.*[42] that does not mention any work up techniques for this compound. Method 2 was performed according to the synthesis of 9-(2-Sulfo)fluorenylmethyloxycarbonylchloride (Smoc-Cl) by *Merrifield et al.*[25] with 2 eq. of chlorosulfonic acid and 24h stirring. The positions of the sulfonate groups on the benzene rings are not fully clear.

protecting group further increases the water solubility hence the substrate scope could be expanded beyond dodecylamine possibly even to secondary amines.

2.3.1 *Synthesis of the new Protecting Group dSmoc-Cl*

The synthesis of 9-(x,x-disulfo)fluorenylmethyloxycarbonylchloride (dSmoc-Cl) was at first performed according to a patent of *Knauer et al.*[42] by treating 9-Fluorenylmethyloxycarbonylchloride (Fmoc-Cl) with concentrated sulfuric acid. It is not clear wether the sulfonate groups are attached at positions 2,9 or 3,8 hence these positions are marked as x,x in the compound name. Accurate synthesis conditions such as temperature, stirring time or work-up are not mentioned by the authors of the patent. In this work the synthesis was carried out by treating 2.93 g (11.33 mmol) Fmoc-Cl with 20 mL concentrated sulfuric acid in a 100 mL round bottom flask equipped with a stirring bar. The reaction mixture was clear and dark blue. After 5 h of stirring at room temperature the mixture became light blue and a precipitate started to form. The suspension was stirred for another 15 h followed by vacuum filtration of the light brown solid and washing the solid with a mixture of hexane/dichloromethane (DCM) (1:1). Due to clogging of the filter the suspension was neutralized by slowly adding a saturated sodium carbonate solution under cooling. With raising the pH closer to neutral range the color of the solution changed from cherry red to light yellow. The solvent was evaporated and the light brown solid dried in vacuum. The ^{1}H-NMR in Figure 2.3.1 (a) shows that the double sulfonation seemed to be successful. However, it is very likely that during the neutralization

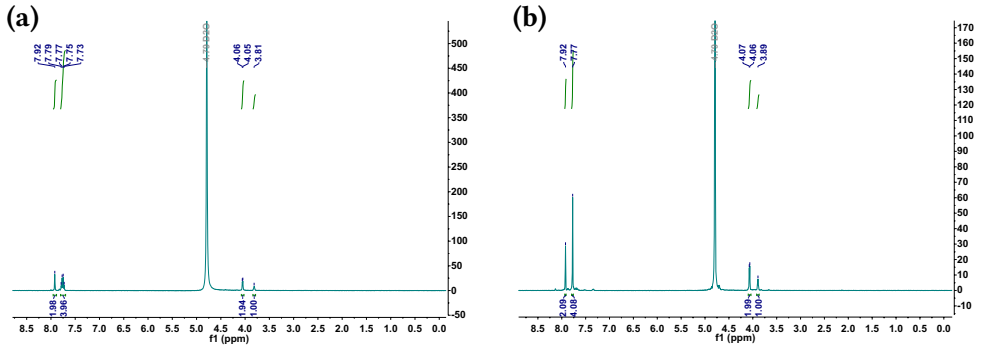

Figure 17: ^{1}H-NMR in deuterium oxide of a designed synthesis taking **(b)** the patent of *Knauer et al.*[42] and **(a)** the protocol for Smoc-Cl from *Merrifield et al.*[25] as basis. The signal in **(a)** at 3.81 ppm shows a slightly different shift in **(b)** at 3.89 ppm. It is possible that **(a)** shows the acid and **(b)** the chloride.

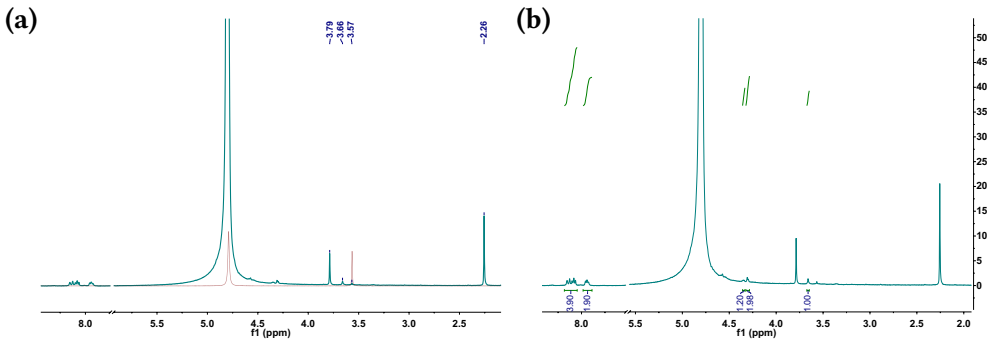

Figure 18: ^{1}H-NMR in deuterium oxide of **(a)** stacked spectra of glycine (red line) and dSmocGly (green line) showing a shift of the glycine signal from 3.57 ppm to 3.66 ppm in the dSmocGly spectrum (acetone: 2.26 ppm, dioxane: 3.79 ppm) meaning that the coupling to the dSmoc group worked. The ^{1}H-NMR spectrum in **(b)** shows the integrated spectrum of dSmocGly.

procedure the conversion from the chloride to the acid happened and thus cannot be used without further activation for coupling it to an amine.

Another synthesis method that was used is an adjusted procedure for the synthesis of the mono sulfonated Smoc-Cl. In a 100 mL round bottom flask equipped with a stir bar 2.66 g (10.28 mmol) was dissolved in 25 mL DCM and 1.5 mL (22.53 mmol) chlorosulfonic acid dissolved in 10 mL DCM was added in a dropwise fashion over a period of 7 min under cooling with an ice bath. Afterwards the reaction mixture was stirred for 20 h at ambient temperature. A brownish precipitate formed which was vacuum filtrated and intensively washed with hexane/DCM (2:1) and the brownish powder finally dried under vacuum. The ^{1}H-NMR in Figure 2.3.1 (b) shows that the double sulfonation seemed to be successful. However, the synthesis and workup should be carried out under inert gas since the product seems to be very hygroscopic.

2.3.2 *Synthesis of dSmoc-glycine*

In a 10 mL round bottom flask equipped with a stir bar 202 mg (0.45 mmol) dSmoc-Cl were dissolved in 1.5 mL dioxane and 20 mg (0.27 mmol) glycine dissolved in a 10% Na_2CO_3 solution was added dropwise under cooling with a water bath. A white precipitate formed and 1 mL dioxane with 0.5 mL 10% Na_2CO_3 solution was added. The mixture became clear with some white agglomerates. The reaction mixture showed a pH of 8 and was stirred for 3 h at ambient temperature where it finally became turbid. Afterwards it was acidified with a 1 M HCl to a pH 2-3. The remaining solid was vacuum filtrated, washed with dioxane and dried in vacuum.

The ^{1}H-NMR in Figure 2.3.2 (a) shows that the coupling seems to have worked since the glycine peak at 3.57 ppm is shifted to 3.66 ppm meaning that the protons experience a stronger electroning withdrawing effect coming from the carbamate group. However, the white precipitate was very likely salt that had some remaining product from the solution phase and is thus visible in the ^{1}NMR spectrum. The synthesis should be repeated with a purification of the solution by chromatography using a water/ACN gradient.

2.3.3 *Outlook*

The dSmoc protecting group shows great potential to expand the substrate scope of the self-replicator to more apolar substrates that are not accessible with the Fmoc- or Smoc-group due to hydrophibicity reasons.

As a next step after dSmoc-glycine (dSmocGly) was isolated, kinetic UV measurements should be performed for determining the catalytic rate of the dSmocGly deprotection by the self-replicator. This should be compared to the deprotection rates of FmocGly and SmocGly. These results might confirm or negate the trend that each sulfonate group enhances the deprotection rate. An enhanced rate might be caused through a possibly more favored arrangement between substrate and replicator by higher attractive coulomb forces between the negatively charged sulfonate group of the substrate and positive lysine residues of the replicator.

After the confirmation that the standard substrate glycine can be deprotected by the self-replicator, more hydrophobic molecules such as dodecylamine or even secondary amines should be protected by the dSmoc group.

2.4 CONTRIBUTIONS

The question about the behavior of the self-replicator in presence of surfactants as well as the substrate scope and deprotection kinetics of protected aliphatic single tail amines was proposed by the author. Kayleigh van Esterik, BSc, synthesized the standard substrate SmocGly, carried out the UV measurement in Figure 7 and prepared the HEPES buffer (50 mM, pH 7.5). The negative stain TEM was done by Jim Ottelé, MSc and cryo TEM by Guillermo Monreal Santiago, MSc. The ^{1}H-NMRs of Smoc-hexylamine and Smoc-octylamine were taken by Paul Adamsky, MSc. and the mass spectra were carried out by Marcel Eleveld, MSc.

The research question about the deptrotection of coacervate forming molecules was proposed by Guillermo Monreal Santiago, MSc.

The author carried out the remaining synthesis', UV measurements, ^{1}H-NMR spectra and data evaluation as well as drew the conclusions in this chapter.

2.5 EXPERIMENTAL

2.5.1 *Synthesis*

9-(2-Sulfo)fluorenylmethyloxycarbonyl chloride *(Smoc-Cl)*

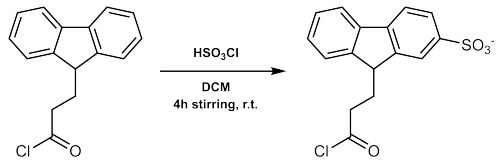

Fmoc-Cl (2.59 g, 0.01 mol) was dissolved in 20 mL DCM (technical grade) in a 100 mL round bottom flask equipped with a magnetic stir bar. The solution was slightly yellow. Then, chlorosulfonic acid (0.56 mL, 8.4 mmol) was dissolved in 10 mL DCM and transferred dropwise to the stirred solution of Fmoc-Cl under cooling with an ice-water bath over a time period of 10 minutes. The solution turned yellow and then dark green. After the addition of chlorosulfonic acid was finished, the solution was allowed to reach room temperature. A light brown precipitate was formed so that the magnetic stir bar got stuck. The mixture was left in this condition for 2 hours.

Then, 20 mL of n-hexane were poured on to the mixture and the precipitate then vacuum filtrated. The old-white solid was washed intensively with a 1:1 mixture of n-hexane:DCM (100 mL). The product was dried in vacuo for 2 days yielding 2.57 g (76% of theory). The ^{1}H-NMR in CD_3CN showed the pure product.

^{1}**H-NMR** (400 MHz, Acetonitrile-d3): δ = 8.14 (s, 1H), 8.04 – 7.93 (m, 3H), 7.70 (d, J = 7.2 Hz, 1H), 7.55 – 7.43 (m, 2H), 4.90 (dd, J = 10.8, 5.7 Hz, 1H), 4.81 (dd, J = 10.8, 6.0 Hz, 1H), 4.47 (t, J = 5.9 Hz, 1H).

Fmoc-hexylamine

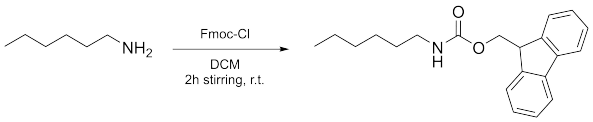

In a 50 mL round bottom flask equipped with a magnetic stir bar, Fmoc-Cl (384,3 mg, 1.5 mmol) was dissolved in 10 mL DCM and cooled with an ice-water bath. Then, n-hexylamine (71.6 mg, 0.7 mmol) dissolved in 4 mL DCM was transferred dropwise to the stirred solution of Fmoc-Cl. Afterwards, the clear and colourless solution was stirred for 20 min under cooling and then at room temperature for another 2 hours. The reaction was controlled by thin layer chromatography (TLC) using a 1:1 mixture of ethylacetate (EA):n-heptane.

The organic phase was washed 3 times excessively with doubly distilled water (ddH_2O) in a 50 mL separation funnel, then with 5% hydrochloric acid (HCl) and finally with saturated NaCl solution. The organic phase was dried over anhydrous magnesium sulfate (Mg_2SO_4), filtered an evaporated leading to 120 mg (53% of theory) of a white solid. The ^{1}H-NMR in $CDCl_3$ showed the pure product.

^{1}**H-NMR** (400 MHz, Chloroform-d): δ = 7.77 (d, J = 7.6 Hz, 2H), 7.60 (d, J = 7.5 Hz, 2H), 7.40 (t, J = 7.4 Hz, 2H), 7.31 (t, J = 7.4 Hz, 2H), 4.40 (d, J = 6.9 Hz, 2H), 4.22 (t, J = 6.9 Hz, 1H), 3.19 (q, J = 6.8 Hz, 2H), 1.50 (s, 2H), 1.30 (s, 6H), 0.88 (d, J = 7.1 Hz, 3H).

Smoc-hexylamine

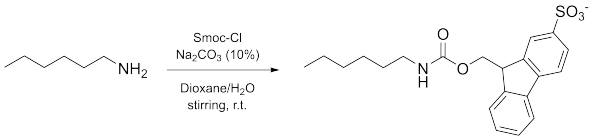

In a 25 mL round bottom flask equipped with a magnetic stir bar, Smoc-Cl (310 mg, 0.9 mmol) was dissolved in 1.6 mL 1,4-dioxane. Then, n-hexylamine (71.6 mg, 0.71 mmol) dispersed in 1.3 mL of a 10% aqueous sodium carbonate (Na_2CO_3) solution and transferred dropwise under cooling with a water bath to the stirred Smoc-Cl solution. The reaction was stirred at room temperature and controlled by TLC using a 1:9 mixture of MeOH:DCM. The dispersion became turbid and a white solid was formed.

After 4 hours of stirring, the reaction was acidified with 1 M HCl aqueous solution to a pH of 2-3 resulting in a clear yellow solution. The crude was purified by reversed phase (RP) flash chromatography using a H_2O/acetonitrile (ACN) gradient. The solvent was evaporated yielding 121 mg (43% of theory) of a white solid. The ^{1}H-NMR in deuterated water (D_2O) showed the pure product.

^{1}**H-NMR** (400 MHz, DMSO-d6): δ = 7.91 – 7.85 (m, 2H), 7.82 (d, J = 7.9 Hz, 1H), 7.70 – 7.65 (m, 2H), 7.36 (dtd, J = 34.0, 7.5, 1.1 Hz, 2H), 7.21 (t, J = 5.7 Hz, 1H), 4.54 (dd, J = 10.2, 5.3 Hz, 1H), 4.28 – 4.09 (m, 2H), 2.94 (q, J = 6.6 Hz, 2H), 1.36 (q, J = 6.9 Hz, 2H), 1.23 (hept, J = 5.4, 4.2 Hz, 6H), 0.85 (t, J = 6.8 Hz, 3H).

Smoc-octylamine

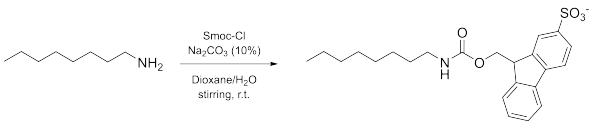

In a 25 mL round bottom flask equipped with a magnetic stir bar, Smoc-Cl (304 mg, 0.9 mmol) was dissolved in 1.6 mL 1,4-dioxane. Then, n-octylamine (90.5 mg, 0.7 mmol) dispersed in 1.3 mL of a 10% aqueous Na_2CO_3 solution and transferred dropwise under cooling with a water bath to the stirred Smoc-Cl solution. The reaction was stirred at room temperature and controlled by TLC using a 1:9 mixture of MeOH:DCM. The dispersion became turbid and a white solid formed.

After 4 hours of stirring, the reaction was acidified with 1 M HCl aqueous solution to a pH of 2-3 resulting in a clear yellow solution. The solvent was evaporated and dissolved in 4 mL ddH_2O and purified by RP flash chromatography using a H_2O/ACN gradient. The solvent was evaporated yielding 260 mg (86% of theory) of a white solid. The ^{1}H-NMR in D_2O showed the pure product.

^{1}**H-NMR** (400 MHz, DMSO-d6): δ = 7.91 – 7.85 (m, 2H), 7.82 (d, J = 7.9 Hz, 1H), 7.71 – 7.66 (m, 2H), 7.41 (td, J = 7.5, 1.2 Hz, 1H), 7.32 (td, J = 7.5, 1.2 Hz, 1H), 7.21 (t, J = 5.7 Hz, 1H), 4.54 (dd, J = 10.3, 5.4 Hz, 1H), 4.21 (t, J = 6.2 Hz, 1H), 4.15 (dd, J = 10.3, 7.0 Hz, 1H), 2.94 (q, J = 6.6 Hz, 2H), 1.36 (p, J = 6.7 Hz, 2H), 1.23 (s, 10H), 0.85 (t, J = 6.7 Hz, 3H).

Smoc-decylamine

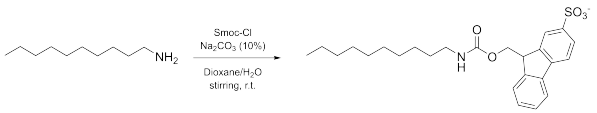

In a 25 mL round bottom flask equipped with a magnetic stir bar, Smoc-Cl (300 mg, 0.9 mmol) was dissolved in 1.6 mL 1,4-dioxane. Then, n-decylamine (94 mg, 0.6 mmol) dispersed in 1.3 mL of a 10% aqueous Na_2CO_3 solution was transferred dropwise under cooling with a water bath to the stirred Smoc-Cl solution. The reaction was stirred at room temperature. After 3 hours a white solid formed so that the magnetic stir bar got stuck. Cold water was (5 mL) added to the reaction and then the mixture was vacuum filtrated. The white solid was washed intensively with ice cold water. The product was dried in vacuum yielding 95 mg (34% of theory) of a white solid. The ^{1}H-NMR in DMSO-d6 showed the pure product.

^{1}**H-NMR** (400 MHz, DMSO-d6): δ = 7.86 (d, J = 6.3 Hz, 2H), 7.80 (d, J = 7.8 Hz, 1H), 7.66 (t, J = 7.9 Hz, 2H), 7.39 (t, J = 7.4 Hz, 1H), 7.30 (t, J = 7.4 Hz, 1H), 7.19 (t, J = 5.7 Hz, 1H), 4.51 (dd, J = 10.0, 5.3 Hz, 1H), 4.22 – 4.09 (m, 2H), 3.55 (s, 1H), 2.92 (d, J = 6.8 Hz, 2H), 1.34 (s, 2H), 1.21 (s, 16H), 0.83 (t, J = 6.5 Hz, 3H).

Smoc-dodecylamine

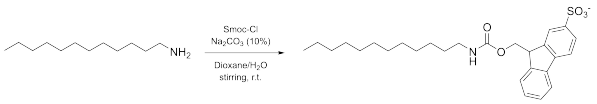

In a 25 mL round bottom flask equipped with a magnetic stir bar, Smoc-Cl (315 mg, 0.9 mmol) was dissolved in 1.6 mL 1,4-dioxane. Then, n-dodecylamine (115 mg, 0.6 mmol) was suspended in 1.3 mL of a 10% aqueous Na_2CO_3 solution and transferred dropwise under cooling with a water bath to the stirred Smoc-Cl solution. The reaction was stirred at room temperature. After 2 hours a white solid formed so that the magnetic stir bar got stuck. A bit of cold water was added to the mixture and then vacuum filtrated. The solid was washed intensively with ice cold water. The product was dried in vacuum yielding 154 mg (53% of theory) of a white solid. The ^{1}H-NMR in DMSO-d6 showed the pure product.

^{1}**H-NMR** (400 MHz, DMSO-d6): δ = 8.11 – 7.62 (m, 5H), 7.45 – 7.19 (m, 2H), 4.20 (s, 1H), 2.93 (s, 2H), 1.23 (s, 20H), 0.97 – 0.76 (m, 3H).

4xSmoc-spermine

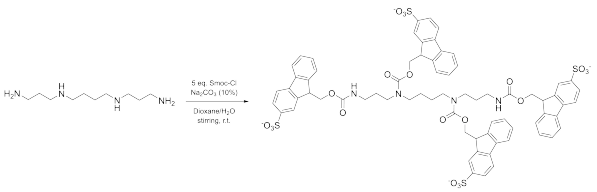

In a 25 mL round botton flask equipped with a magnetic stir bar, Smoc-Cl (303 mg, 0.9 mmol) was dissolved in 1.6 mL 1,4-dioxane. Then, spermine (37 mg, 0.18 mmol) dissolved in 1.3 mL of a 10% aqueous Na_2CO_3 solution was transferred dropwise under

cooling with a water bath to the stirred Smoc-Cl solution. The reaction was stirred at room temperature and a white precipitate formed. The reaction was controlled by TLC using a 1:4 mixture of MeOH:DCM.

After 4 hours of stirring, the reaction was acidified with 1 M HCl aqueous solution to a pH of 2-3 resulting in a clear yellow solution, which was poured as it was on a RP flash column. A H_2O:ACN gradient was used for purification. The solvent was evaporated yielding 200 mg (16% of theory) of a white solid. The ^{1}H-NMR in D_2O showed the pure product.

^{1}**H-NMR** (400 MHz, D_2O): δ = 8.13 – 6.57 (m, 28H), 4.57 – 0.04 (m, 32H).

9-(x,x-disulfo)fluorenylmethyloxycarbonylchloride

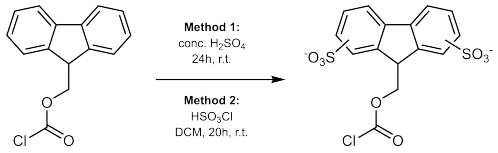

Method I:

In a 100 mL round bottom flask equipped with a stir bar 2.66 g (10.28 mmol) was dissolved in 25 mL DCM and 1.5 mL (22.53 mmol) chlorosulfonic acid dissolved in 10 mL DCM was added in a dropwise fashion over a period of 7 min under cooling with an ice bath. Afterwards the reaction mixture was stirred for 20 h at ambient temperature. A brownish precipitate formed which was vacuum filtrated and intensively washed with hexane/DCM (2:1) and the brownish powder finally dried under vacuum yielding 2.1 g (49% of theory). The ^{1}H-NMR in D_2O showed the pure product.

^{1}**H-NMR** (400 MHz, D_2O): δ = 7.92 (s, 2H), 7.76 (q, J = 8.1 Hz, 4H), 4.05 (d, J = 4.4 Hz, 2H), 3.81 (s, 1H).

Method II:

Fmoc-Cl (2.93 g, 11.33 mmol) was treated with 20 mL concentrated sulfuric acid in a 100 mL round bottom flask equipped with a stirring bar. The reaction mixture was clear and dark blue. After 5 h of stirring at room temperature the mixture became light blue and a precipitate started to form. The suspension was stirred for another 15 h, which was followed by vacuum filtration of the light brown solid and washing the solid with a mixture of hexane/DCM (1:1). Due to clogging of the filter the suspension was neutralized by slowly adding a saturated Na_2CO_3 solution under cooling. With raising the pH closer to neutral range the color of the solution changed from cherry red to light yellow. The solvent was evaporated and the light brown solid dried in vacuum. The ^{1}H-NMR in D_2O showed the pure product. However, the white solid was a mixture of the product and Na_2CO_3.

^{1}**H-NMR** (400 MHz, D_2Oe): δ = 7.92 (s, 2H), 7.77 (s, 4H), 4.07 (d, J = 4.6 Hz, 2H), 3.89 (t, J = 4.7 Hz, 1H).

dSmoc-glycine

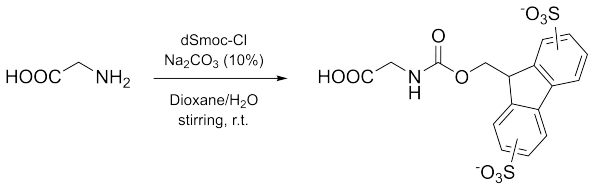

In a 10 mL round bottom flask equipped with a stir bar 202 mg (0.45 mmol) dSmoc-Cl were dissolved in 1.5 mL dioxane and 20 mg (0.27 mmol) glycine dissolved in a 10% Na_2CO_3 solution was added dropwise under cooling with a water bath. A white precipitate formed and 1 mL dioxane with 0.5 mL 10% Na_2CO_3 solution was added. The mixture became clear with some white agglomerates. The reaction mixture showed a pH of 8 and was stirred for 3 h at ambient temperature where it finally became turbid. Afterwards it was acidified with a 1 M HCl to a pH 2-3. The remaining solid was vacuum filtrated, washed with dioxane and dried in vacuum leading to a white solid in a quantitative yield. The ^{1}H-NMR in D_2O showed the product.

^{1}**H-NMR** (400 MHz, D_2O): δ = 8.18 – 8.05 (m, 4H), 7.94 (t, J = 6.8 Hz, 2H), 4.35 (s, 1H), 4.30 (d, J = 4.6 Hz, 2H), 3.66 (s, 1H).

2.5.2 *Buffer preparation*

Buffer	Preparation
Borax buffer (50 mM, pH 8.2)	Borax $Na_2B_4O_7x10H_2O$ (953.4 mg, 2.5 mmol) was dissolved in 45 mL ddH_2O. The pH was adjusted to 8.2 with HCl (1 M) and NaOH (1 M), respectively.
PBS buffer (118 mM, pH 7.4)	$Na_2HPO_4x12H_2O$ (179 mg, 0.5 mmol) and KH_2PO_4 (12.25 mg, 0.09 mmol) were dissolved in 45 mL ddH_2O. The pH was adjusted to 7.4 with HCl (1 M) and NaOH (1 M), respectively.
HEPES buffer (50 mM, pH 7.5)	HEPES (596 mg, 2.5 mmol) was dissolved in 45 mL ddH_2O. The pH was adjusted to 7.5 with HCl (1 M) and NaOH (1 M), respectively.

2.5.3 *Libary preparation*

Library	Preparation
Atmospheric oxygen oxidized libary (2 mM)	The monomer featuring the peptide chain -GLKFK (2.96 mg, 0.003 mmol) was dissolved in 1.5 mL buffer and stirred under atmospheric oxygen with 1200 rpm. The hexamer formation was monitored by ultrahigh pressure liquid chromatography (UPLC) after 7 days.
Perborate pre-oxidized oxidized libary (2 mM)	The monomer featuring the peptide chain -GLKFK (2.96 mg, 0.003 mmol) was dissolved in 493.75 µL buffer including 6.25 µL $NaBO_3x4H_2O$ (40 mM) for a 50% pre-oxidation and stirred under atmospheric oxygen with 1200 rpm. The hexamer formation was monitored by UPLC after 7 days.

2.5.4 *Analysis*

TEM measurements

Samples were diluted to approximately 0.80 mM using doubly distilled water. A small drop (5 µL) of the sample was deposed on a 400 mesh carbon-coated copper grid (Agar Scientific) and blotted on filter paper after 30 s. The sample was stained twice using 4 µL of 2% uranyl acetate solution. The grids were imaged in a Philips CM12 electron microscope operating at 120 kV using a slow scan CCD camera.[8]

cryo-TEM measurements

A 10 µL drop of the sample was placed on a Quantifoil 3.5/1 holey carbon coated grid. Blotting and vitrification in ethane was done in a Vitrobot (FEI, Eindhoven, the Netherlands). The grids were observed in a Tecnai T20 cryo-electron microscope operating at 200 keV with a Gatan model 626 cryo-stage. Images were recorded under low-dose conditions with a slow-scan CCD camera.[11]

UV measurements

A stock solution of the substrate was prepared in the reaction medium. The concentration of the hexamer libary was 2 mM in 50 mM borate buffer pH 8.2. The substrate stock solution was diluted with the reaction medium in a UV quartz glass cuvette and equilibrated in the UV meter JASCO-II for 20-30 min. Afterwards the self-replicator was added to the substrate. It was mixed by shaking the cuvette and a time course measurement was performed by using the detection wavelength of 308 nm.

^{1}*H-NMR*

^{1}H-NMR spectra were recorded on a 300 MHz spectrometer. The spectra were referenced to the used solvent.

3

DEPROTECTION OF A ORGANOCATALYSTS BY A SYNTHETIC SELF-REPLICATOR

The implementation of a reaction cascade that involves the self-replicator starting the deprotection of a Smoc-protected organocatalyst capable of catalyzing the Aldol or Knoevenagel reaction, leading to products featuring a surfactant structure, could be another approach of achieving compartmentalization. Furthermore, a better knowledge about the deprotection rate - substrate hydrophobicity correlation will be gained by expanding the substrate scope through a reaction cascade.

3.1 IMPLEMENTATION OF A CASCADE REACTION

In nature, biochemical reaction cascades which involve a series of chemical reactions such as signaling cascades causing cell responses are very common and essential for keeping the biochemical machinery alive.[36] This was taken as a model in order to achieve compartmentalization induced by the self-replicator. A reaction cascade involving the deprotection of a Smoc-protected organocatalyst, with the following catalysis of a reaction by the released organocatalyst leading to a reaction product that features a surfactant structure, was introduced.

Various aldol reactions catalyzed by organocatalysts such as the aminobase pyrrolidine or the amino acid L-proline in aqueous media have been reported in literature,[34,43,44] among others the aldol reaction between p-nitrobenzaldehyde and aliphatic ketones in PBS buffer.[45] The synthetic self-replicator emerges faster in buffered aqueous media than in just water and previous works in the *Otto* group have shown that the replicator emerges in PBS buffer as well. Hence, aldol reactions that can be catalyzed by pyrrolidine in PBS buffer pH 7.5 were taken for the approach described in Figure 19.

3.1.1 *Selection of Aldol Reactions for the Proof of Concept*

The reaction between p-nitrobenzaldehyde and cyclohexanone in PBS buffer pH 7.5 was used according to *Córdova et al.*[45] as a first starting point for the proof of concept. The ^{1}H-NMR in Figure 21 (a) shows that the reaction works under pyrrolidine catalysis but not in the negative sample with just the reactants in PBS

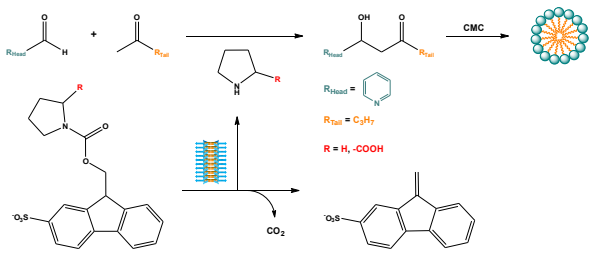

Figure 19: The reaction cascade approach. By the Smoc-protection of the nitrogen of an organocatalyst, in this current example pyrrolidine (R=H) and L-proline (R=−COOH), the catalyst is not able to catalyze for instance an aldol reaction. The organocatalyst is trapped and only capable of catalyzing the given reaction until the self-replicator deprotects it. The released organocatalyst then catalyzes the aldol reaction which ideally leads to a product featuring a surfactant structure resulting in compartmentalization of the aldol product as shown in the scheme.

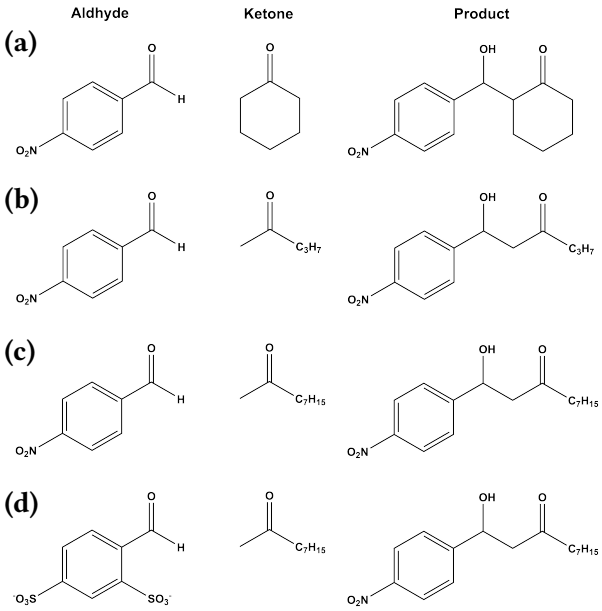

Figure 20: Starting materials and products of pyrrolidine catalyzed aldol reactions for the proof of principle. In 118 mM PBS buffer pH 7.5 **(a)** p-nitrobenzaldehyde and cyclohexanone yielding 2-(hydroxy(4-nitrophenyl)methyl)cyclohexan-1-one **(b)** p-nitrobenzaldehyde and 2-pentanone yielding 1-hydroxy-1-(4-nitrophenyl)hexan-3-one **(c)** p-nitrobenzaldehyde and 2-nonanone yielding 1-hydroxy-1-(4-nitrophenyl)decan-3-one and **(d)** 4-formylbenzene-1,3-disulfonate and 2-nonanone yielding 1-hydroxy-1-(4-nitrophenyl)decan-3-one were used according to the conditions described in literature.[45] The aldol reactions between the starting materials in **(a)** - **(c)** do not lead to products that feature a surfactant structure while the reaction **(d)** yields a negatively charged surfactant as product.

buffer. In order to achieve products with surfactant-like structures the ketones were expanded in this thesis to longer alkyl chains (Figure 20 (b)-(c)). The ^{1}H-NMRs in Figure 21 show that the expanded substrate scope can be catalyzed by pyrrolidine but not in the negative sample. For finally achieving a surfactant structure in the

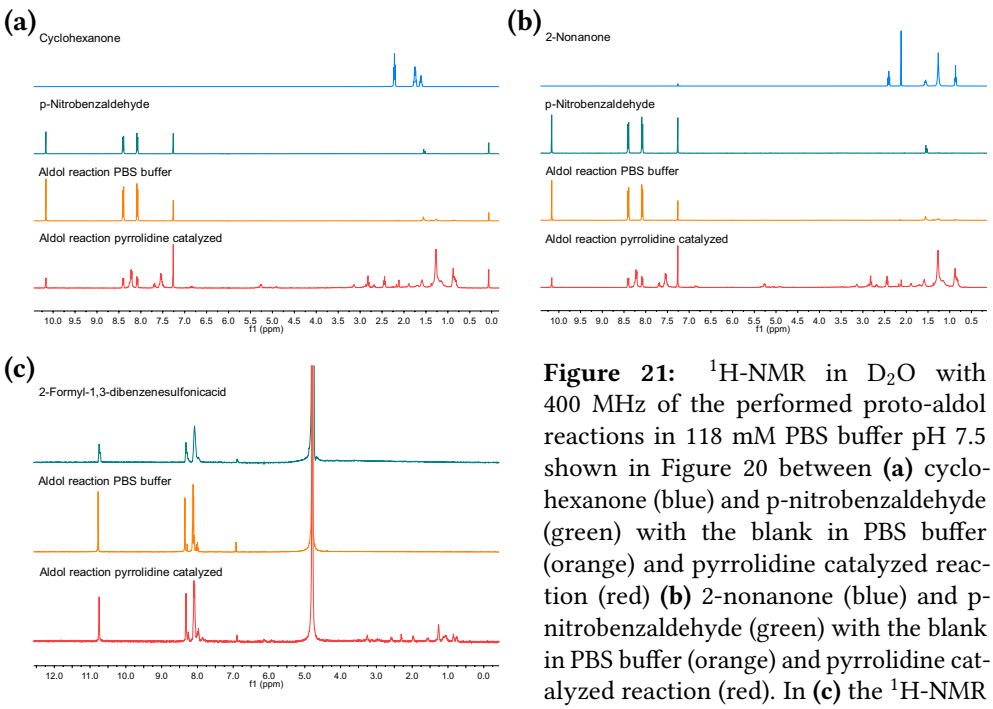

Figure 21: ^{1}H-NMR in D_2O with 400 MHz of the performed proto-aldol reactions in 118 mM PBS buffer pH 7.5 shown in Figure 20 between **(a)** cyclohexanone (blue) and p-nitrobenzaldehyde (green) with the blank in PBS buffer (orange) and pyrrolidine catalyzed reaction (red) **(b)** 2-nonanone (blue) and p-nitrobenzaldehyde (green) with the blank in PBS buffer (orange) and pyrrolidine catalyzed reaction (red). In **(c)** the ^{1}H-NMR in D_2O between 4-formylbenzene-1,3-disulfonate (green) and 2-pentanone (not shown) with the blank in PBS buffer (orange) and pyrrolidine catalyzed reaction (red) is shown. The ketones are not visible in the spectra of the crude reactions due to evaporation on the rotary evaporator during sample preparation.

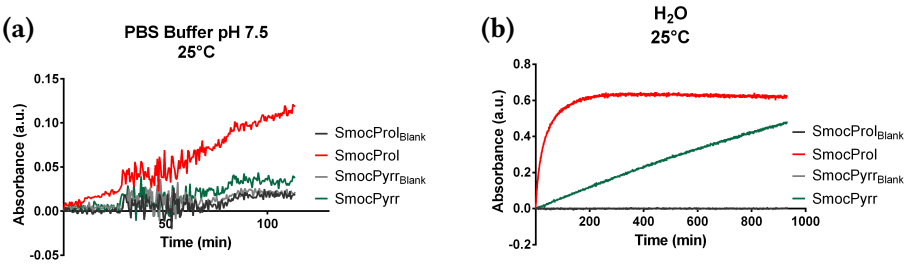

	PBS	H_2O
	Catalytic rate $*10^{-5}$ [Abs/min]	**Catalytic rate** $*10^{-5}$ [Abs/min]
$Blank_{Prol}$	-10 ± 20	60 ± 20
Prol	220 ± 40	3290 ± 20
$Blank_{Pyr}$	96 ± 22	-30 ± 20
Pyr	100 ± 20	850 ± 10

Figure 22: Proto kinetic UV measurements of the Smoc-L-proline (SmocProl) and Smoc-pyrrolidine (SmocPyr) deprotection by the self-replicator in **(a)** 50 mM PBS buffer pH 7.5 and **(b)** water. The measurements were performed without stirring at 25°C **(a)**, as well as 40°C **(b)**, using 308 nm as the detection wavelength for SDBF. Each blank was the Smoc protected organocatalyst in the corresponding reaction medium. The catalytic rates ($*10^{-5}$ Abs/min) are given in the table below the graphs.

aldol product, the proto-aldehyde was changed to 4-formyl-1,3-dibenzenesulfonic acid which bears two negatively charged sulfonate groups. The ^{1}H-NMR in Figure 20 (d) shows that the reaction seems to work under pyrrolidine catalysis but not in the negative sample. Hence, it is possible to achieve surfactant structures through the aldol reaction in PBS buffer.

The Smoc-protected organocatalysts pyrrolidine and L-proline were synthesized since literature reports aldol reactions that can be catalyzed by amino acids like L-proline as well.[43–45] UV measurements of their deprotection by the self-replicator

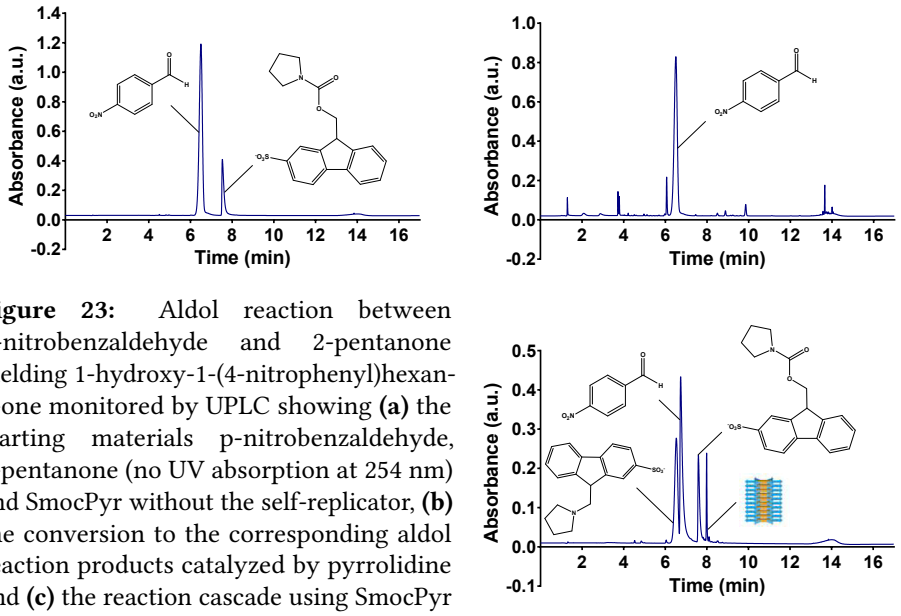

Figure 23: Aldol reaction between p-nitrobenzaldehyde and 2-pentanone yielding 1-hydroxy-1-(4-nitrophenyl)hexan-3-one monitored by UPLC showing **(a)** the starting materials p-nitrobenzaldehyde, 2-pentanone (no UV absorption at 254 nm) and SmocPyr without the self-replicator, **(b)** the conversion to the corresponding aldol reaction products catalyzed by pyrrolidine and **(c)** the reaction cascade using SmocPyr as the trapped catalyst. In UPLC **(c)** the first peak after 6 min is suspected to be the addition product between pyrrolidine and SDBF trapping the organicatalyst again and hence no conversion to the aldol reaction products can be observed.

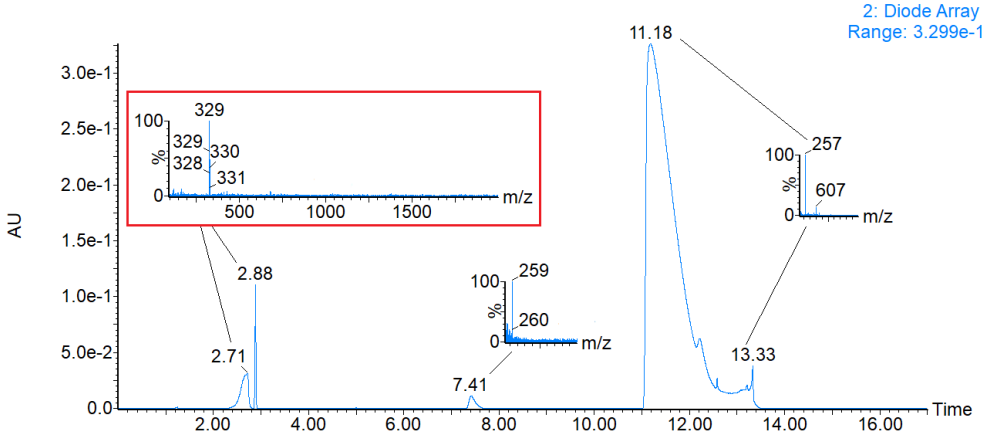

Figure 24: UPLC/ESI-MS of SmocPyr deprotected by pyrrolidine in order to confirm the possible addition product of Figure 25 **(a)** with the exact mass of 328,10 g/mol. The peaks at 2.72 min and 2.88 min show the mass of 328 g/mol which confirms that pyrrolidine is trapped by SDBF after it was deprotected, hence is not able to catalyze a reaction anymore.

in PBS buffer (Figure 22, (a)) were performed. Interestingly, in PBS buffer pH 7.5 the self-replicator cannot deprotect SmocPyr at all and SmocProl just slowly. Figure 22 (b) shows that the replicator is able to deprotect both substrates very efficiently thus water was chosen as the reaction medium for all further experiments.

The proto-reaction between p-nitrobenzaldehyde and 2-pentanone is catalyzed by pyrrolidine not only in PBS buffer but in water as well. Hence, the reaction cascade of the deprotection of SmocPyr by the self-replicator, with the following aldol reaction catalyzed by the released pyrrolidine, was tested in water and monitored by UPLC. Figure 23 shows the chromatograms of all measured samples including the reference (a), which shows that the self-replicator is not destroyed by the starting materials. Chromatogram (b) shows the aldol reaction catalyzed by pyrrolidine but when compared to chromatogram (c) where the reaction cascade was tested, it seems that only the deprotection of SmocPyr but no aldol reaction happens. It is suspected that the addition of the released pyrrolidine to the double bond of SDBF happens, which traps the released organocatalyst again hindering it from catalyzing the aldol reaction. In order to confirm this assumption a mass spectrum in negative mode was taken. The mass of 328 g/mol found in the mass spectrum in Figure 24 confirms that the addition of pyrrolidine to SDBF happens, which prohibits the aminobase from catalyzing the aldol reaction. Hence, in order to prevent that the organocatalyst is trapped by SDBF, a scavenger needs to be found that forms the addition product rather than pyrrolidine.

3.1.2 *Screening for SDBF Scavengers*

For an efficient scavenging of SDBF, compounds that are more nucleophilic than pyrrolidine are needed (Figure 25). Test reactions of pyrrolidine deprotecting SmocPyr with the scavenger as additive were carried out and analyzed via ultrahigh pressure liquid chromatography couled to mass spectrometry (UPLC-MS) in negative mode shown in Figure 26.

As a first starting point the secundary amine dibutylamine was tested, due to the benefit that if it competes against pyrrolidine a double tailed surfactant is formed

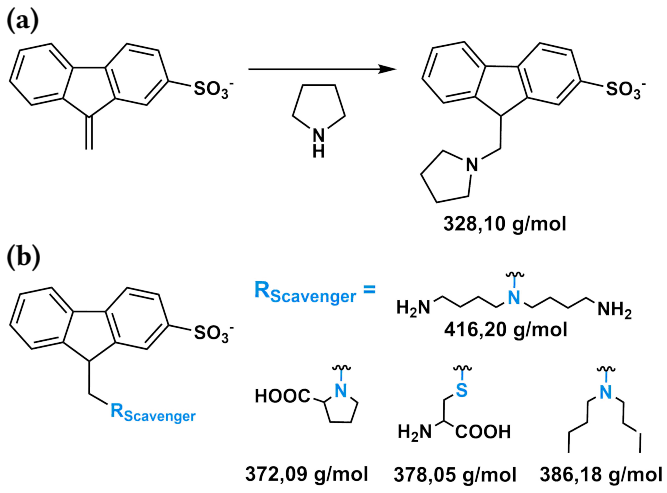

Figure 25: Possible additions of certain nucleophiles to the SDBF double bond. Scheme **(a)** shows the addition of pyrrolidine to the double bond trappring the organocatalyst after it was released through the deprotection of SmocPyr by the self-replicator. Scheme **(b)** shows the addition of possible scavengers to the double bond of SDBF. Compounds featuring a secundary nitrogen (spermidine, ditbutylamine, L-proline) as nucelophile or thiol (L-cysteine) as an even better nucleophile were tested. Since L-proline could serve as an organocatalyst it was also tested if it forms the addition product to SDBF as well.

through the addition of dibutylamine to SDBF, which would lead to even more compartmentalization. However, Figure 26 (a) shows that dibutylamine does not work as a scavenger in presence of pyrrolidine, since only the masses of pyrrolidine and water addition products to SDBF could be found. Also spermidine, which is a triamine featuring one primary amine and two secundary ones, did not work as a scavenger in presence of pyrrolidine. L-proline was tested as well for two reasons: on one hand to exclude that the amino acid becomes trapped through the formation of the addition product since it could also be used as a catalyst for the aldol reaction. On the other hand to check if L-proline could work as a scavenger. However, Figure 26 (c) only shows the masses of the pyrrolidine and water addition products.

Since the amines did not work as scavengers in presence of pyrrolidine, L-cysteine, which features a thiol group that is more nucleophilic compared to nitrogen, was tested. Figure 26 (d) shows that L-cysteine is able to scavenge SDBF in a very efficient way through the addition of the thiol. Another interesting information included in the mass spectrum, is the mass of cystine, which is the oxidation product of two cysteine molecules. SDBF enhances the disulfide oxidation hence it is not surprising that the disulfide cystin is formed in this reaction as well. Since L-cysteine is able to efficiently trap SDBF in presence of pyrrolidine it was used as a scavenger for the further experiments.

3.1.3 *Proof of Concept with the Aid of a Scavenger*

Literature reported aldol reactions between pyridinecarbaldehydes and ketones catalyzed by pyrrolidine and L-proline respectively in water. Hence, the protoaldehyde was changed to pyridine-2-carbaldehyde since the transition from the pyridine to a charged pyridinium head group for having a surfactant structure can be easily achieved by methylation of the nitrogen. Furthermore, pyridine-2-carbaldehyde is miscible with water which facilitates the handling of the reactions in aqueous systems.

The cascade reaction of the SmocPyr deprotection with the following aldol reaction catalyzed by the released pyrrolidine was monitored by UPLC (Figure 27) including the reference (b). Chromatogram (d) shows the aldol reaction catalyzed by pyrrolidine with the product peaks at 2-3 minutes. Interestingly, when compared to

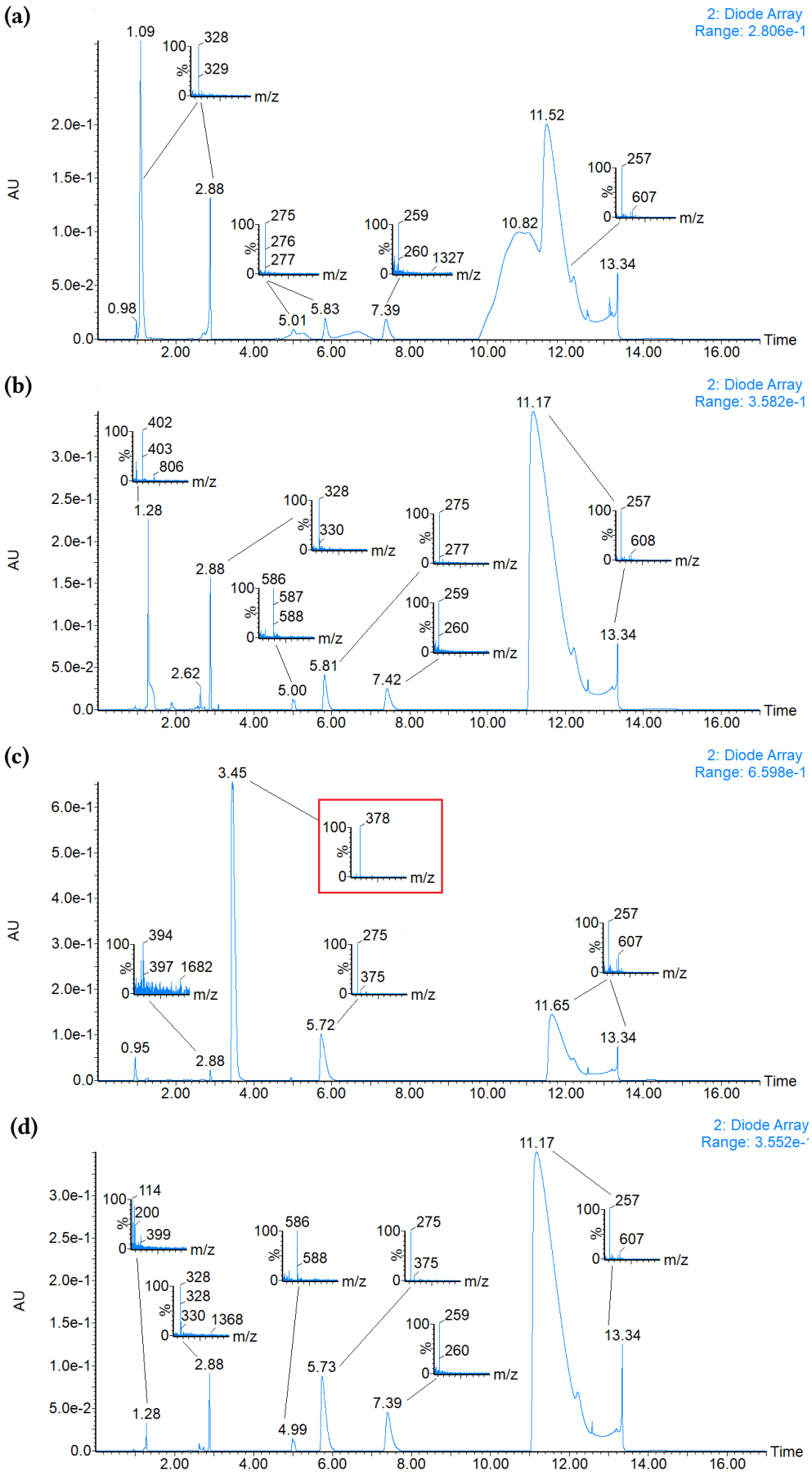

Figure 26: UPLC/ESI-MS in negative mode to investigate a possible scavenging capability of **(a)** dibutylamine **(b)** spermidine **(c)** L-cysteine and **(d)** L-proline.

chromatogram (c) of the reaction cascade a new peak appears at approximately 2 minutes which is different from the reference. A UPLC-MS (Figure 28) was performed for further investigation of this new appeared peak. The mass of 210 g/mol which was found for this peak corresponds to the azathioacetal between the scavenger L-cysteine and pyridine-2-carbaldehyde. L-cysteine, which appeared to be a very efficient scavenger for SDBF, cannot be used in presence of aldehydes since L-cysteine traps the starting material before SDBF is released through the deprotection of the

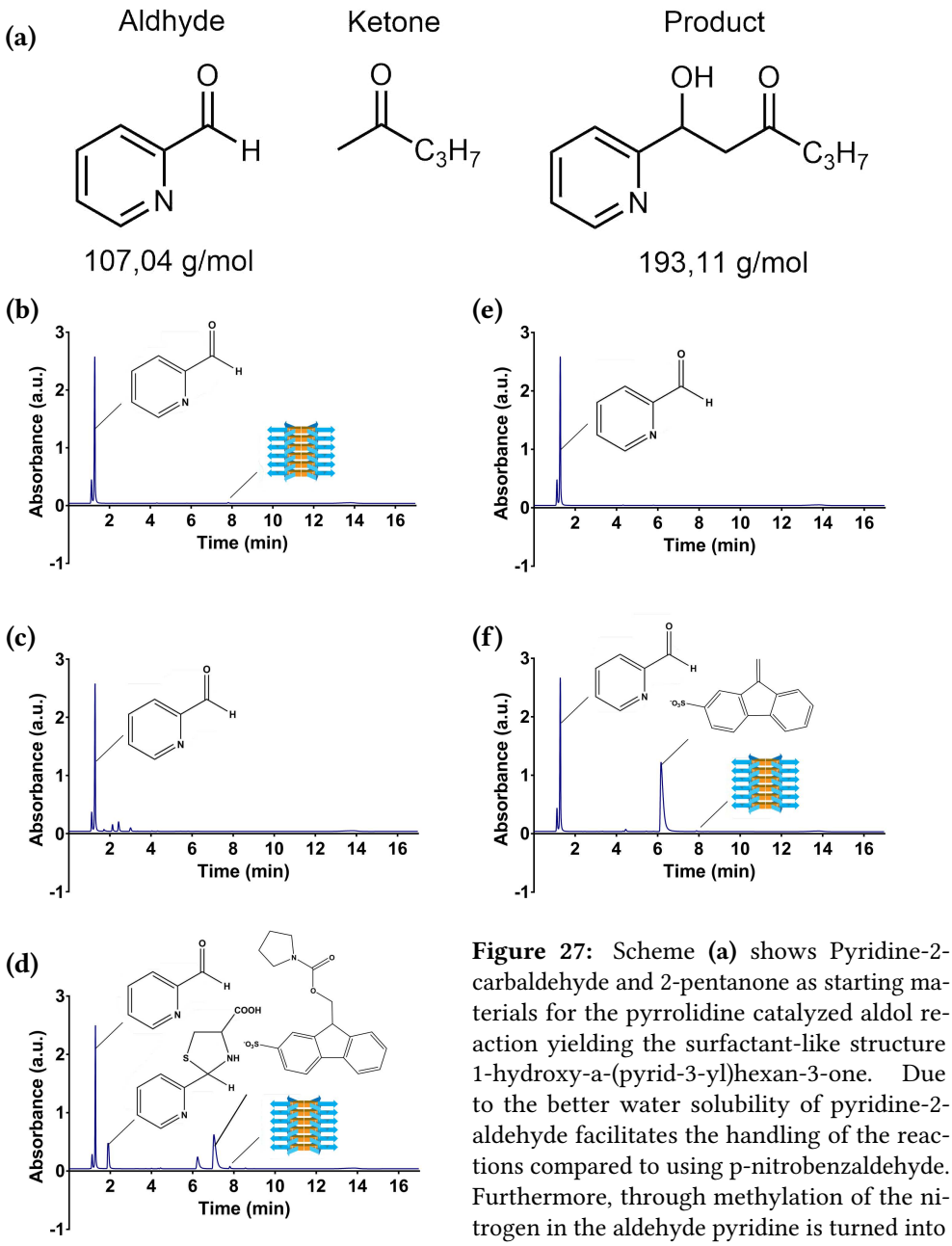

Figure 27: Scheme **(a)** shows Pyridine-2-carbaldehyde and 2-pentanone as starting materials for the pyrrolidine catalyzed aldol reaction yielding the surfactant-like structure 1-hydroxy-a-(pyrid-3-yl)hexan-3-one. Due to the better water solubility of pyridine-2-aldehyde facilitates the handling of the reactions compared to using p-nitrobenzaldehyde. Furthermore, through methylation of the nitrogen in the aldehyde pyridine is turned into a pyridinium cation featuring a permanent positively charged nitrogen. The UPLC shows **(b)** the starting materials in presence of the self-replicator **(c)** the pyrrolidine catalyzed aldol reaction with the corresponding products between 2-3 min **(d)** the reaction cascade using SmocPyr where the peak at 2 min is possibly the aza-thioacetal between pyridine-2-carbaldehyde and the scavenger L-cysteine **(e)** L-proline catalyzed aldol reaction showing no conversion **(f)** the reaction cascade using SmocProl showing no aldol product.

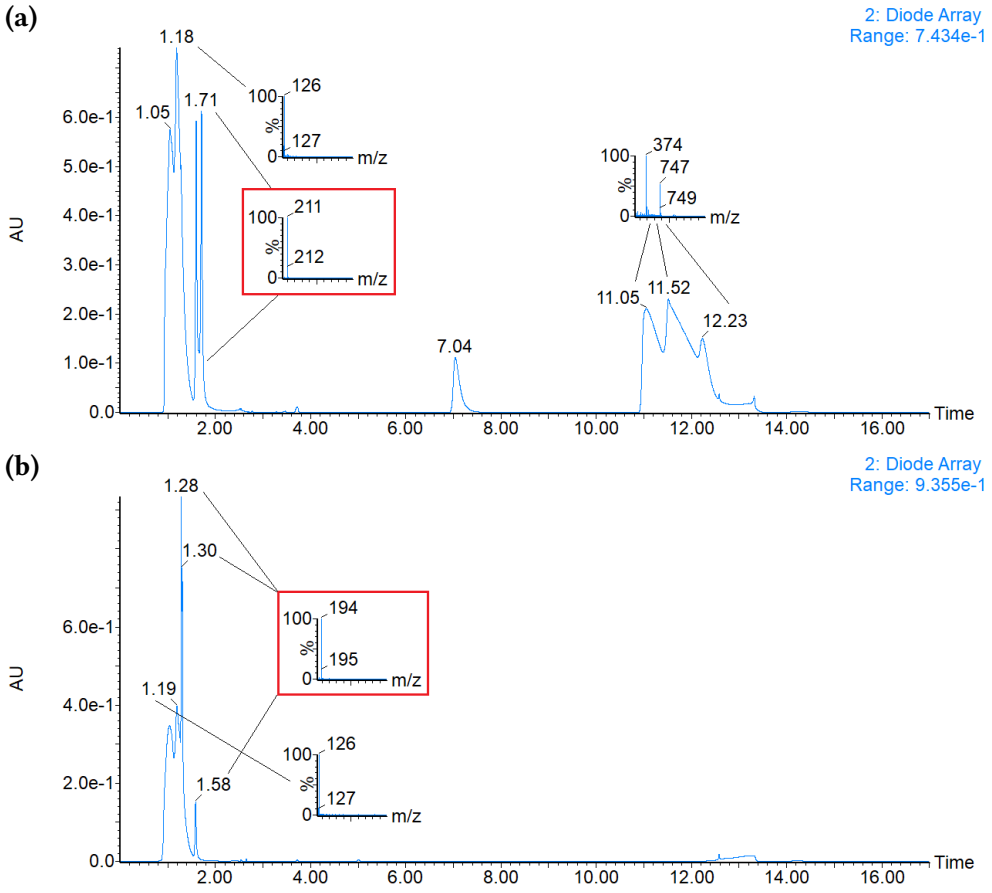

Figure 28: UPLC/ESI-MS of **(a)** the cascade aldol reaction showing the mass of the aza-thioacetal (210 g/mol, 1.71 min) of L-cysteine to pyridine-2-carbaldehyde but not the product 1-hydroxy-a-(pyrid-3-yl)hexan-3-one (196 g/mol) of the aldol reaction with 2-pentanone and **(b)** the pyrrolidine catalyzed aldol reaction showing the mass of the product (193 g/mol).

organocatalyst by the replicator. After being trapped, the aldehyde is not reactive enough to undergo the aldol reaction and hence another scavenger needs to be found. A scavenger, which can be used in presence of aldehydes for a functional reaction cascade by the usage of pyrrolidine as the organocatalyst. However, this was not done in this thesis.

Since literature reports aldol reactions that can be catalyzed by L-proline in water,[43–45] the same reaction cascade as with SmocPyr was performed with SmocProl which does not require a scavenger since L-proline does not form the addition product to SDBF which makes the reaction mixture less complicated. Figure 27 shows the performed UPLC measurements of the reaction cascade including the reference (e). Chromatogram (f) shows that L-proline seems not to be able to catalyze this specific aldol reaction and hence also the reaction cascade does not work.

3.2 DEPROTECTION KINETICS OF SMOC-PROTECTED AMINES

Previous works in the *Otto* group as well as the results from Chapter 2 in this thesis have shown that the catalytic ability of the self-replicator depends on the substrate. In order to study influences on deprotection kinetics such as temperature and reaction medium in correlation with the substrate hydrophobicity, the compounds SmocProl

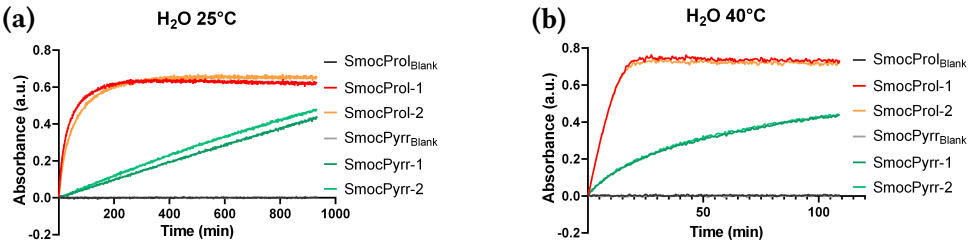

	25°C	40°C
	Catalytic rate $*10^{-5}$ [Abs/min]	**Catalytic rate** $*10^{-5}$ [Abs/min]
Blank_{Prol}	60 ± 20	3 ± 1
Prol-1	3030 ± 30	5540 ± 30
Prol-2	3290 ± 20	5610 ± 30
Mean	**3160** ± 190	**5570** ± 50
Blank_{Pyr}	-30 ± 20	-3 ± 1
Pyr-1	850 ± 10	1500 ± 20
Pyr-2	840 ± 20	1430 ± 30
Mean	**850** ± 10	**1460** ± 50

Figure 29: Kinetic UV measurements of SmocProl and SmocPyr deprotection by the self-replicator in water. The measurements were performed without stirring at 25°C **(a)** as well as 40°C **(b)** using 308 nm as the detection wavelength for SDBF. Each blank was the Smoc protected organocatalyst in water. The catalytic rates ($*10^{-5}$ Abs/min) are given in the table below the graphs.

and SmocPyr are used as substrates since the only structural difference between these two compounds is the carboxylic acid group of L-proline which is ideal to study how an additional functional group in the substrate changes the kinetics.

In water (Figure 29) there is no significant background reaction for the Smoc-protected amines, neither at 25°C nor at 40°C. Since the slope of the SmocPyr blank is negative at both temperatures, which does not make sense in this measurement set up, the background reaction is considered to be 0 Abs/min.

Both substrates can be deprotected by the replicator at 25°C as well as 40°C. However, at both temperatures there is a difference between the substrates concerning their deprotection rate. SmocProl is faster deprotected than SmocPyr. It could be that hydrophobic and electrostatic effects play a role since the amino acid L-proline features a carboxylic acid group while pyrrolidine does not. It is very likely that the carboxylic acid is deprotonated and hence electrostatically more attracted to the positively charged lysine residues of the replicator. This attraction brings the substrate closer to the replicator which could result in a tighter and more favored arrangement between replicator and substrate and thus results in a faster deprotection.

It seems that the catalytic rate also correlates with hydrophibicity, as shown in Chapter 2. Due to the missing carboxylic acid group pyrrolidine is more hydrophobic compared to L-proline, which could cause an adverse interaction with the self-replicator and hence slows down the deprotection rate. Furthermore, the carboxylic acid group shows an electronic withdrawn mesomeric effect (-M) which could cause a higher driving force for the decarboxylation during the deprotection and thus increases the catalytic rate.

The reached plateau at 25°C was 0.7 a.u. for SmocProl and 0.4 a.u. for SmocPyr. A temperature of 40°C did not change the reached plateaus, neither for SmocProl

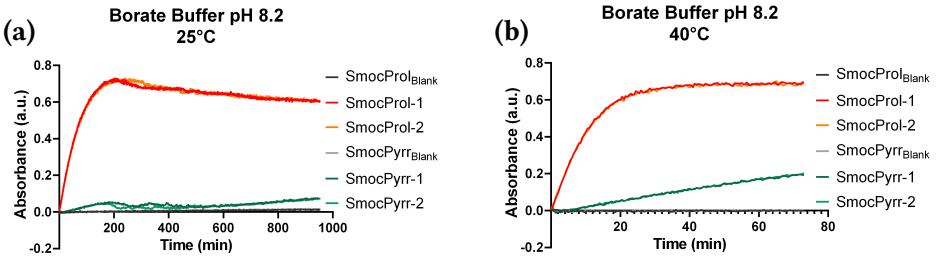

	25°C	40°C
	Catalytic rate $*10^{-5}$ [Abs/min]	**Catalytic rate** $*10^{-5}$ [Abs/min]
Blank$_{Prol}$	-30 ± 40	-50 ± 30
Prol-1	940 ± 30	2260 ± 70
Prol-2	900 ± 40	2350 ± 50
Mean	**920** ± 30	**2310** ± 60
Blank$_{Pyr}$	-40 ± 40	-70 ± 30
Pyr-1	160 ± 40	440 ± 40
Pyr-2	80 ± 40	370 ± 20
Mean	**120** ± 60	**410** ± 50

Figure 30: Kinetic UV measurements of SmocProl and SmocPyr deprotection by the self-replicator in 50 mM borate buffer pH 8.2. The measurements were performed without stirring at 25°C **(a)** as well as 40°C **(b)** using 308 nm as the detection wavelength for SDBF. Each blank was the Smoc protected organocatalyst in buffer. The catalytic rates ($*10^{-5}$ Abs/min) are given in the table below the graphs.

nor SmocPyr. The difference in a.u. between the substrates is either caused by an incomplete deprotection of SmocPyr or side reactions. Since L-proline does not in terms of an addition to the double bond of SDBF, while pyrrolidine reacts very efficiently, it is very likely that the released SDBF during the SmocPyr deprotection could not be detected due to a shift of the absorption maximum by the addition of pyrrolidine to SDBF. A temperature of 40°C increases the catalytic rate by a factor of ~ 1.7 for SmocProl as well as for SmocPyr. Hence the temperature seems to have a comparable impact for both substrates.

In 50 mM borate buffer pH 8.2 (Figure 30) there is no significant background reaction for the Smoc-protected amines, neither at 25°C nor at 40°C. Since the slope of all blanks are negative at both temperatures, which does not make sense in this measurement set up, the background reaction is considered to be 0 Abs/min.

In borate buffer there is a remarkable difference between the two substrates. While at 25°C SmocProl is deprotected quite fast by the replicator, the deprotection rate for SmocPyr is almost 8 times slower and it seems that the latter is not fully deprotected since it is close to the blank. However, a temperature of 40°C increases the catalytic rate for SmocProl by a factor of 2.5 and for SmocPyr the rate is increased by a factor of ~ 3.3 times. This could be due to a higher kinetic energy that comes with an increased temperature. It is possible that in borate buffer a higher kinetic energy is needed in order to start the deprotection. This means 25°C are not enough for SmocPyr, which already shows a smaller attraction to the replicator anyway due to the lack of the carboxylic acid group. Hence, temperature seems to have a higher impact on the deprotection rate of SmocPyr than SmocProl.

Furthermore, the reached plateau for SmocProl (0.7 a.u.) is almost equal at both temperatures, while for SmocPyr the plateau is increased from 0.03 a.u. to 0.2 a.u.

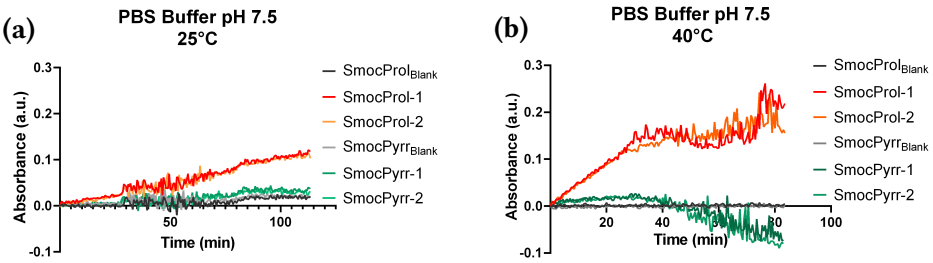

	25°C	40°C
	Catalytic rate $*10^{-5}$ [Abs/min]	**Catalytic rate** $*10^{-5}$ [Abs/min]
Blank$_{Prol}$	-6 ± 20	40 ± 20
Prol-1	220 ± 40	530 ± 30
Prol-2	150 ± 20	530 ± 40
Mean	**180** ± 50	**530** ± 2
Blank$_{Pyr}$	100 ± 20	-100 ± 30
Pyr-1	100 ± 20	270 ± 40
Pyr-2	50 ± 20	210 ± 30
Mean	**80** ± 30	**240** ± 40

Figure 31: Kinetic UV measurements of SmocProl and SmocPyr deprotection by the self-replicator in 50 mM PBS buffer pH 7.5. The measurements were performed without stirring at 25°C **(a)** as well as 40°C **(b)** using 308 nm as the detection wavelength for SDBF. Each blank was the Smoc protected organocatalyst in buffer. The catalytic rates ($*10^{-5}$ Abs/min) are given in the table below the graphs.

This could be caused by the fact that for the deprotection of SmocPyr a higher kinetic energy is needed, which is achieved by an increased temperature and hence results in a release of more SDBF that can be detected at 40°C leading to a higher plateau.

In 118 mM PBS buffer pH 7.5 (Figure 30) there is no significant background reaction for the Smoc-protected amines, neither at 25°C nor at 40°C. Since the slope of SmocProl at 25°C and SmocPyr at 40°C is negative, the background reaction is considered to be 0 Abs/min.

At 25°C SmocProl is just slowly deprotected and SmocPyr shows a catalytic rate that is in the range of the blank. A temperature of 40°C increases the deprotection rate of both substrates by factor 3. Hence, temperature seems to have the same impact for both substrates. Interestingly, at both temperatures there is a lot of noise noticeable. A possible explanation for this could be the salts NaCl and KCl present in the PBS buffer, which seems to cause aggregation of the replicator, since in all samples showed turbidity, including the reference.

In 50 mM HEPES buffer pH 7.5 (Figure 30) there is no significant background reaction for the Smoc-protected amines, neither at 25°C nor at 40°C. Since the slope of SmocProl at both temperatures is negative, the background reaction is considered to be 0 Abs/min.

At both temperatures SmocProl showed a remarkable high deprotection rate compared to SmocPyr, which showed just ~ 1/10 and ~ 1/5 of the SmocProl deprotection rate, respectively. At 25°C a plateau of 0.7 a.u. is reached for SmocProl and 0.3 a.u. for SmocPyr. While at 40°C for SmocProl the reached plateau of 0.8 a.u. does not significantly differ from 25°C, the reached plateau for SmocPyr is doubled to 0.6 a.u. Furthermore, for SmocProl the catalytic rate at 40°C is increased by a factor of ~ 1.7 while for SmocPyr it is increased by a factor of 2.8. It seems that temperature has

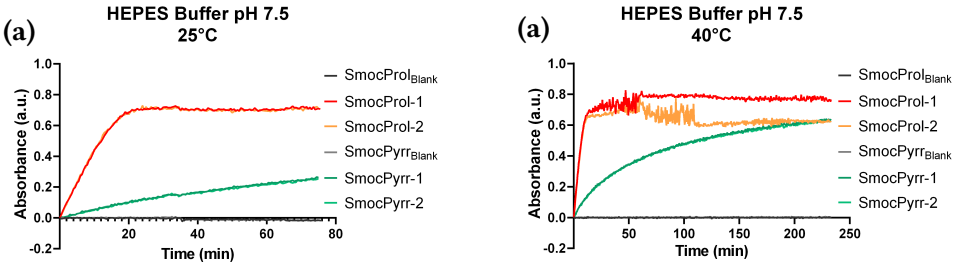

	25°C	40°C
	Catalytic rate $*10^{-5}$ [Abs/min]	**Catalytic rate** $*10^{-5}$ [Abs/min]
$Blank_{Prol}$	-10 ± 2	-30 ± 20
Prol-1	4560 ± 50	7730 ± 60
Prol-2	4650 ± 30	7430 ± 60
Mean	**4610** ± 70	**7580** ± 210
$Blank_{Pyr}$	20 ± 30	30 ± 20
Pyr-1	520 ± 30	1400 ± 30
Pyr-2	470 ± 30	1380 ± 30
Mean	**490** ± 30	**1390** ± 20

Figure 32: Kinetic UV measurements of SmocProl and SmocPyr deprotection by the self-replicator in 50 mM HEPES buffer pH 7.5. The measurements were performed without stirring at 25°C **(a)** as well as 40°C **(b)** using 308 nm as the detection wavelength for SDBF. Each blank was the Smoc protected amineorganocatalyst in buffer. The catalytic rates ($*10^{-5}$ Abs/min) are given in the table below the graphs.

a higher impact on the more hydrophobic SmocPyr than on SmocProl. A possible explanation for this is the zwitterionic structure of HEPES at pH 7.5. It could be that additionally to the attraction between the replicator and the carboxylic acid group, the buffer ions stabilize this pre-organization. The stabilization could be due to the zwitterionic properties with the negatively charged sulfonate group in the substrate and the positively charged nitrogen from the piperazine ring. SmocPyr does not feature a carboxylic acid group which could explain why it shows just ~ 1/10 of the catalytic rate of SmocProl at 25°C.

Table 12 shows a summary of all catalytic rates mentioned in this section for a better overview. Previous works in the *Otto* group show that the standard substrate SmocGly is faster deprotected than FmocGly. It can be assumed that the negatively charged sulfonate moiety of the Smoc protecting group facilitates the deprotection. This could be due to a stronger electrostatic interaction between the positively charged lysine residues of the self-replicator and the negatively charged sulfonate group in the Smoc group. Hence, the interaction with the negative sulfonate group

	H_2O	Borate	PBS	HEPES
	Catalytic rate $*10^{-5}$ [Abs/min]	**Catalytic rate** $*10^{-5}$ [Abs/min]	**Catalytic rate** $*10^{-5}$ [Abs/min]	**Catalytic rate** $*10^{-5}$ [Abs/min]
$Prol_{25C}$	3100 ± 200	920 ± 30	180 ± 50	4610 ± 70
$Prol_{40C}$	5570 ± 60	2300 ± 60	533 ± 2	7600 ± 200
$Pyrr_{25C}$	847 ± 9	120 ± 60	80 ± 30	490 ± 30
$Pyrr_{40C}$	1460 ± 50	400 ± 60	240 ± 40	1390 ± 20

Table 12: Summary of the mean values of the deprotection rates of SmocProl and SmocPyr received by the kinetic UV measurements at 25°C and 40°C in different reaction media.

could cause some sort of pre-organization between the substrate and catalyst. This brings the deprotonated lysines of the replicator closer to the crucial proton of the Smoc protecting group and hence facilitates the accessibility causing a faster deprotection. The Fmoc group does not feature a negative charge, resulting in a weaker attraction between self-replicator and substrate.

In general, SmocProl is faster deprotected by the self-replicator than SmocPyr. The reason for this trend could be a more favored interaction between SmocProl due to the carboxylic acid group which is not present in SmocPyr. It could be that through electrostatic interactions between the deprotonated negatively charged carboxylic acid of L-proline in combination with the negative sulfonate moiety of the Smoc protecting group and the positively charged lysine residues of the self-replicator a stronger pre-organization of substrate and catalyst is enabled so that the crucial proton of the Smoc protecting group is brought closer to the deprotonated lysine residues of the replicator compared SmocPyr which does not feature the additional carboxylic acid group.

Another possible explanation for the increased deprotection rate of SmocProl compared to SmocPyr could be the enhanced driving force for the decarboxylation due to the electron withdrawing effect of the carboxylic acid group.

Furthermore, the carboxylic acid makes L-proline more polar compared to pyrrolidine. A more polar substrate could show a more favored interaction with the polar self-replicator compared to the less polar pyrrolidine moiety. As shown in Chapter 2 the deprotection rate could also correlate with the hydrophobicity of the substrate. The more hydrophobic the substrate is, the less is the interaction with the replicator and hence the slower is the deprotection.

Another interesting aspect is that the reaction medium has a remarkable influence on the catalytic rate. For SmocProl the highest catalytic rates at both temperatures were achieved in 50 mM HEPES buffer pH 7.5 while for SmocPyr the highest catalytic rates were achieved in water. In general the order from highest to lowest catalytic rate at both temperatures for SmocProl is HEPES 7.5 > H_2O > borate 8.2 > PBS 7.5 and for SmocPyr H_2O > HEPES 7.5 > borate 8.2 > PBS 7.5 but at 40°C the catalytic rates in water and HEPES are very similar.

The order from highest to lowest catalytic rate at both temperatures for SmocPyr is H_2O > HEPES 7.5 > borate 8.2 > PBS 7.5 where at 40°C the catalytic rates in water and HEPES are very similar. Hence, the reaction media has almost the same impact on both substrates.

The substrate SmocPyr shows the same order of reaction media as the Smoc-amine substrates in Chapter 2 where SmocProl shows a slightly different order with having the fastest deprotection rate in HEPES buffer and not water. As discussed in Chapter 2, a possible explanation for the order of reaction media could be that the buffered solutions charged molecules. The amount of charges depends on the dissociation grade, which is linked to the pK_a of the buffer molecules. This could cause an inhibition effect by blocking the positively charged replicator and negatively charged sulfonate group of the substrate by electrostatic attractions to the buffer salts. This is in agreement with the order of reaction media for the substrates Smoc-hexylamine, Smoc-octylamine and SmocPyr but not exactly for SmocProl, since it shows the highest catalytic rates in HEPES buffer and not water. A possible explanation for the different order of water and HEPES, especially at 25°C, could be an interaction between the deprotonated negatively charged carboxylic acid group of L-proline with the zwitterionic buffer species. This facilitates the deprotection through the stabilization of a pre-organization between SmocProl and the replicator. However,

pyrrolidine does not feature this additional negative charge. It could be even possible that the zwitterionic buffer species rather slows down the catalytic rate through blocking the catalytic sides of the replicator than facilitating it through stabilization.

Temperature seems to have almost the same impact on the deprotection rate of both substrates. As shown in Chapter 2 the temperature has more impact on the deprotection rate of Smoc-octylamine, probably since more aggregates are broken compared to Smoc-hexylamine. Compared to the substrates used in this chapter, in borate and HEPES buffer there is a slight difference of temperature impact on the SmocPyr deprotection rate compared to SmocProl. This could be linked to a possible inhibition of the replicator by buffer ions rather than a buffer ion stabilized pre-organization, which is possibly present during the SmocProl deprotection. After all, the substrates in this chapter do not show surfactant like structures hence the substrates do not aggregate and the assumption that temperature should have a similar effect on the catalytic rate of both substrates is confirmed.

All in all, both substrate pairs Smoc-hexylamine/Smoc-octylamine and SmocProl/SmocPyr showed that the deprotection rate clearly depends on the substrate's hydrophobicity. Wherever a slower deprotection rate of a more hydrophobic substrate is caused, the accessibility of the crucial proton in position 9 of the Smoc-group is hindered. This happens either by aggregation in case of Smoc-protected primary amines, or by a possibly less favored pre-organization due to a lack of additional charges in case of SmocPyr. The overall conclusion of the tested substrate pairs in this thesis is the more hydrophobic a substrate is, the more the accessibility to of the proton in position 9 is hindered, hence the slower is the deprotection by the self-replicator.

3.3 CONTRIBUTIONS

The research question about a reaction cascade that should lead to compartmentalization as well as the substrate scope and deprotection kinetics of Smoc-protected amines was proposed by the author. The synthesis of all products, screenings, UV measurements, ^{1}H-NMR spectra and data evaluation as well as the drawn conclusions in this were made by the author. The HEPES buffer (50 mM, pH 7.5) was prepared by Kayleigh van Esterik, BSc and all the mass spectra were carried out by Marcel Eleveld, MSc.

3.4 EXPERIMENTAL

3.4.1 *Synthesis*

Smoc-pyrrolidine:

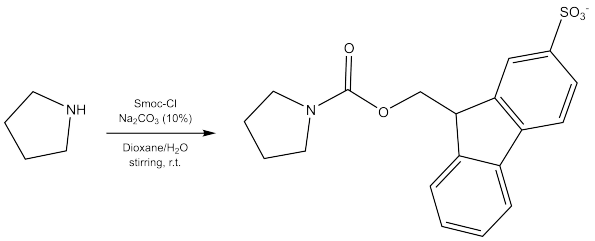

In a 25 mL round botton flask equipped with a magnetic stir bar, Smoc-Cl (563 mg, 1.7 mmol) was dissolved in 3 mL 1,4-dioxane. Then, pyrrolidinde (71 mg, 1 mmol) mixed with 2.1 mL of a 10% aqueous Na_2CO_3 solution was transferred dropwise to the stirred Smoc-Cl solution over a time period of 15 minutes under cooling with a water bath. The reaction was stirred at room temperature and a white precipitate was formed. The reaction was controlled by TLC using a 1:4 mixture of methanol (MeOH):DCM.

After 3 hours of stirring 3 mL ddH_2O were added and the mixture was then acidified to a pH of 2-3 with HCl (1 M) resulting in a yellow solution which was poured as it was on a RP flash column. A H_2O:ACN gradient was used for purification. Afterwards, the solvent was evaporated yielding 100 mg (27% of theory) of a white solid. The ^{1}H-NMR in D_2O showed the pure product.

^{1}**H-NMR** (400 MHz, Deuterium Oxide): δ = 7.92 (s, 1H), 7.79 (q, J = 8.1 Hz, 2H), 7.71 (d, J = 7.5 Hz, 1H), 7.46 (d, J = 7.3 Hz, 1H), 7.32 (dt, J = 22.8, 7.4 Hz, 2H), 4.35 (dd, J = 10.6, 5.8 Hz, 1H), 4.15 (dd, J = 10.6, 6.5 Hz, 1H), 3.99 (t, J = 6.1 Hz, 1H), 3.13 (s, 2H), 2.92 (t, J = 6.3 Hz, 2H), 1.70 (q, J = 7.1, 6.5 Hz, 4H).

Smoc-proline:

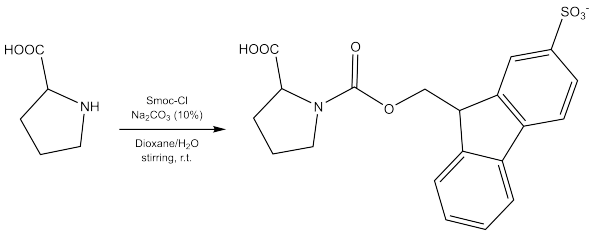

In a 25 mL round botton flask equipped with a magnetic stir bar, Smoc-Cl (306 mg, 0.9 mmol) was dissolved in 1.6 mL 1,4-dioxane. Then, L-proline (101 mg, 0.9 mmol) dissolved in 1.5 mL of a 10% aqueous Na_2CO_3 solution was transferred dropwise to the stirred Smoc-Cl solution under cooling with a water bath. The reaction was stirred at room temperature and a white precipitate was formed. The reaction was controlled by TLC using a 1:4 mixture of MeOH:DCM.

After 3 hours of stirring the mixture was then acidified to a pH of 2-3 with HCl (1 M) resulting in a yellow solution which was poured as it was on a RP flash column. A H_2O:ACN gradient was used for purification. Afterwards, the solvent was evaporated

yielding 73 mg (19% of theory) of a white solid. The ^{1}H-NMR in D_2O showed the pure product.

^{1}**H-NMR** (400 MHz, Deuterium Oxide): δ = 7.70 – 7.60 (m, 1H), 7.55 (d, J = 7.9 Hz, 1H), 7.44 – 7.22 (m, 2H), 7.20 – 6.90 (m, 3H), 4.27 – 3.81 (m, 2H), 3.72 – 3.51 (m, 1H), 3.33 (ddd, J = 33.9, 9.0, 3.8 Hz, 1H), 3.10 – 2.71 (m, 2H), 1.98 – 1.36 (m, 4H).

3.4.2 *Screenings*

Aldol reaction screening

In a 1.5 mL vial, the aldehyde (0.05 mmol) and ketone (0.04 mmol) were mixed with 25 mol-% catalyst. The mixture was filled up to a total volume of 1000 µL with water and buffer, respectively. The reaction was stirred at ambient temperature for 24 h with 1200 rpm and monitored by UPLC and ^{1}H-NMR.

Scavenger screening

In a 1.5 mL vial, Smoc-Cl (0.01 mmol) was mixed with the scavenger (0.01 mol) and an excess of pyrrolidine (1.4 mmol). The mixture was filled up to a total volume of 1000 µL with water and stirred for 24 h with 1200 rpm at ambient temperature. The reaction was monitored by UPLC-MS.

Cascade reaction without a scavenger

In a 1.5 mL vial, the aldehyde (150 µM) and ketone (500 µM) were mixed with Smoc-protected catalyst (150 µM) and a 2 mM stock of the self-replicator (40 µM). The mixture was filled up to a total volume of 1000 µL with water and buffer, respectively. For the reference only the original catalyst without the self-replicator was used. The reaction was stirred at ambient temperature for 24 h with 1200 rpm and monitored by UPLC and ^{1}H-NMR.

Cascade reaction with a scavenger

In a 1.5 mL vial, the aldehyde (150 µM) and ketone (500 µM) were mixed with Smoc-protected catalyst (150 µM), scavenger (150 µM) and a 2 mM stock of the self-replicator (40 µM). The mixture was filled up to a total volume of 1000 µL with water and buffer, respectively. For the reference only the original catalyst without the self-replicator was used. The reaction was stirred at ambient temperature for 24 h with 1200 rpm and monitored by UPLC and ^{1}H-NMR.

3.4.3 *Analysis*

UV measurements

A stock solution of the substrate was prepared in the reaction medium. The concentration of the hexamer libary was 2 mM in 50 mM borate buffer pH 8.2. The substrate stock solution was diluted with the reaction medium in a UV quartz glass cuvette and equilibrated in the UV meter JASCO-II for 20-30 min. Afterwards the self-replicator was added to the substrate. It was mixed by shaking the cuvette and a time course measurement was performed by using the detection wavelength of 308 nm.

4 SYNTHESIS OF SURFACTANTS BY THE SYNTHETIC SELF-REPLICATOR

Compartmentalization formed by surfactants that were synthesized through a reaction catalyzed by the self-replicator would be the ultimate goal of combining the three fundamental parts of life self-replication, metabolism and compartmentalization. The knowledge about the self-replicator being able to catalyze the deprotection of Fmoc- and Smoc-protected compounds enables the exploration to more reaction types that can possibly be catalyzed by the self-replicator, among others the aldol and Knoevenagel reaction. The expansion to new reaction types, which could result in the possibility the replicator being able to catalyze the synthesis of surfactants, would lead to a huge progress concerning the question about the origin of life.

4.1 CATALYSIS OF CARBON-CARBON BOND FORMATION REACTIONS MEDIATED BY A PEPTIDE-BASED SELF-REPLICATOR

In nature, C–C carbon bond formations are crucial for metabolism reactions such as the formation of fructose-1,6-biphosphate out of dihydroxyacetonephosphate and glycerinaldehydephosphate through an aldol reaction. This is just one example out of a variety of metabolism reactions and hence the reactions, that can be catalyzed by the self-replicator, should be expanded in order to come one step closer to understand the question about life.

The proton of the Fmoc-protecting group at position 9 that the self-replicator is capable to deprotonate, shows a pK_a of ~25.[23] Usually, the Fmoc-deprotection is carried out by secondary amino bases like piperidine (pK_a ~11.22), pyrrolidine (pK_a ~11.27) or morpholine (pK_a ~8.36). As it is reported in literature,[35,46–48] the mentioned amines can also serve as organocatalysts under aqueous conditions catalyzing various C–C carbon bond formations such as the aldol reaction or Knoevenagel condensation. The self-replicator is capable of performing the Fmoc- and Smoc-deprotection just like the cyclic amino bases do. Hence, the scope of catalyzed reactions by the self-replicator should be explored to C–C carbon bond formations which could be used for the synthesis of surfactants catalyzed by the self-replicator itself (Figure 33).

4.1.1 *The Self-Replicator and the Knoevenagel Reaction*

Knoevenagel condensations catalyzed by organocatalysts such as the aminobases piperidine, pyrrolidine and morpholine or even amino acids like L-proline in aqueous media have been reported in various publications.[35,46,47]

Figure 34 shows the substrates which were tested in 50 mM borate buffer pH 8.2 for the proof of concept. In order to achieve a surfactant structure in the product, a charged head group and an aliphatic tail must be connected through the Knoevenagel condensation. The initial idea behind the first tested substrates (a) was that a charge has to be present in one of the starting materials, either at the CH active methylene compound or at the aldehyde. In (a) both components bear a negative charge hence if this reaction may be catalyzed by the replicator, the residues in the

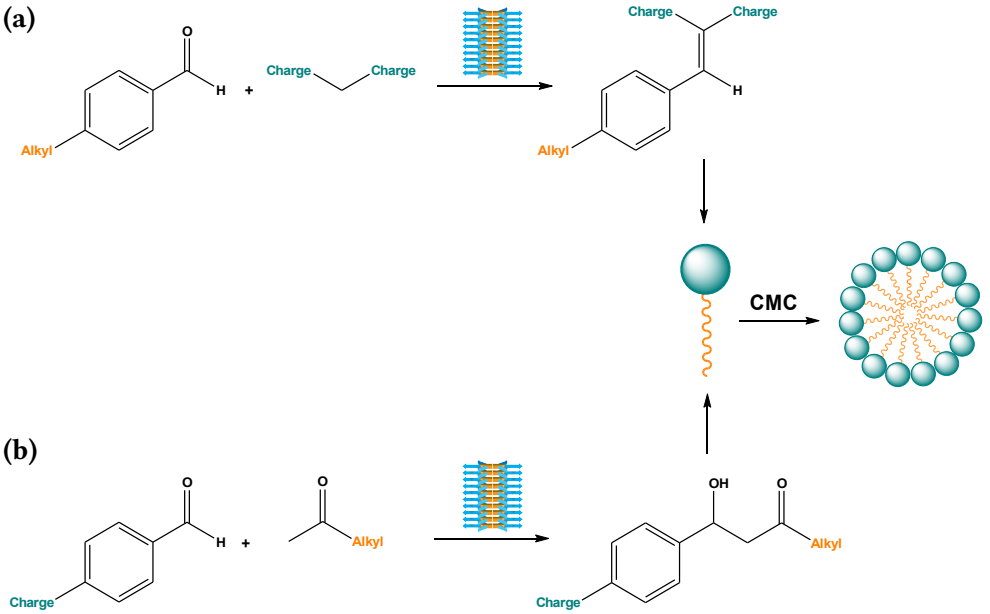

Figure 33: Achieving surfactant structures by connecting a charged with an uncharged moiety through a reaction catalyzed by the self-replicator. Via the Knoevenagel condensation **(a)** a CH-active methylene compound bearing a charge should be deprotonated by the self-replicator resulting in a nucleophilic attack on the aldehyde which features a hydrophopic tail leading to a connection of charged and uncharged part of the final surfactant through a C=C bond. Via the aldol reaction **(b)** a ketone bearing an apolar aliphatic chain should be deprotonated by the self-replicator resulting in a nucleophilic attack on the aldehyde which features a charge leading to a connection of charged and uncharged part of the final surfactant through a C–C bond. Above the critical micelle concentration (CMC) the synthesized surfactants in both reactions **(a)** and **(b)** form micelles in case of a single tail surfactant.

starting materials can be varied in order to design the product composition that leads to a surfactant structure. Figure 35 shows the UPLC measurements of this initial experiment including the reference that was catalyzed by piperidine. Chromatogram (b) shows that the conversion was achieved by piperidine catalysis but not in (c) where the self-replicator should have served as the catalyst. A reason for this could be that too many negative charges are involved. At pH 8.2 malonic acid bears two and 2-formylbenzenesulfonic acid one negative charge which could result in a strong electrostatic attraction to the positively charged replicator hindering the active lysine residues from deprotonating the CH active methylene compound which would further result in an additional negative charge.

Hence, the CH active methylene compound was changed to a more apolar but also more acidic acetylacetone (Figure 34 (b)). However, due to the sulfonate group present in the aromatic aldehyde as well as in the product, starting material and product peaks are hard to separate by UPLC. Hence, the aldehyde was changed to 4-hydroxybenzaldehyde as shown in Figure 34 (b).

After all, acetylacetone shows a keto-enol tautomerism with a strongly shifted equilibrium to the enol conformation and hence is highly reactive which results in various reaction products already in the buffer without any catalyst. The CH active methylene compounds in Figure 34 (d) and (e) were too reactive as well since the reaction already happened in the buffer without any catalyst.

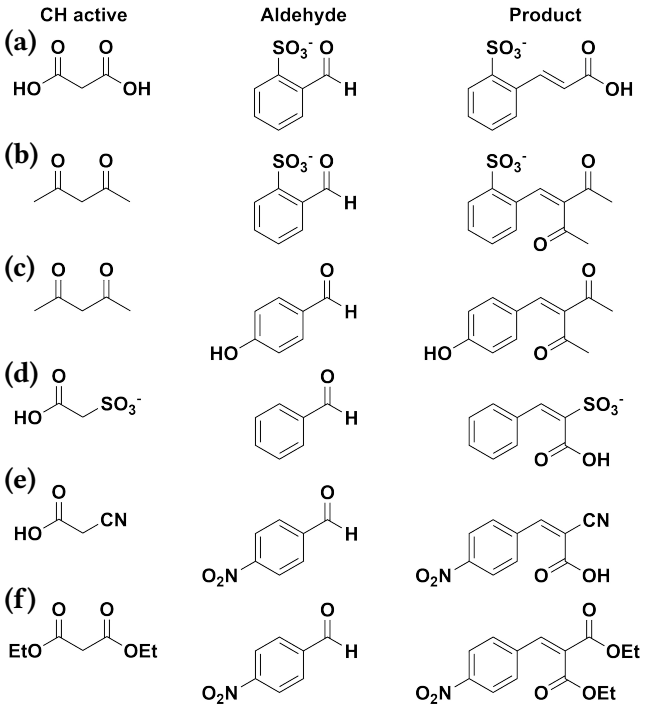

Figure 34: Starting materials and products of piperidine catalyzed Knoevenagel condensations for the proof of principle. In 50 mM borate buffer pH 8.2 **(a)** malonic acid and 2-formylbenzenesulfonic acid **(b)** acetylacetone and 2-formylbenzenesulfonic acid **(c)** acetylacetone and p-hydroxybenzaldehyde **(d)** 2-sulfoacetic acid and benzaldehyde and **(e)** 2-cyanoacetic acid and p-nitrobenzaldehyde were mixed together with piperidine as reference, with the self-replicator as proof of concept and without any catalyst as negative sample. In water **(f)** diethylmalonate and p-nitrobenzaldehyde were mixed together as **(a)** - **(e)**. Reactions **(a)** - **(d)** as well as **(f)** were controlled by TLC and UPLC. Reaction **(e)** already showed product formation by precipitation in the negative sample hence the reaction took place without any organic catalyst.

In literature various Knoevenagel and aldol reactions are reported where p-nitrobenzaldehyde was used as the proto-aldehyde,[35,45,48] hence the starting materials were changed to p-nitrobenzaldehyde and (f) diethylmalonate. Since the borate buffer as the reaction medium has an important influence on the reaction rate or can even hinder the replicator from catalyzing a reaction due to charged buffer salts, the medium was changed to water. Chromatogram (d) in Figure 35 shows a conversion of the starting materials with a retention time of 4 min catalyzed by L-proline.

Chromatogram (b) shows the cascade reaction of SmocProl deprotection by the replicator with following catalysis of the Knoevenagel reaction by the released L-proline. However, the chromatogram shows no conversion to the products of the Knoevenagel condensation. Since L-proline seems in general not as efficient as the aminobases piperidine or pyrrolidine the concentration of SmocProl should be increased so that more L-proline is released by the replicator and hence could possibly catalyze the Knoevenagel condensation which was not done in this thesis.

In chromatogram (c), which shows the starting materials with the self-replicator, it seems that a conversion happened especially when compared to the negative sample containing just the starting materials in buffer (a) which also seems to show a conversion but with less peaks than the starting materials with the replicator. Furthermore (c) shows more peaks than the reference reaction catalyzed by L-proline. It could be that the replicator interacts with the starting materials and forms additional reaction products. In order to confirm that, a mass spectrum in negative mode was taken, which is shown in Figure 37.

Possible reaction products that would fit with their masses to those ones that appear in the mass spectrum (a) are shown in (e) and include the hydrolyzed and decarboxylated cinnamic acid derivative and partly- as well as non-hydrolyzed products

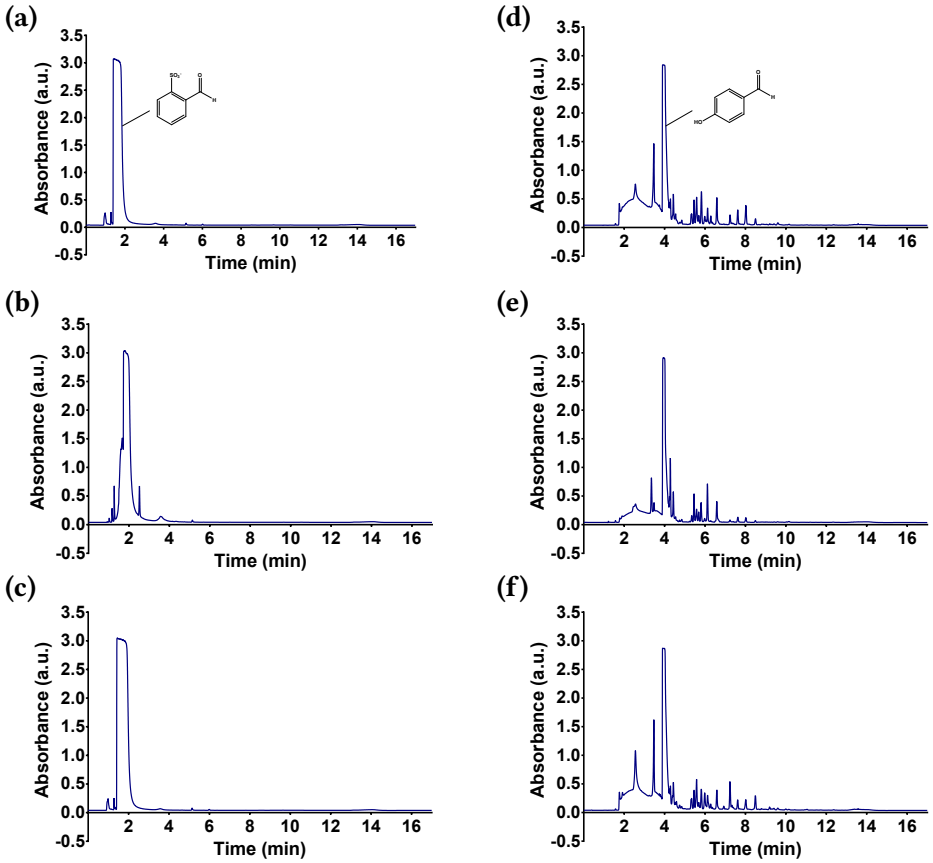

Figure 35: UPLC measurements of the Knoevenagel condensation between 2-formylbenzenesulfonic acid and malonic acid in 50 mM Borax buffer pH 8.2 **(a)** without any additional catalyst **(b)** with piperidine as the organocatalyst **(c)** with the self-replicator as the catalyst and Knoevenagel condensation between 2-formylbenzenesulfonic acid and acetylacetone in 50 mM Borax buffer pH 8.2 **(d)** without any additional catalyst **(e)** with piperidine as the organocatalyst **(f)** with the self-replicator as the catalyst

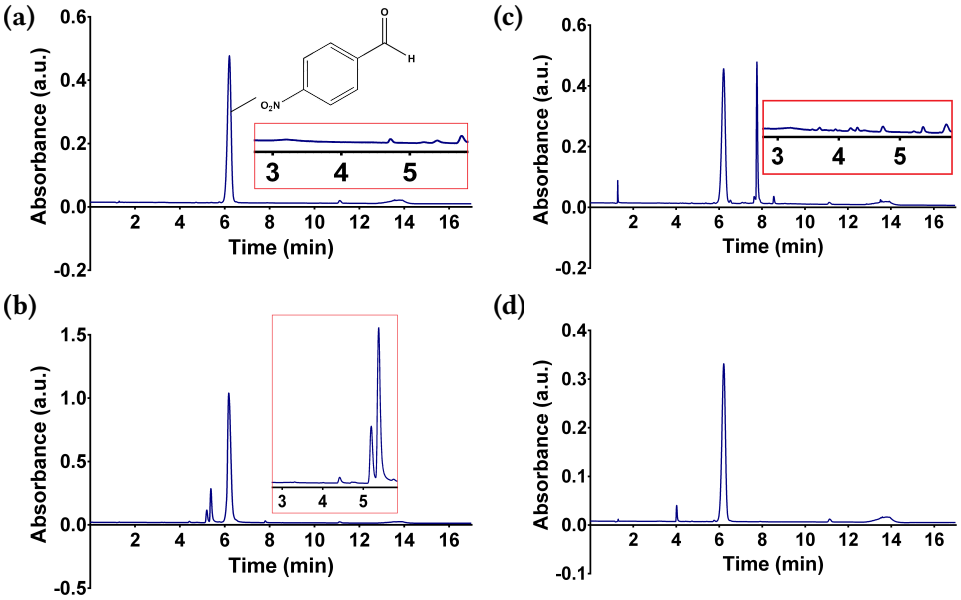

Figure 36: UPLC measurements of the Knoevenagel condensation between p-nitrobenzaldehyde and diethylmalonate in water **(a)** without any additional catalyst **(b)** using the reaction cascade of Smoc-L-proline (SmocProl) deprotection by the self-replicator **(c)** the self-replicator as the catalyst and **(d)** L-proline as the organocatalyst. Differences of the relevant chromatogram part between **(a)** - **(c)** are shown in the red boxes.

all obtained via the Knoevenagel reaction. Further masses that appear in the spectrum are those ones of the replicator dimer and interactions between the monomeric and dimeric structures of the replicator with the starting materials. However, in order to confirm that the self-replicator catalyzed this specific Knoevenagel reaction, a series of experiments including references that contain only the starting materials, a reference reaction catalyzed by pyrrolidine as well as the reaction catalyzed by the self-replicator should be performed and monitored by UPLC and UPLC-MS with an adjusted chromatography protocol in order to achieve a better separation of the peaks, which was not done in this thesis.

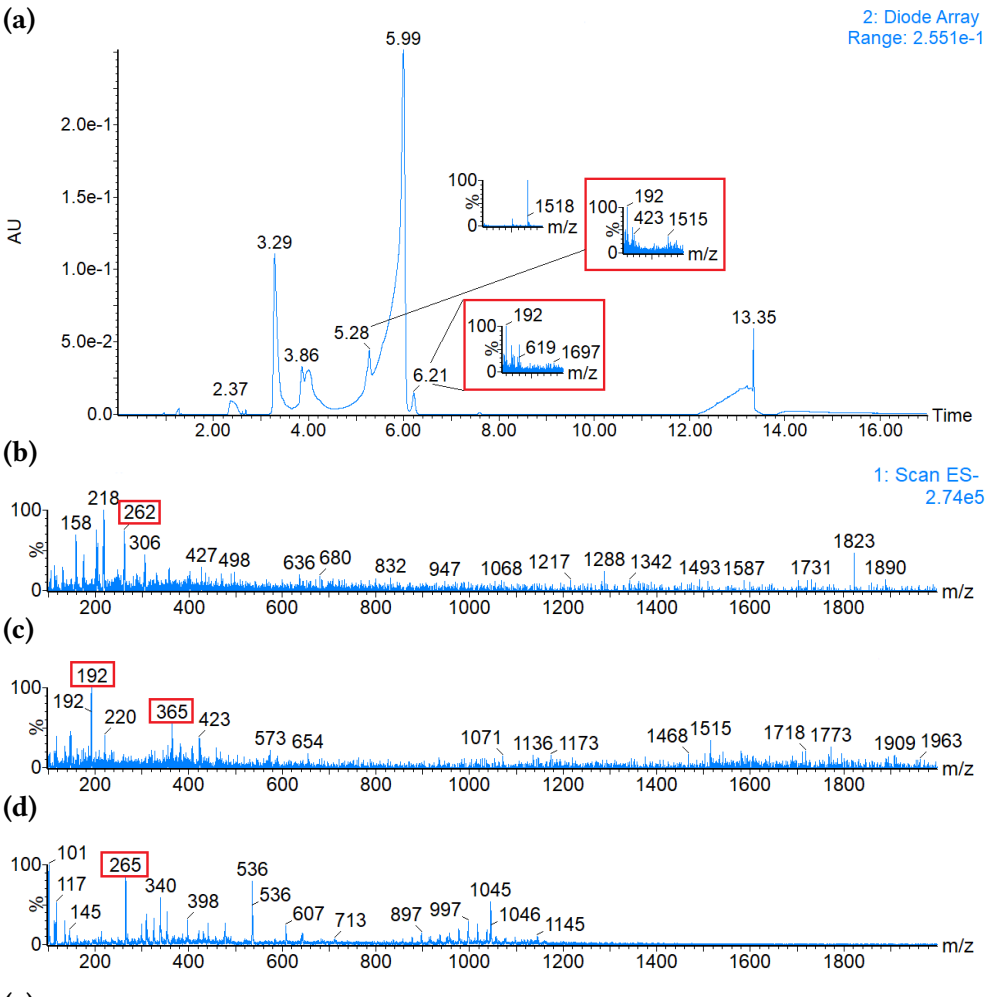

Figure 37: UPLC/ESI-MS **(a)** in negative mode of the Knoevenagel condensation between p-nitrobenzaldehyde and diethylmalonate possibly catalyzed by the self-replicator. Spectra **(b)** at 1.07 min and **(d)** in the wash show the mass of a partly hydrolyzed product and spectrum **(c)** at 5.31 min the cinnamic acid derivative and water addition to the Knoevenagel product. Masses, which fit to compounds resulting from the condensation reaction, are marked in red and shown in **(b)**. The more accurate UPLC/ESI-MS spectrum is shown in the appendix.

4.1.2 *The Self-Replicator and the Aldol Reaction*

Previous works in the *Otto* group have shown that the self-replicator might not be able to catalyze the aldol reaction in aqueous buffered media. Since reactions can be hindered by buffer salts, the medium was changed to water and the aldol reaction between pyridine-2-carbaldehyde and 2-pentanone was taken as a prototype of reaction.

Figure 38 shows the chromatograms of the reference (a) containing just the starting materials and (b) the starting materials with the self-replicator. The reference reaction

catalyzed by pyrrolidine shows product peaks between 2-4 min.[i] Taking a closer look on this time window the starting materials mixed with the replicator (d) seem to show more peaks and also more intensive ones compared to the reference (b) containing just the starting materials in water. In order to confirm a possible product formation, mass spectra in positive as well as negative mode were taken from both, the reference as well as starting materials mixed with the replicator. The mass spectra are shown in Figure 39.

Possible reaction products that would fit with their masses to those ones that appear in Figure 39 are shown in (d) and include products resulting from a reaction of 2-pentanone with itself, through a Knoevenagel reaction with the aldehyde as well as hydrates of the products. Masses that arise from interactions between replicator building blocks and starting materials do not appear. However, in order to confirm that the self-replicator catalyzed this specific Aldol reaction, multiple series of experiments including references that contain only the starting materials, a reference reaction catalyzed by pyrrolidine as well as the reaction catalyzed by the self-replicator should be performed and monitored by UPLC and UPLC-MS, which was not done in this thesis.

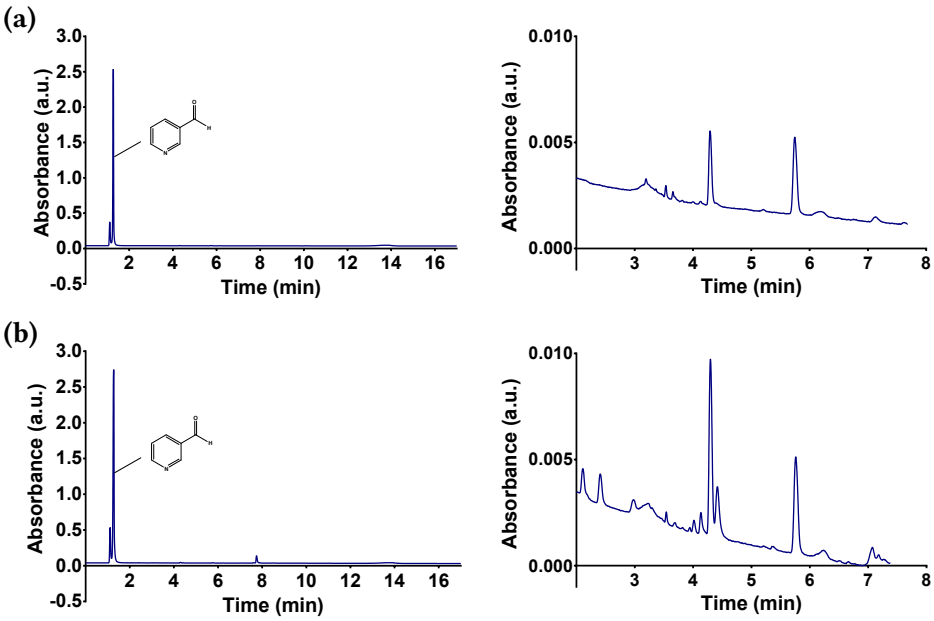

Figure 38: UPLC measurements of the aldol reaction between pyridine-2-carbaldehyde and 2-pentanone in water **(a)** without any additional catalyst **(b)** using the self-replicator as the catalyst. The relevant parts of the chomatogram are each shown to the right.

[i]Note that the retention time depends on the solvent composition and can differ from run to run.

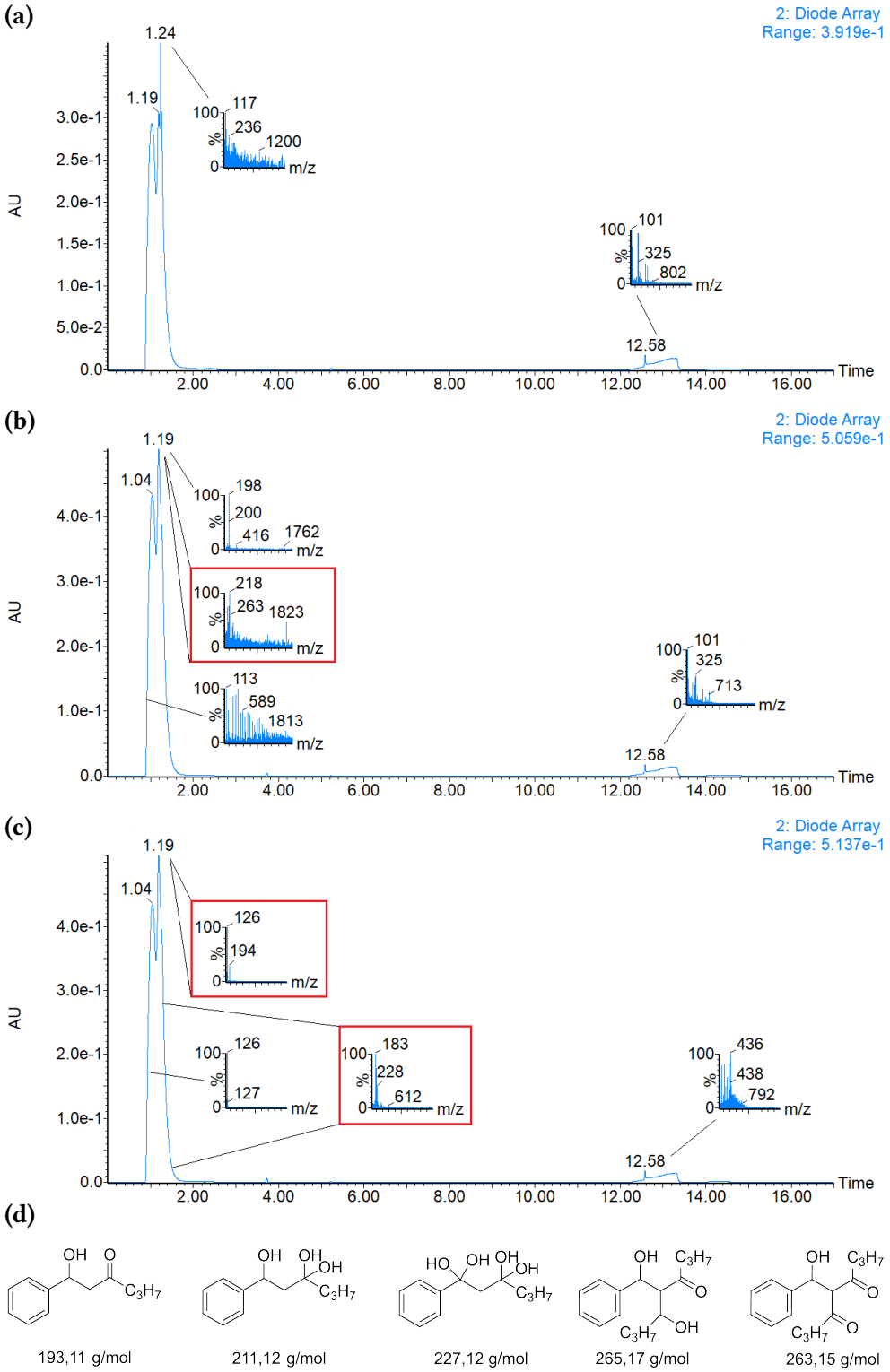

Figure 39: UPLC/ESI-MS of the aldol reaction between pyridine-2-carbaldehyde and 2-pentanone in **(a)** in water without any additional catalyst in negative mode as a control as well as with the self-replicator in negative mode **(b)** and positive mode **(c)**. Masses and structures, which have been found are shown in **(d)** where 3-(1-hydroxy-3-oxohexyl)-1-pyridine with an exact mass of 193,11 g/mol would have been the desired product of the aldol reaction.

4.2 THE SELF-REPLICATOR AND THE IMINE FORMATION

Another reaction that can be induced by the self-replicator in order to achieve reaction products that are capable of forming compartments is the process of imine formation shown in Figure 40. In order to achieve a surfactant structure in the final product, the self-replicator deprotects a Smoc-amine and through imine formation between the free amine and an aldehyde a surfactant is formed. Above the critical aggregation concentration (CAC) compartmentalization is finally induced.

Usually, imines are not stable in water and the equilibrium is mostly on the side of the free amine and carbonyl compound. However, the formation of surfactants finally leading to supramolecular structures has a stabilizing effect. This pulls the equilibrium towards the imine, meaning in this case the formed surfactant.[27]

4.2.1 *Imine Formation of Amino Acids*

Amino acids show a great potential for being the amine component during the imine formation leading to compartment forming molecules since amino acids bear a negative charge at the carboxylic acid group that finally forms the headgroup of the surfactant as it is described in Figure 40 (a). Furthermore, some amino acids are ideal candidates for the formation of double tail surfactants finally leading to vesicles. Kayleigh van Esterik investigated the potential of lysine forming surfactants through imine formation. Lysine features an additional amine group in the side chain. Hence, it this amino acid is suggested to form double tail surfactants through imine

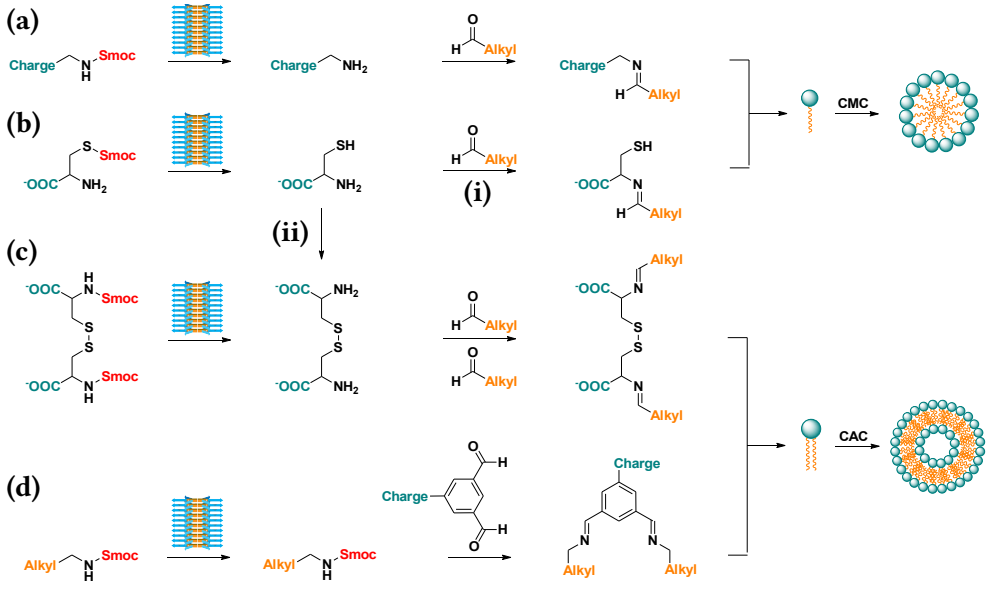

Figure 40: Achieving surfactant structures by imine formation. In general **(a)** a Smoc-protected amine is hindered by the protecting group to form an imine with a carbonyl compound until the self-replicator deprotects it and releases the free amine, which can then undergo imine formation resulting in surfactant structures. The use of **(b)** Smoc protected cysteine can result, after deprotection, in single tail surfactants **(i)** or **(ii)** double tail surfactants through oxidation to the dimer cystine by sulfo-dibenzofulvene (SDBF). L-cysteine can also be pre-oxidized **(c)** already starting from the dimer. Another possibility achieving double tail surfactant structures is **(d)** the deprotection of Smoc-protected primary amines forming imines with charged aromatic dialdehydes.

formation with an aliphatic aldehyde in a ratio of 1:2. In this case the carboxylate forms the negatively charged head group.

Another amino acid that shows a great potential for forming double tail surfactants through imine formation is cysteine which bears just one amino group but a thiol in the side chain. Previous works in the *Otto* group have shown that the side product of the Fmoc- and Smoc-deprotection dibenzofulvene (DBF) and SDBF respectively, enhances the oxidation of thiols to disulfides through a radical mechanism. Cysteine bears just one amine nevertheless it shows potential to form a double tail surfactant through imine formation and an additional oxidation to a disulfide by SDBF that is released during the deprotection of the amine or thiol component induced by the self-replicator as it is described in Figure 40 (b). However, the thiol group could interact with the replicator leading to undesired products and destruction of the replicator. Furthermore, even by a pre-oxidation to the disulfide cystine as described in Figure 40 (c), an interaction with the self-replicator cannot be fully avoided. However, in order to keep the experiments to a simpler level, the oxidation step was skipped and the experiment started from the thiol as a first starting point.

L-cysteine was protected with the Smoc-group according to the standard protocol mentioned in the experimental section. Figure 41 shows the mass spectra of the received products, where L-cysteine was protected on the one hand at the N-terminus Smoc-N-Cys yielding a carbamate (a) and on the other hand at the thiol group resulting in a thiocarbonate (b). Since both compounds share the same mass of

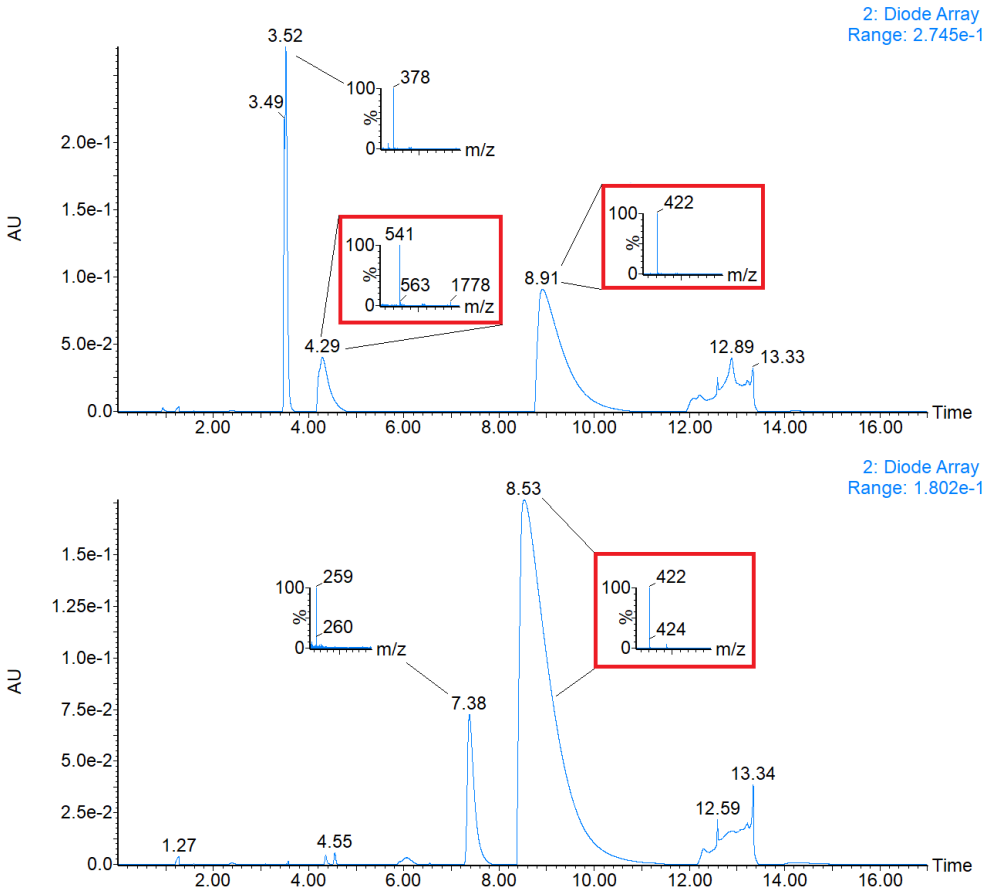

Figure 41: UPLC/ESI-MS in negative mode of the Smoc-protection of L-cysteine leading to the two different products **(a)** Smoc-N-Cys (N-terminus) and **(b)** Smoc-S-Cys (side chain).

422 g/mol the spectra were analyzed for different characteristics in order to identify the products.

Evidence has been found suggesting (a), which shows the spectrum of the carbamate Smoc-N-Cys is the mass of 541 g/mol belonging to the dimer cystine which is protected on just one nitrogen. Furthermore, the mass of 378 g/mol belongs to the addition product of cysteine to SDBF. It is very likely that a certain amount of Smoc-N-Cys decomposed into L-cysteine and SDBF, which enhances the formation of disulfides. The free L-cysteine is on the one hand able to form an adduct with SDBF as well as a disulfide with Smoc-N-Cys, which has a free thiol leading to the dimer cystine which is protected on just one amino group. The product Smoc-S-Cys is not able to form a disulfide with L-cysteine, since the thiol group is protected thus the mass of 541 g/mol must not appear. Hence, it is suspected that spectrum (b) shows Smoc-S-Cys due to the absence of a peak with the mass 541 g/mol. However, the mass of the addition product of Smoc-N-Cys to SDBF was not found in one of the mass spectra. Although spectrum (b) shows the mass of SDBF, no thiol addition products were found. It could be that SDBF formed during the synthesis and could not be separated properly with flash chromatography. It is suggested that spectrum (b) shows the thiocarbonate Smoc-S-Cys, since it does not show the masses of any thiol addition products or disulfide compounds.

UV-measurements for monitoring the deprotection of Smoc-N-Cys as well as Smoc-S-Cys by the self-replicator were carried out in water and are shown in Figure 42. The replicator is able to deprotect both compounds, Smoc-N-Cys as well as Smoc-S-Cys, with a catalytic rate being in the same magnitude for both substrates.

In order to confirm that the double imine of the disulfide cystine forms vesicles, L-cysteine was pre-oxidized with sodium perborate in water followed by the addition of hexanal in the same amount as L-cysteine. The mixture was stirred at room temperature for 24 hours and analyzed by confocal microscopy shown in Figure 43 (a) and (b) as well as cryo transmission electron microscopy (TEM) (c). However, the structures shown in the cryo TEM images appear to be oil droplets and not vesicular structures. The reason for the formation of oil droplets instead of vesicular structures could be the fact that long chained aliphatic carboxylic acids in general show an increased pK_a, meaning a weaker acidity due to the +I-effect of the alkyl chain, which lowers the tendency to release a proton from the −COOH group. In combination with aggregation, where more alkyl chains come closer, the pK_a could be even more

	Catalytic rate $*10^{-5}$ [Abs/min]
Smoc-N-Cys	1890 ± 20
Smoc-S-Cys	2280 ± 30

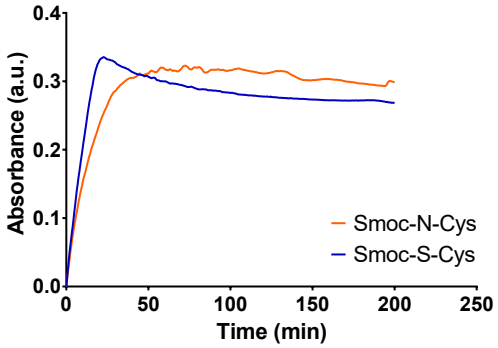

Figure 42: Kinetic UV measurements of th deprotection of the N-terminus protected cysteine Smoc-N-Cys as well as the thiol protected one Smoc-S-Cys in water using 100 µM of the substrate and 20 µM of the replicator. Both can be deprotected fast by the replicator showing catalytic rates in the same magnitude.

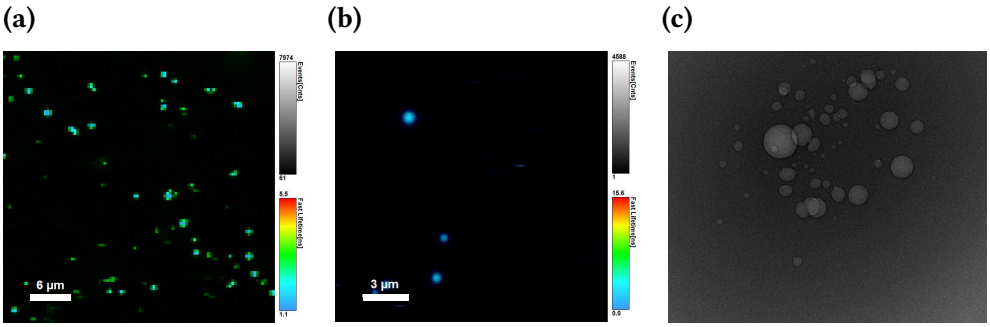

Figure 43: Confocal images **(a)** and **(b)** showing compartment formation. In order to confirm a vesicular structure cryo-TEM **(c)** was performed with the same sample showing oil droplets and not vesicles.

increased, thus the partly deprotonated carboxylic acid is too weak to form the head group of this specific surfactant. After all, the double tail surfactant bears two apolar aliphatic chains that try to have the lowest possible interaction with water oil droplets are formed instead of micelles or vesicles since the head group is not charged enough. A possible solution to this issue could be attaching the more acidic and hence more negatively charged sulfonate group of p-hydroxybenzenesulfonic acid through an esterfication between its −OH group and the −COOH group of L-cysteine, which was not in this thesis.

4.2.2 *Imine Formation of primary amines*

As it was shown in Chapter 2 the self-replicator is able to deprotect Smoc-protected primary amines, which are capable of forming micelles. In order to explore the supramolecular structure to vesicles the approach of forming double tail surfactants through imine formation could be used, which is described in Figure 40 (d). This section will be mainly discussed in a conceptual way.

For achieving a double tail surfactant through imine formation using primary amines, a charged aromatic dialdehyde can be used as the head group part. The armoatic dialdehyde 5-hydroxy-6-methylpyridine-3,4-dicarbaldehyde was synthesized from the vitamin B_6 analogon pyridoxal through oxidation with manganese(II)oxide. In order to attach a permanent positive charge the nitrogen of the pyridine ring should be methylated resulting in a pyridinium cation (Figure 44 (a)) which was not achieved in this thesis. However, this charged dialdehyde shows the ideal structure for serving as a head group since the −OH group on the fifth position is able to stabilize the imine through donation of an H-bond to the nitrogen leading to a six membered arrangement as described in Figure 44 (b). By mixing the charged dialdehyde with a Smoc-protected primary amine, the imine formation is hindered by the protecting group until the self-replicator deprotects it and releases the free amine, which is capable of forming an imine with the aldehyde resulting in a double tail surfactant when mixed in a ratio 1:2.

Since the synthesis of a charged dialdehyde can be challenging due to sensitivity for over reactions of the aldehyde group another possibility that yields double tail surfactants through imine formation is the use of single tail surfactants that carry a carbonyl group as shown in Figure 44 (c). In general, the CAC for single tail surfactants is higher compared to the CAC of double tail surfactants. Through an aldol reaction between a methylated pyridiniumcarbaldehyde and an aliphatic ketone a single tail surfactant is synthesized bearing a carbonyl group and a hydroxy group in position 2, which has a stabilizing effect on imine formation through H-bonding.

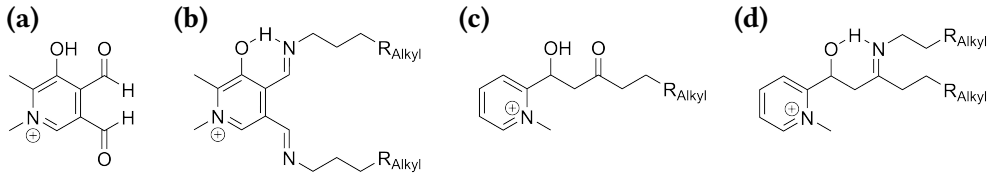

Figure 44: Imine formation between **(a)** the positively charged aromatic dialdehyde 5-hydroxy-6-methylpyridine-3,4-dicarbaldehyde and primary amines resulting in **(b)** double tail surfactants and between **(c)** the single tail surfactant 3-(1-hydroxy-3-oxohexyl)-1-methylpyridin-1-ium and primary amines resulting in **(d)** double tail surfactants. Both imines **(b)** and **(d)** are stabilized by H-bonding and an additional six membered arrangement.

In this work, pyridine-2-carbaldehyde was methylated at the pyridine nitrogen according to *Plater et al.*[49] in order to attach a permanent positive charge followed by the synthesis of 3-(1-hydroxy-3-oxohexyl)-1-methylpyridin-1-ium through an aldol reaction with 2-pentanone according to the conditions of *Chimni.*[50]

In order to continue this approach, it should be confirmed that the imine formation between a primary amine bearing an aliphatic chain from C_6 - C_{10} and the synthesized 3-(1-hydroxy-3-oxohexyl)-1-methylpyridin-1-ium leads the formation of vesicles. If the vesicle formation is successful, the next step should be mixing the synthesized single tail surfactant and a Smoc protected primary amine together with the self-replicator, which should finally induce the formation of compartments. However, this was not done in this thesis.

4.3 CONTRIBUTIONS

The research question about the expansion of reaction scope that can be catalyzed by the self-replicator to C−C carbon bond formation such as the Knoevenagel reaction was proposed by the author. The approach of achieving compartmentalization through imine formation was proposed by Andreas Hussain, MSc and Kayleigh van Esterik, BSc and expanded by the author to L-cysteine as well as primary amines as the amino component. Negative stain TEM was carried out by Guillermo Monreal Santiago, MSc, confocal microscopy images taken by Viktor V. Krasnikov as well as Guillermo Monreal Santiago and mass spectrometry performed by Marcel Eleveld, MSc. The author who also carried out synthesis of all products, screenings, UV measurements, ^{1}H-NMR spectra and data evaluation as well as drew the conclusions in this chapter.

4.4 EXPERIMENTAL

4.4.1 *Synthesis*

Smoc-N-Cys/Smoc-S-Cys

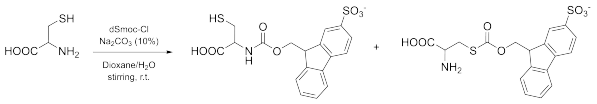

In a 25 mL round bottom flask, L-cysteine (1.35 mmol) was dissolved in 1.3 mL 10% Na_2CO_3 and Smoc-Cl (0.9 mmol) dissolved in 1.6 mL dioxane was transferred to the flask dropwise under cooling with a water bath. The mixture became white turbid and was stirred at ambient temperature for 2h. Afterwards, the mixture was acidified with HCl (1M) to pH 2-3 and then poured as it was on the flash chromatography and purified by using a H_2O/ACN gradient. Then the fractions were concentrated on the rotary evaporator yielding 123 mg of Smoc-N-cysteine and 100 mg of Smoc-S-cysteine. Both products were light yellow solids.

N-methylpyridine-2-carbaldehyde

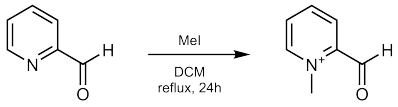

Pyridine-2-carbaldehyde (10.5 mmol) was mixed with methyliodine (40 mmol) in 10 mL DCM and heated under reflux for 24 h. The orange crystals were vacuum filtrated and washed with DCM. The yield were 105 mg (8% of theory).

^{1}**H-NMR** (400 MHz, D_2O): δ 8.78 (d, J = 6.2 Hz, 1H), 8.57 (t, J = 8.0 Hz, 1H), 8.34 (d, J = 8.2 Hz, 1H), 7.98 (t, J = 7.1 Hz, 1H), 6.40 (s, 1H), 4.40 (s, 3H).

2-(1-hydroxy-3-oxoundecyl)-1-methylpyridin-1-ium

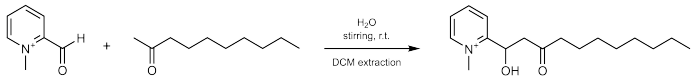

In a 3 mL vial, N-methylpyridine-2-carbaldehyde (0.044 mmol) was dissolved in 1 mL H_2O and 2-decanone (2 mmol) was added. Afterwards, pyrrolidine (0.6 mmol) was added to the mixture and the 2-phase system was intensively stirred at ambient temperature. After 5 min the organic phase turned from colourless to milky. After 2h of stirring the organic phase became red. It was then extracted with 3x4 mL DCM and the organic phase was washed with 25 mL H_2O. The solvent was evaporated leading to a red liquid in a quantitative yield. A ^{1}H-NMR was taken in D_2O.

^{1}**H-NMR** (400 MHz, D_2O): δ 8.78 (d, J = 6.2 Hz, 1H), 8.57 (t, J = 8.0 Hz, 1H), 8.34 (d, J = 8.2 Hz, 1H), 7.98 (t, J = 7.1 Hz, 1H), 6.40 (s, 1H), 4.40 (s, 3H).

5-hydroxy-6-methylpyridine-3,4-dicarbaldehyde

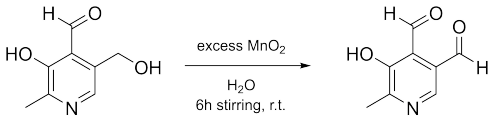

In a 50 mL round bottomflask, manganese(IV)oxide (22 mmol) were suspended in 15 mL H_2O. Afterwards, pyridoxal hydrochloride (1.5 mmol) was dissolved in 2 mL H_2O and transferred to the MnO_2 suspension. The mixture was stirred at ambient temperature for 6h. Afterwards, it was vacuum filtrated and the filtrate evaporated on the rotary evaporator. The crude was dissolved in 3 mL H_2O and filtrated though a syringe filter in order to get rid of MnO_2 residues. The filtered solution was intensively yellow and purified by flash chromatography using a H_2O/ACN gradient. The solvent was evaporated leading to a brownish liquid in a quantitative yield.

4.4.2 *Screening*

Knoevenagel reaction

In a 1.5 mL vial, the aldehyde (1 mM) and CH-active methylene compound (1 mM) were mixed with the catalyst (50 µM) to a total volume of 200 µL with water. For the positive reference pyrrolidine was used as the catalyst and for the testing sample the self-replicator. For the negative reference only the starting materials were mixed together. The reaction was stirred at ambient temperature for 24 h with 1200 rpm and monitored by (MS-)UPLC.

Aldol reaction

In a 1.5 mL vial, the aldehyde (350 µM) and ketone (500 µM) were mixed with the catalyst (14 µM) to a total volume of 1000 µL with water. For the positive reference pyrrolidine was used as the catalyst and for the testing sample the self-replicator. For the negative reference only the starting materials were mixed together. The reaction was stirred at ambient temperature for 24 h with 1200 rpm and monitored by (MS-)UPLC.

Imine formation test reaction

Sodium perborate tetrahydrate (4.61 mg, 0.03 mmol) was dissolved in 1 mL deuterium oxide. L-cysteine (3.63 mg, 0.03 mmol) was added and the clear solution stirred for 4 h at ambient temperature. Then, n-hexanal (2.6 mg, 0,03 mmol) was added and mixed on a shaker. After a few minutes the mixture became turbid. Droplets were visible under a light microscope and the mixture was further analyzed by confocal microscopy as well as cryo-TEM.

4.4.3 *Analysis*

UV measurements

A stock solution of the substrate was prepared in the reaction medium. The concentration of the hexamer libary was 2 mM in 50 mM borate buffer pH 8.2. The substrate stock solution was diluted with the reaction medium in a ultra violett (UV) quartz glass cuvette and equilibrated in the UV meter JASCO-II for 20-30 min. Afterwards the self-replicator was added to the substrate. It was mixed by shaking the cuvette and a time course measurement was performed by using the detection wavelength of sulfodibenzofulvene at 308 nm.

cryo-TEM measurements

A 10 µL drop of the sample was placed on a Quantifoil 3.5/1 holey carbon coated grid. Blotting and vitrification in ethane was done in a Vitrobot (FEI, Eindhoven, the Netherlands). The grids were observed in a Tecnai T20 cryo-electron microscope operating at 200 keV with a Gatan model 626 cryo-stage. Images were recorded under low-dose conditions with a slow-scan CCD camera.[11]

Confocal microscopy

Confocal microscopy experiments were performed using a MicroTime 200 setup (PicoQuant, Germany), using an Olympus IX73 microscope with a 100x oil immersion objective. For the fluorescence images, a standard 120 W mercury lamp (X-Cite® series 120 Q) was used as an irradiation source, together with a fluorescence cube with exciter and emitter wavelengths of 466 ± 20 and 525 ± 25 nm, respectively (Semrock GFP-4050B). For confocal images, a 440 nm laser was used together with a 10%R/90%T beamsplitter, an interference filter with wavelengths of 482 ± 35 nm, and a standard Single-Photon Counting Module (Excelitas Technologies, USA). The laser power remained under 10 µW, and was kept constant for each series of experiments.

Glass slides were coated with PEG to prevent interactions with the coacervate phase, using a protocol modified from *Lau et al.*[51]: 3-[Methoxy(polyethyleneoxy)propyl]trimethoxysilane (6-9 PE-units, ACBR GmbH) (0.5% v/v) and acetic acid (1% v/v) were dissolved in ethanol to make the coating reagent. 50 µL of this solution was placed on top of each microscope slide, placing another slide on top of it to spread the solution through both surfaces. More slides and droplets of coating reagent were put on top of each other in this way, and then heated in an oven to 100 °C for at least 30 minutes. The slides were then submerged in ddH_2O, sonicated, rinsed with more ddH_2O, dried, and stored for use.

APPENDIX

5

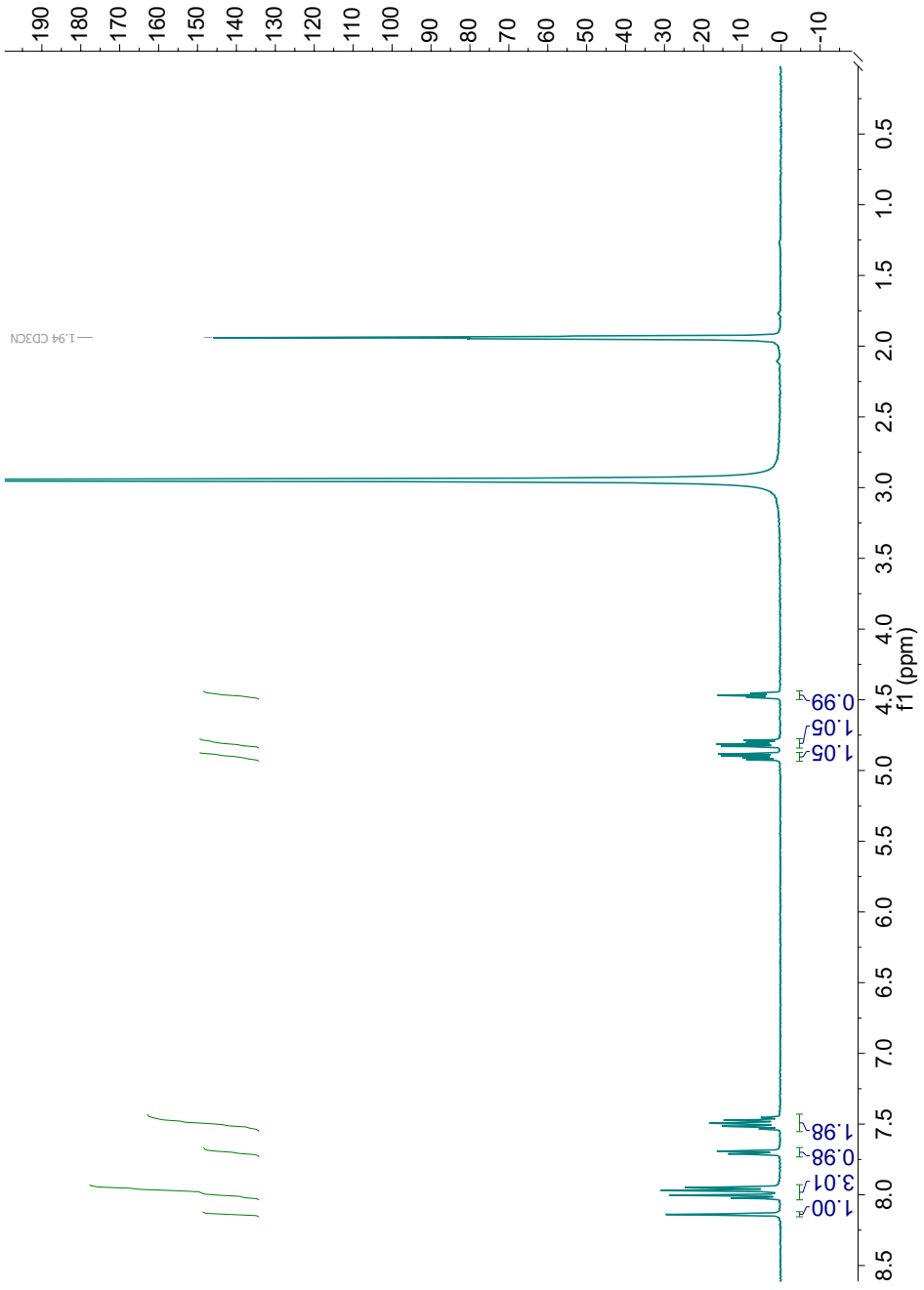

Figure 45: ^{1}H-NMR of 9-(2Sulfo)fluorenylmethyloxycarbonylchloride in acetonitrile-d3 at 400 MHz. The solvent is marked in grey.

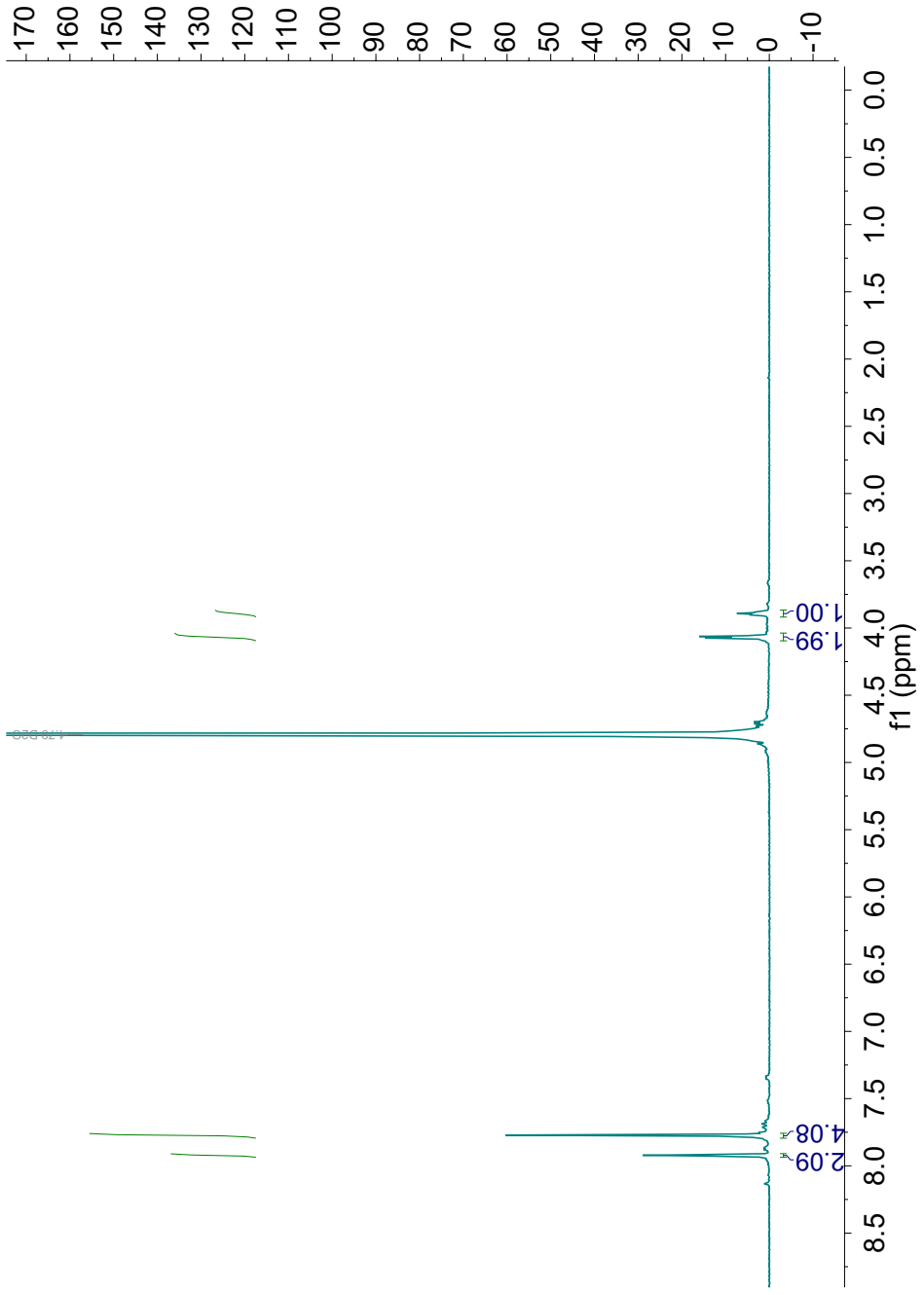

Figure 46: ^{1}H-NMR of 9-(x,x-disulfo)fluorenylmethyloxycarbonylchloride in deuterium oxide at 400 MHz. The solvent is marked in grey.

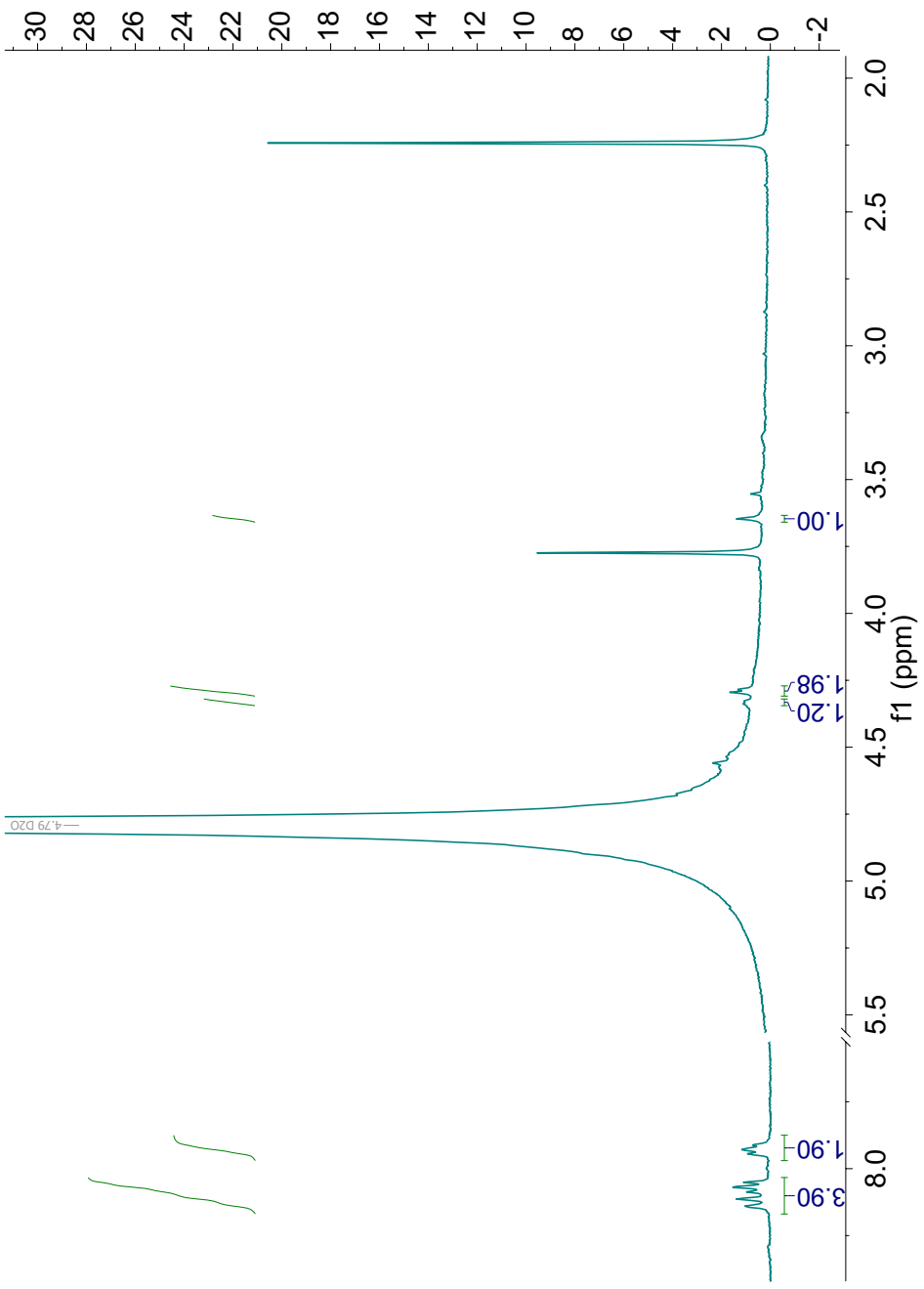

Figure 47: ^{1}H-NMR of dSmoc-glycine in deuterium oxide at 400 MHz. The solvent is marked in grey.

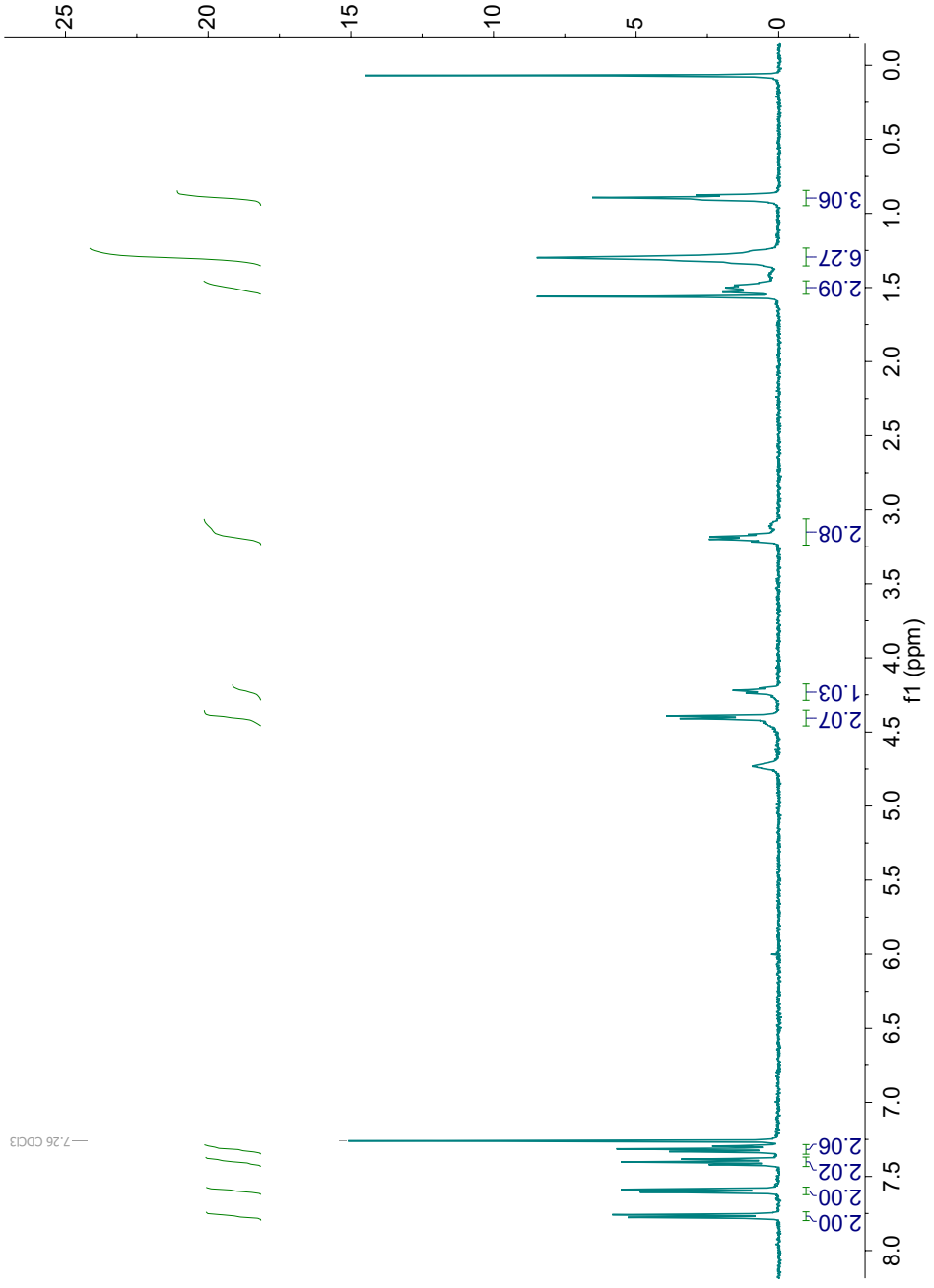

Figure 48: ^{1}H-NMR of Fmoc-hexylamine in chloroform-d at 400 MHz. The solvent is marked in grey.

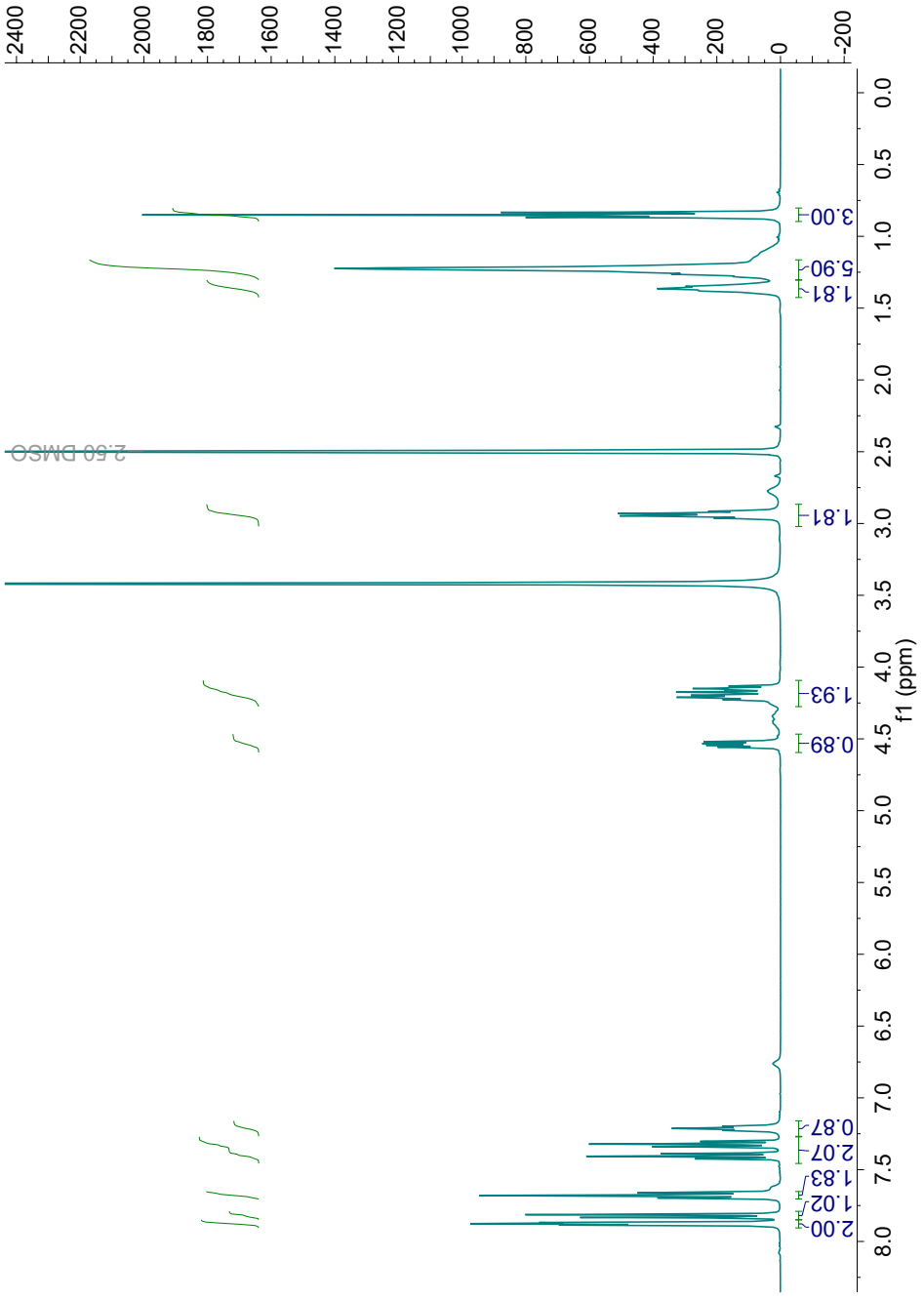

Figure 49: [1]H-NMR of Smoc-hexylamine in DMSO-d6 at 400 MHz. The solvent is marked in grey.

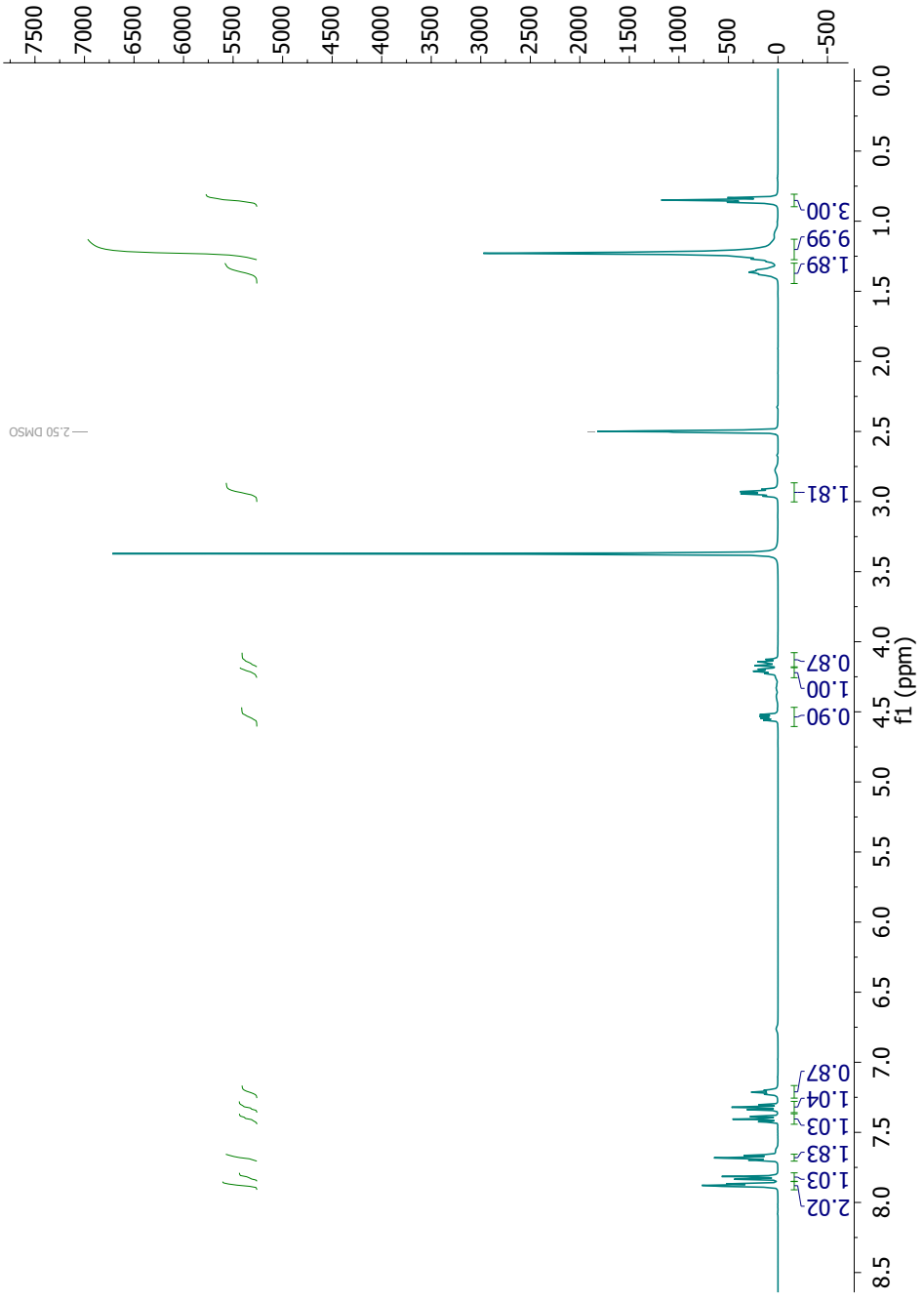

Figure 50: [1]H-NMR of Smoc-octylamine in DMSO-d6 at 400 MHz. The solvent is marked in grey.

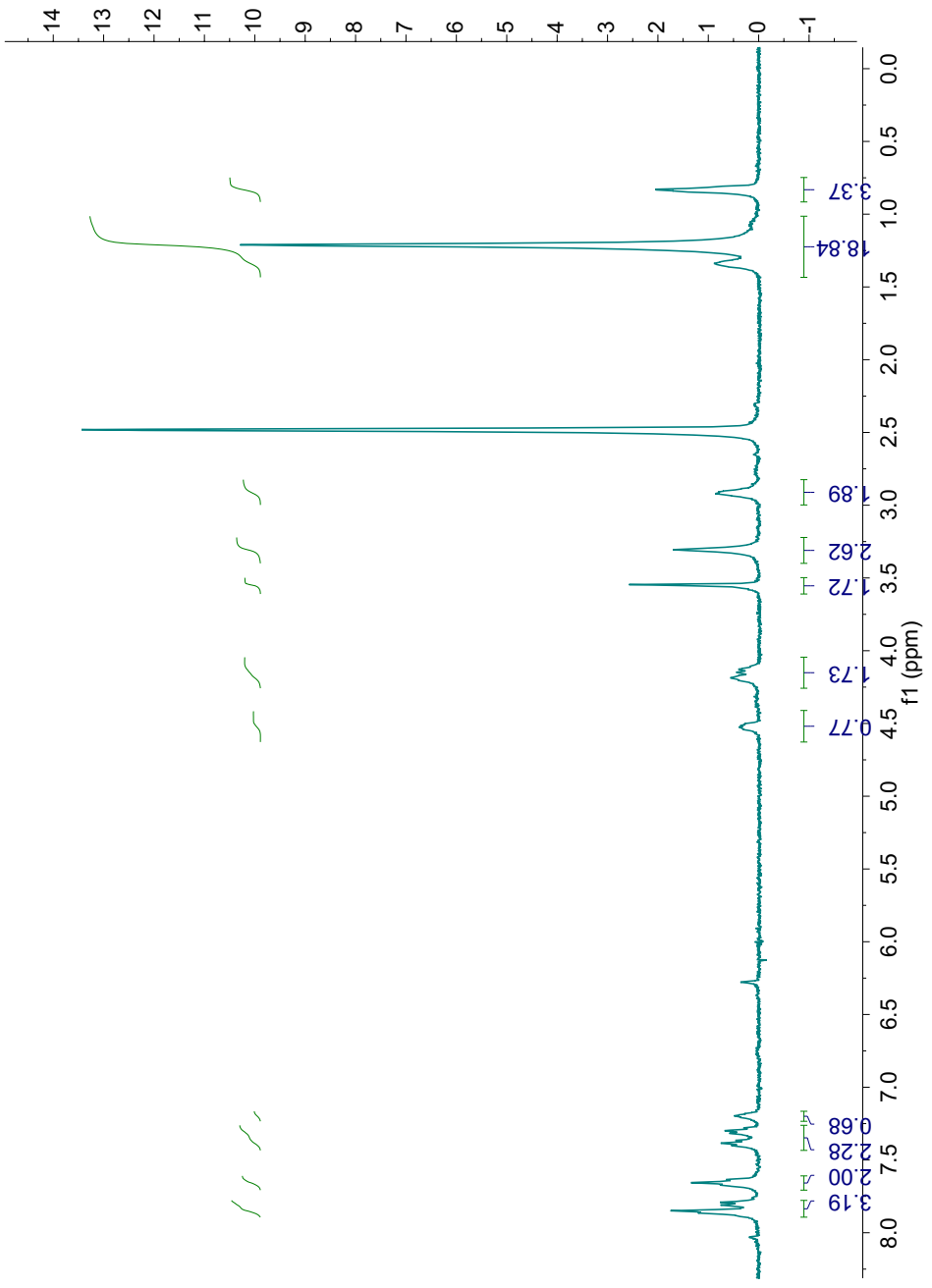

Figure 51: ^{1}H-NMR of Smoc-decylamine in DMSO-d6 at 400 MHz.

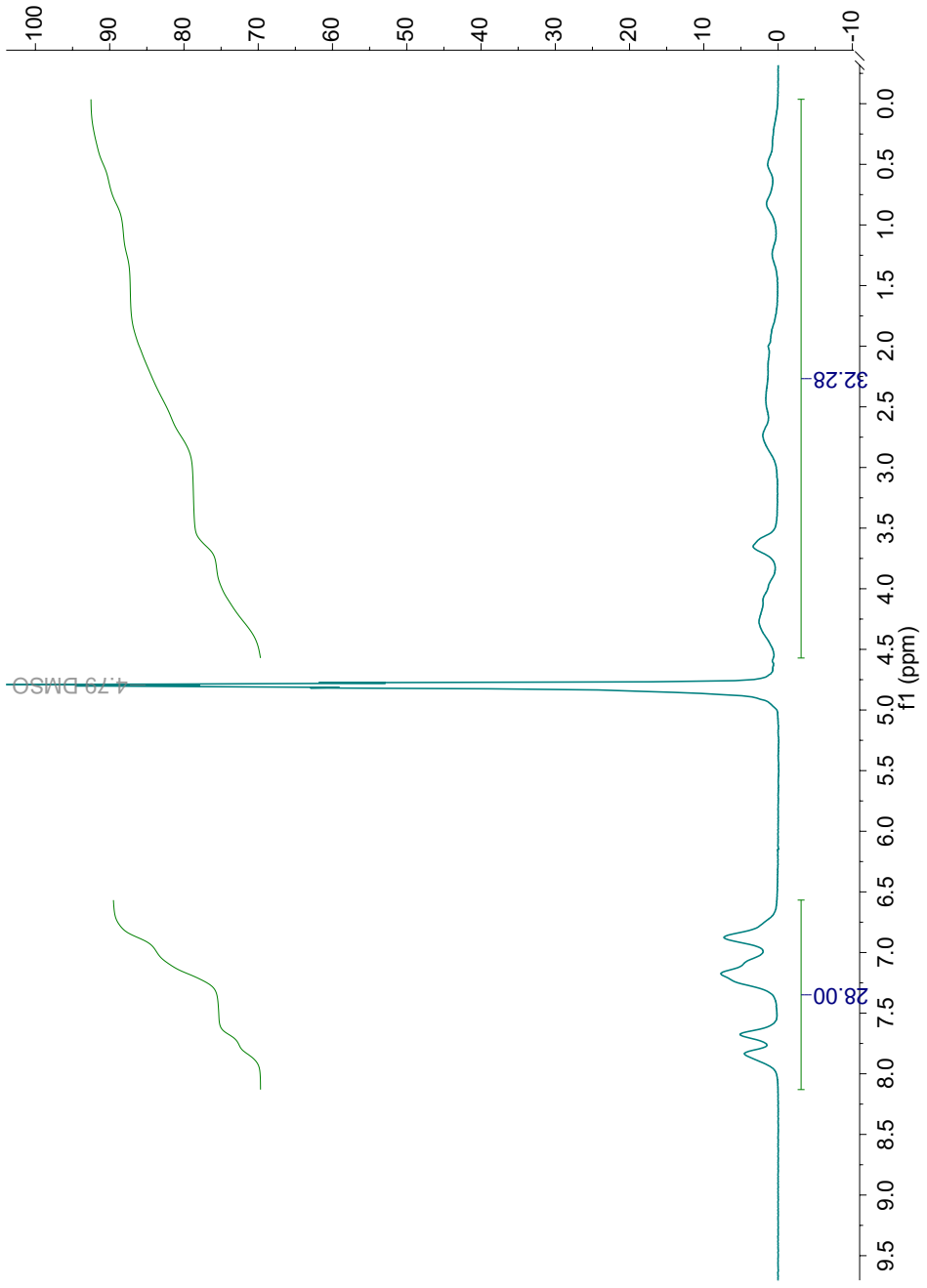

Figure 52: ^{1}H-NMR of 4xSmoc-spermine in deuterium oxide at 400 MHz. The solvent is marked in grey.

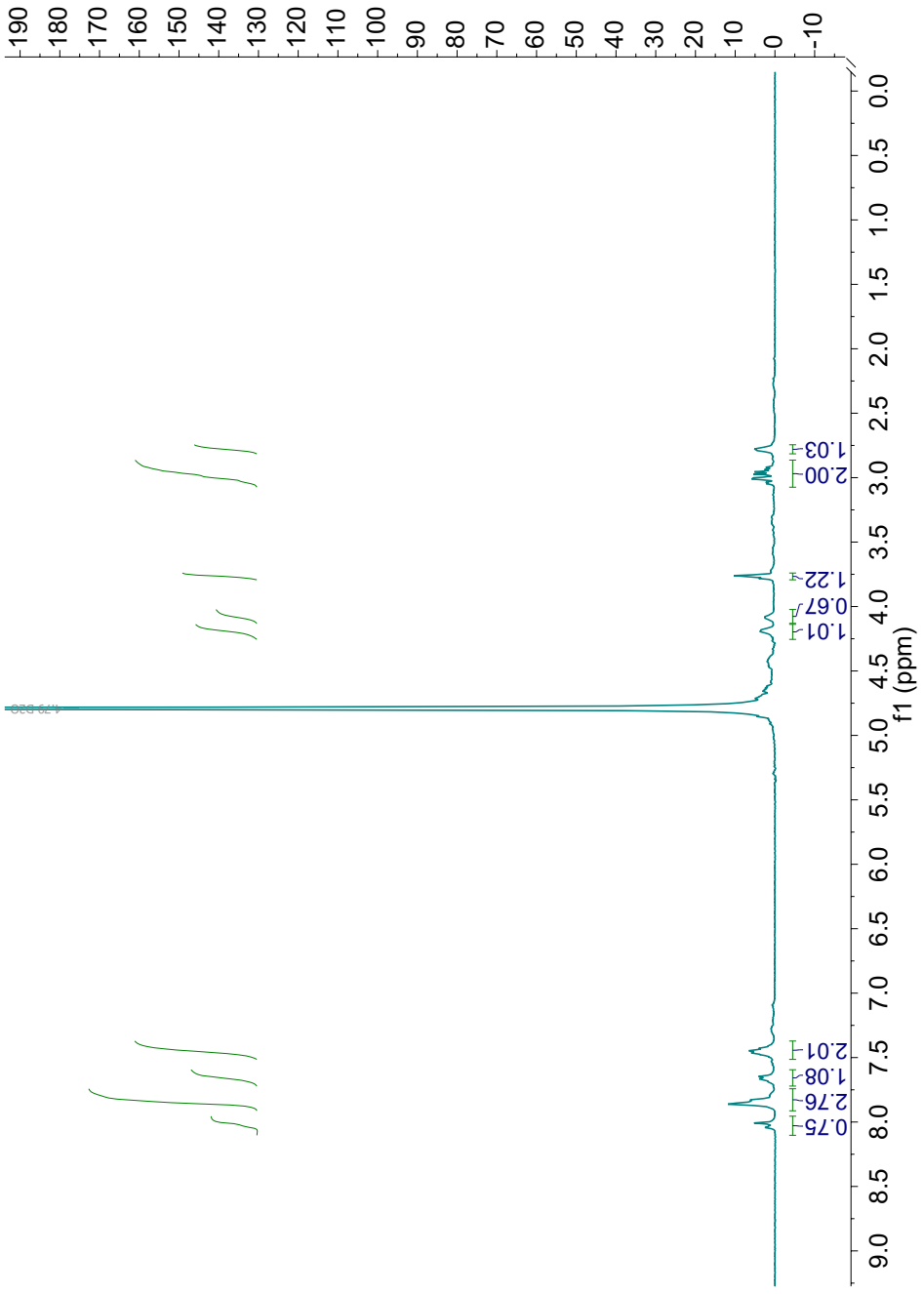

Figure 53: [1]H-NMR of Smoc-N-cysteine in deuterium oxide at 400 MHz. The solvent is marked in grey.

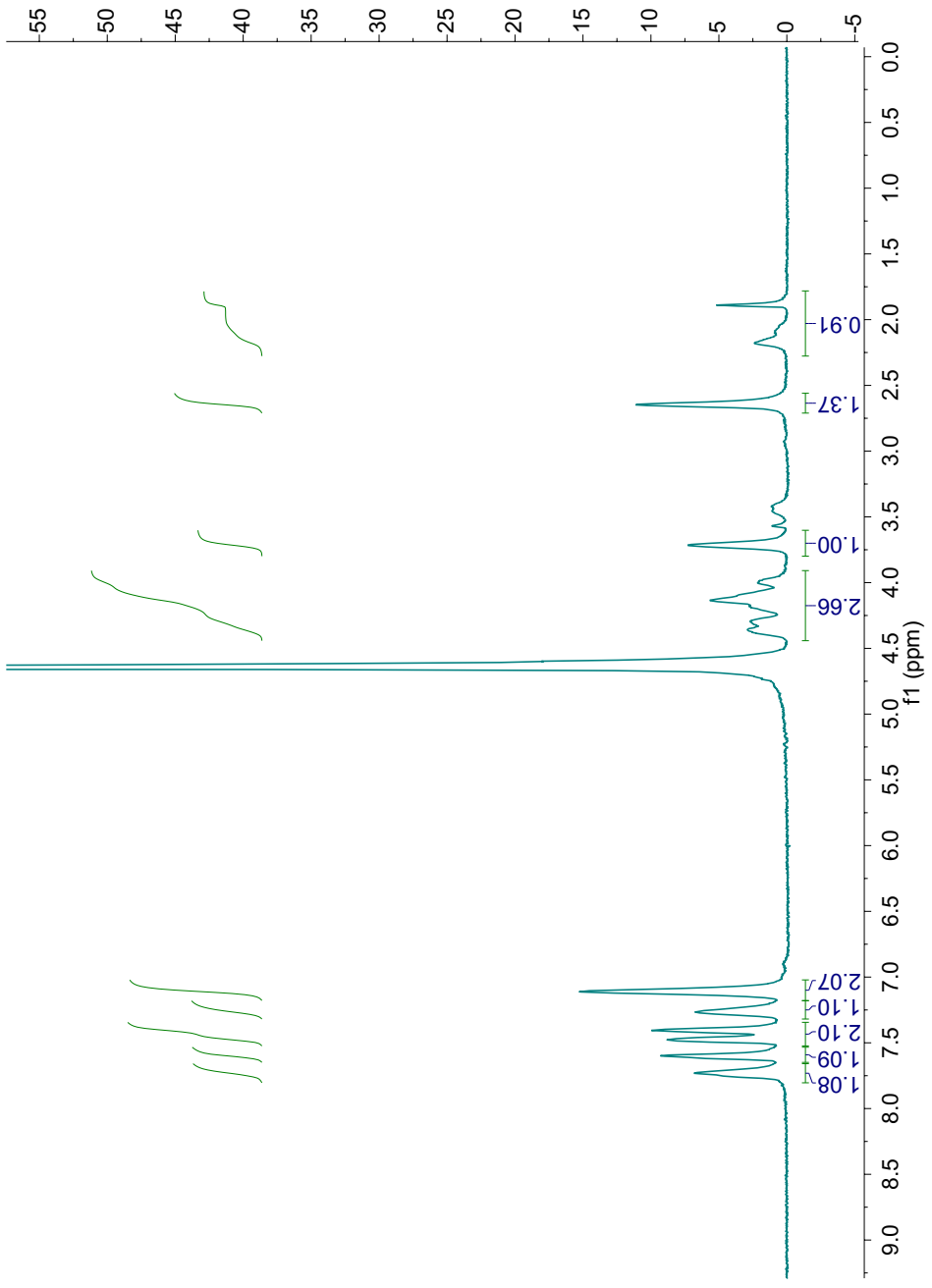

Figure 54: [1]H-NMR of Smoc-S-cysteine in deuterium oxide at 400 MHz.

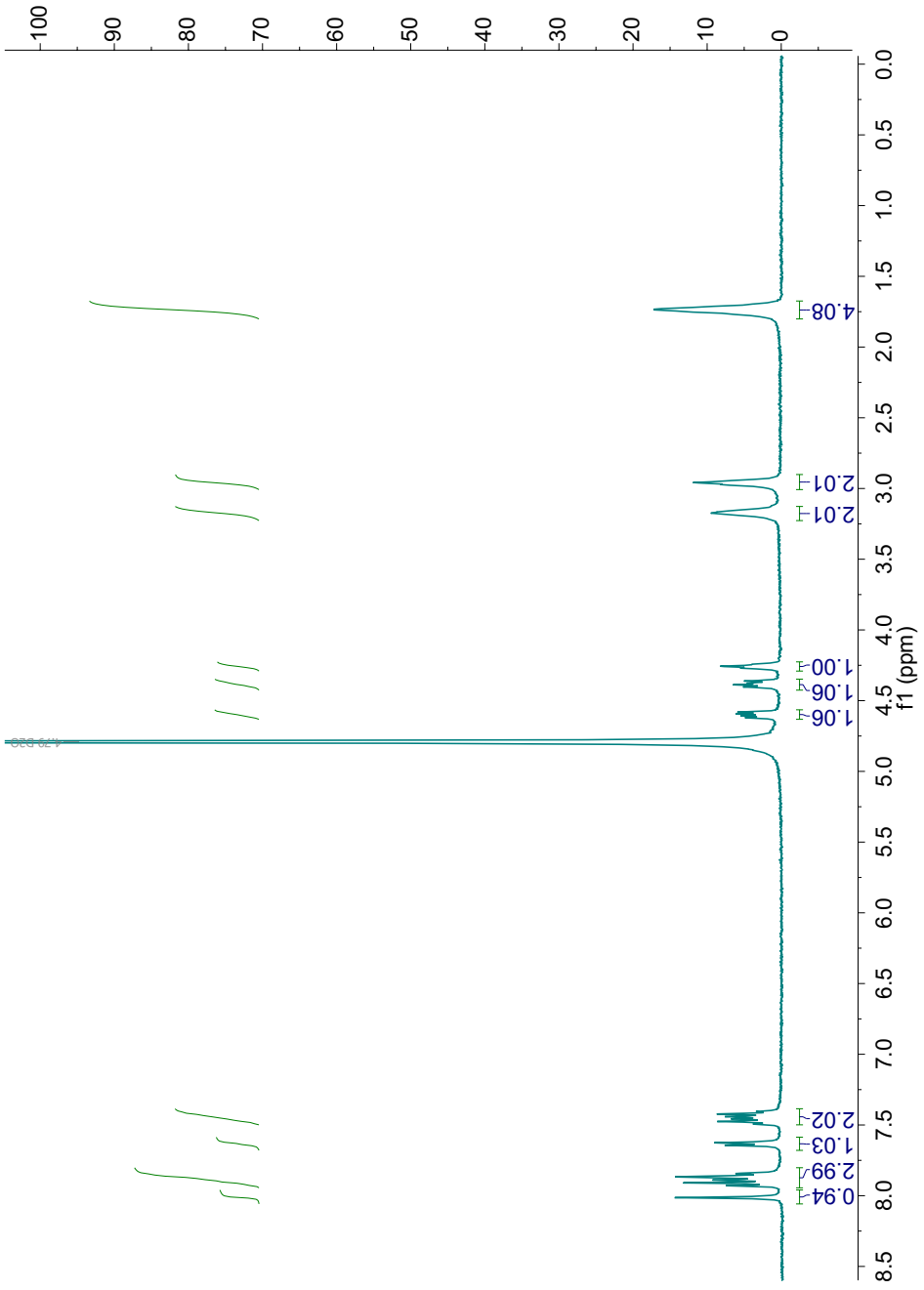

Figure 55: [1]H-NMR of Smoc-pyrrolidine in deuterium oxide at 400 MHz. The solvent is marked in grey.

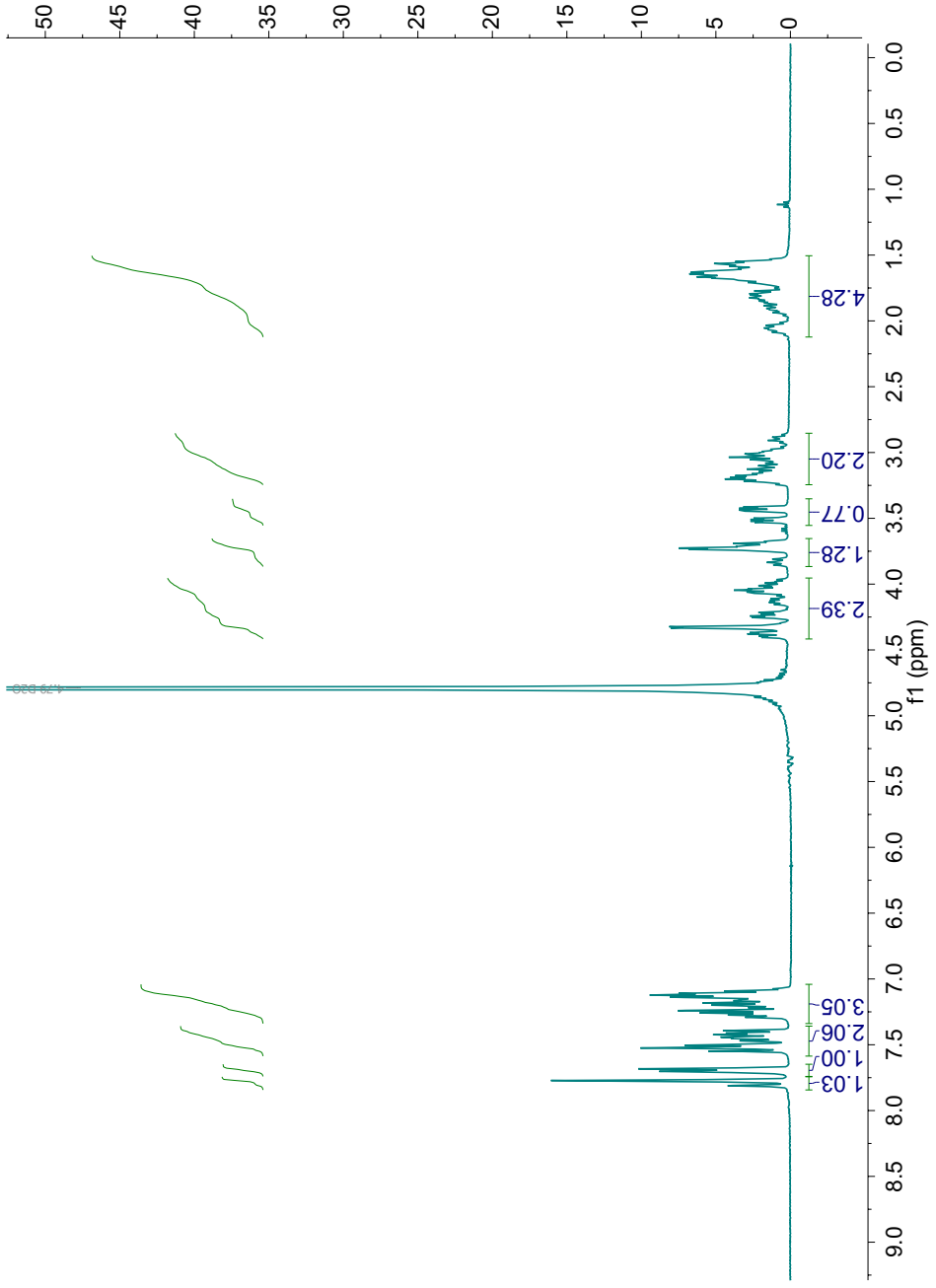

Figure 56: [1]H-NMR of Smoc-proline in deuterium oxide at 400 MHz. The solvent is marked in grey.

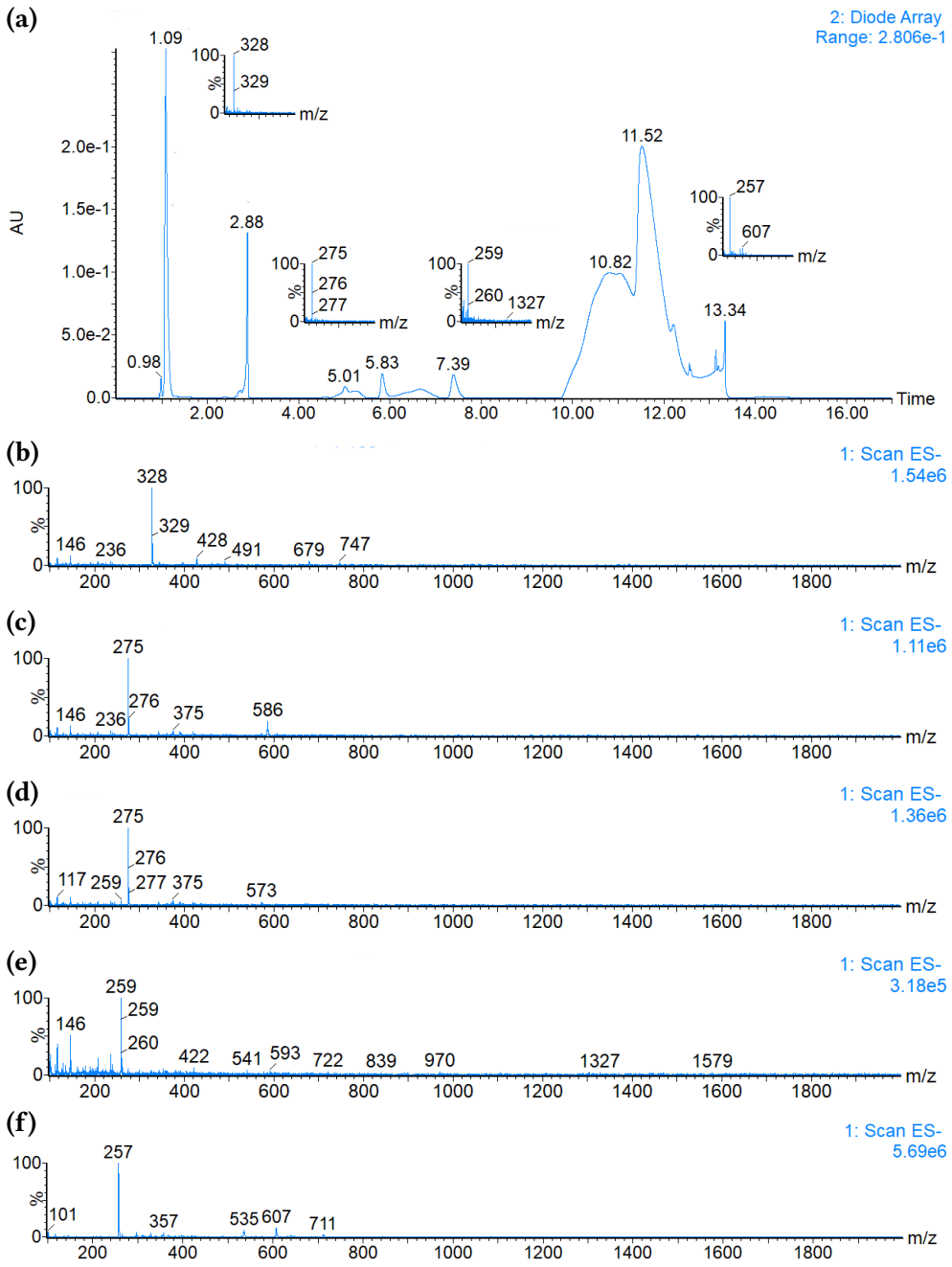

Figure 57: UPLC/ESI-MS in negative mode of Smoc-pyrrolidine deprotection by pyrrolidine with the additive dibutylamine acting as a potential scavenger. The mass spectra are from the peaks at **(b)** 2.90 min **(c)** 5.05 min **(d)** 5.86 min **(e)** 7.39 min **(f)** wash.

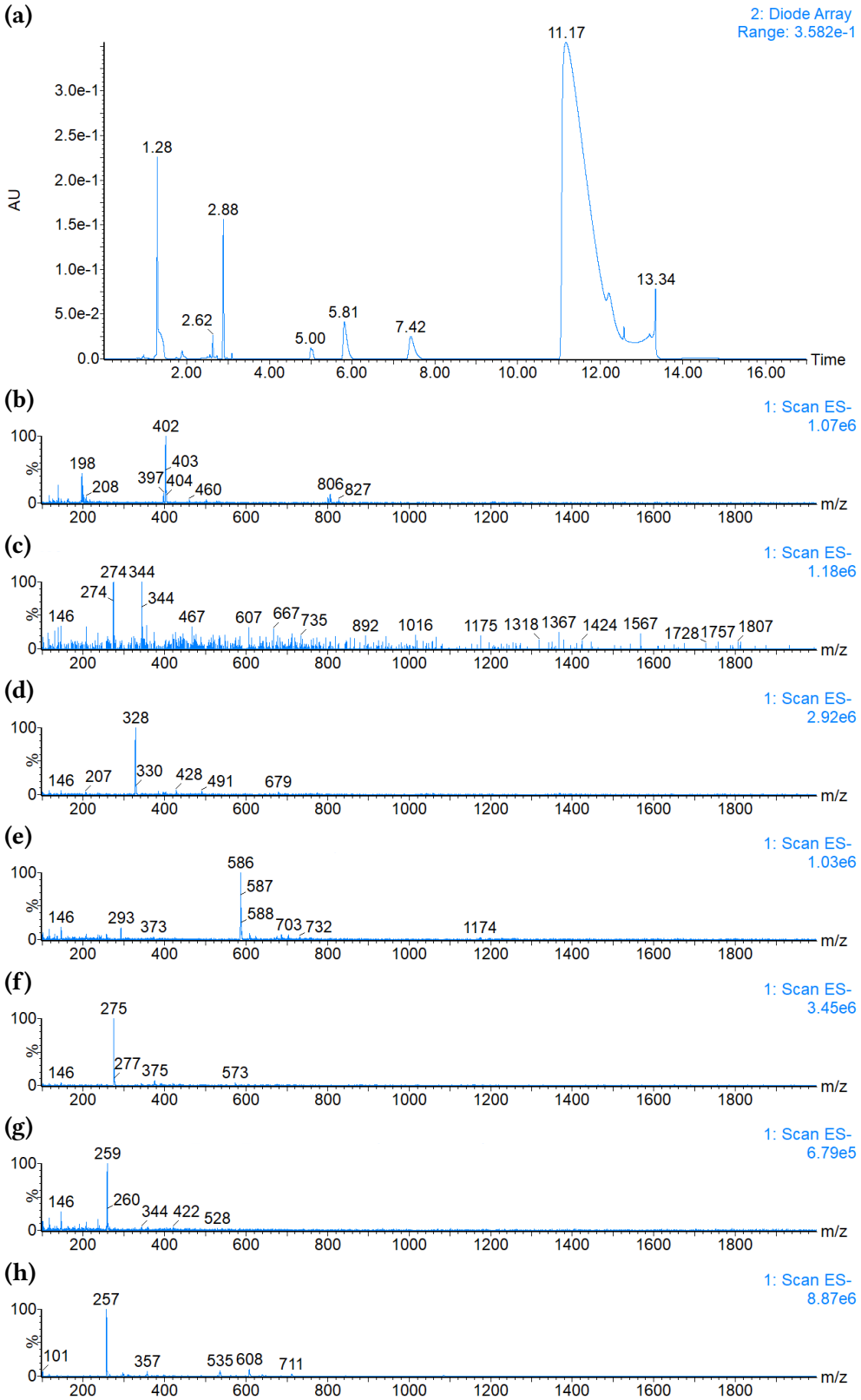

Figure 58: UPLC/ESI-MS in negative mode of Smoc-pyrrolidine deprotection by pyrrolidine with the additive spermidine acting as a potential scavenger. The mass spectra are from the peaks at **(b)** 1.28 min **(c)** 2.66 min **(d)** 2.92 min **(e)** 5.00 min **(f)** 5.81 min **(g)** 7.42 min **(h)** wash.

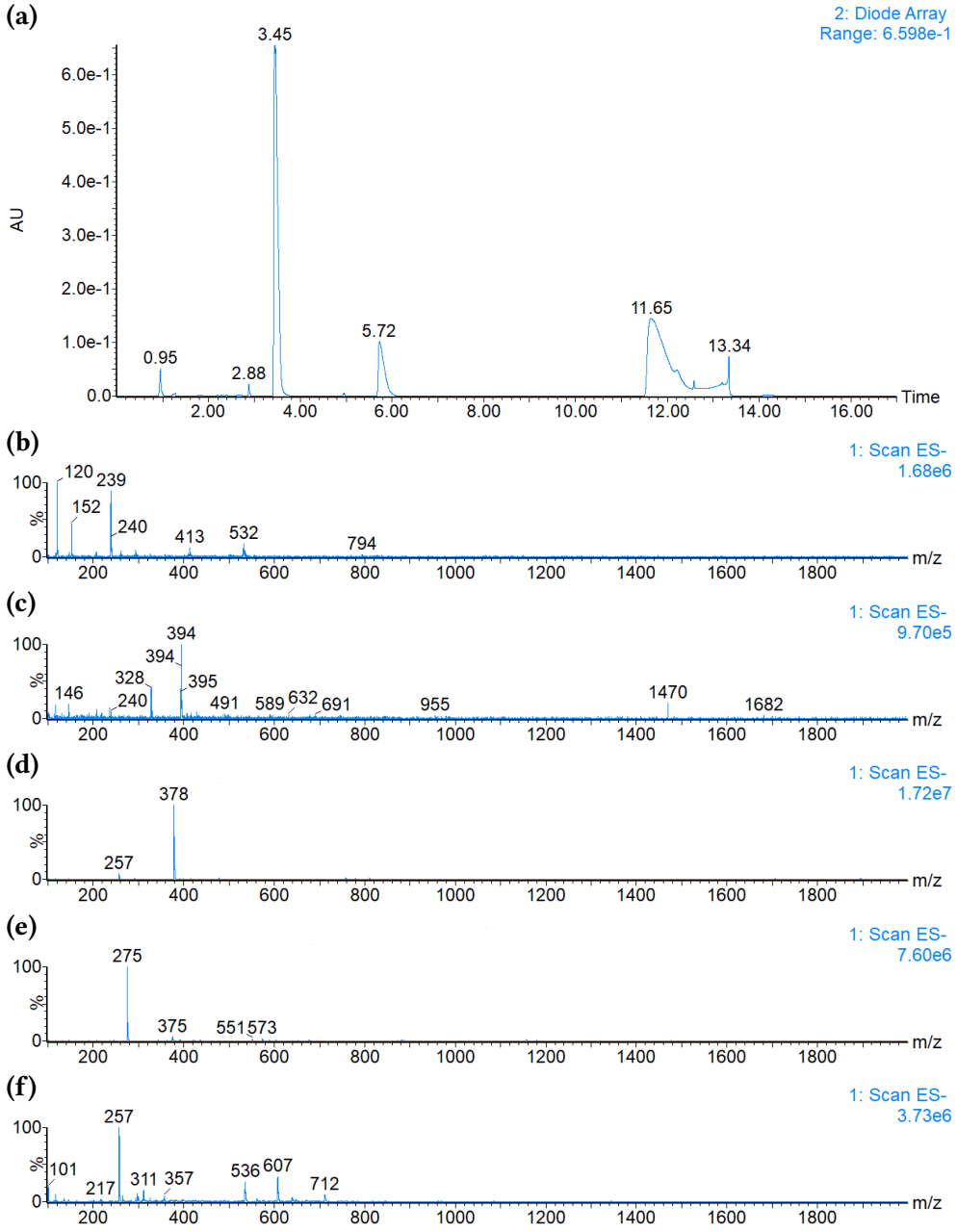

Figure 59: UPLC/ESI-MS in negative mode of Smoc-pyrrolidine deprotection by pyrrolidine with the additive cysteine acting as a potential scavenger. The mass spectra are from the peaks at **(b)** 0.95 min **(c)** 2.88 min **(d)** 3.45 min **(e)** 5.72 min **(f)** wash.

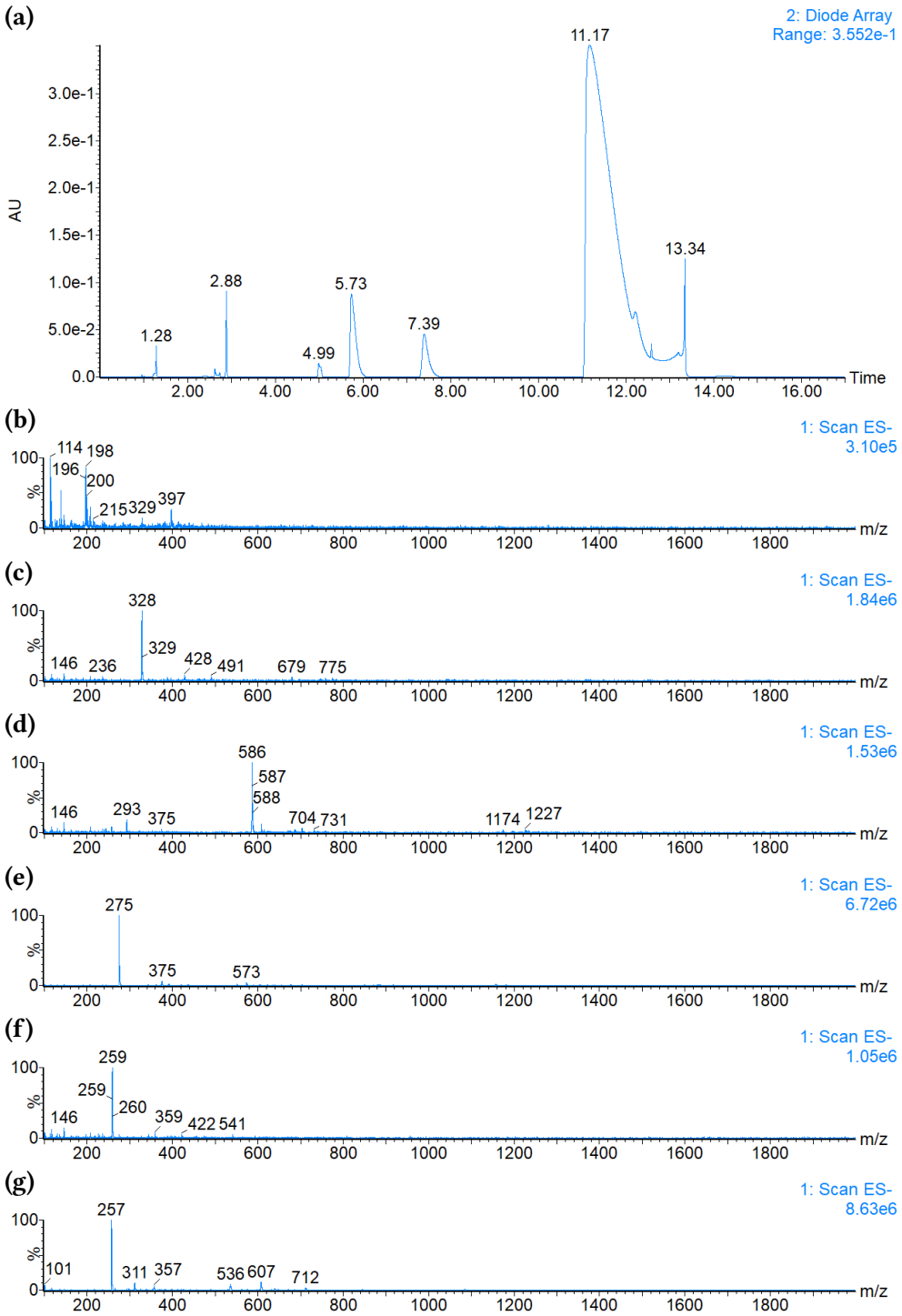

Figure 60: UPLC/ESI-MS in negative mode of Smoc-pyrrolidine deprotection by pyrrolidine with the additive L-proline acting as a potential scavenger. The mass spectra are from the peaks at **(b)** 1.28 min **(c)** 2.88 min **(d)** 4.99 min **(e)** 5.73 min **(f)** 7.39 min **(g)** wash.

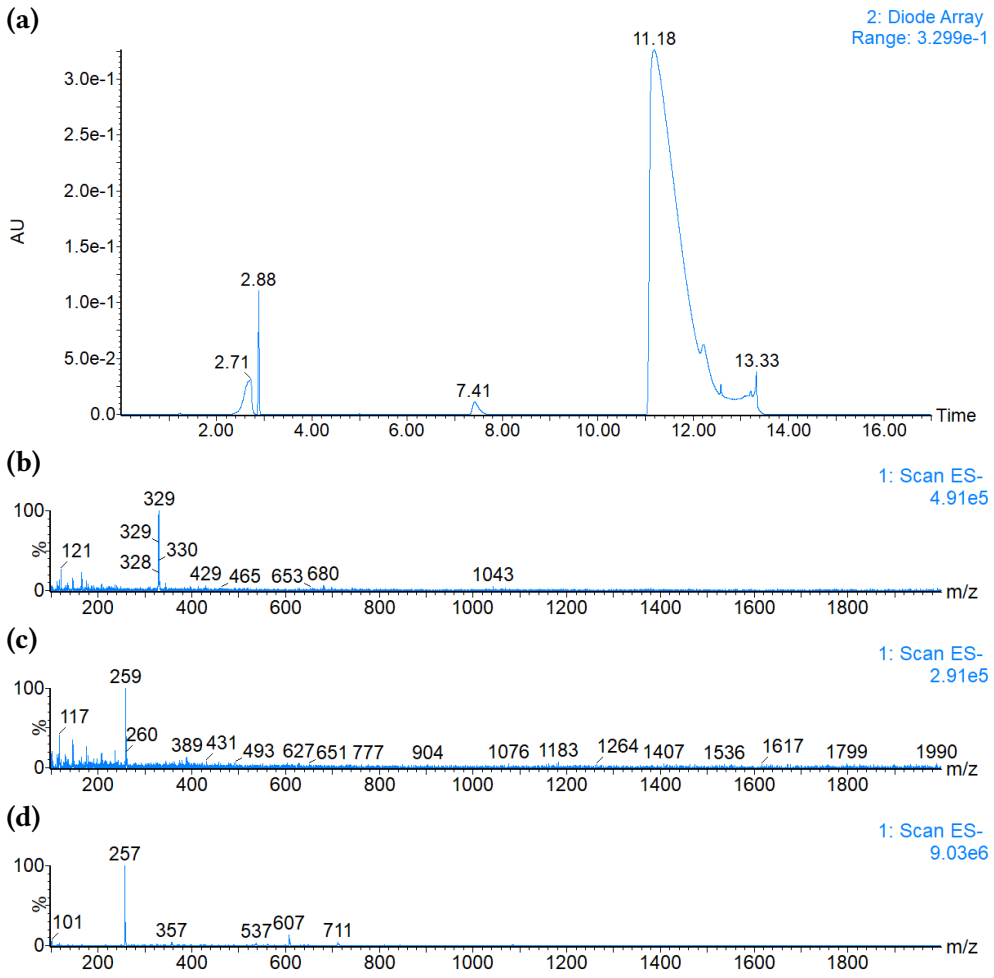

Figure 61: UPLC/ESI-MS in negative mode of Smoc-pyrrolidine deprotection by pyrrolidine showing the addition product of pyrrolidine to SDBF. The mass spectra are from the peaks at **(b)** 2.71/2.88 min **(c)** 7.41 min **(d)** wash.

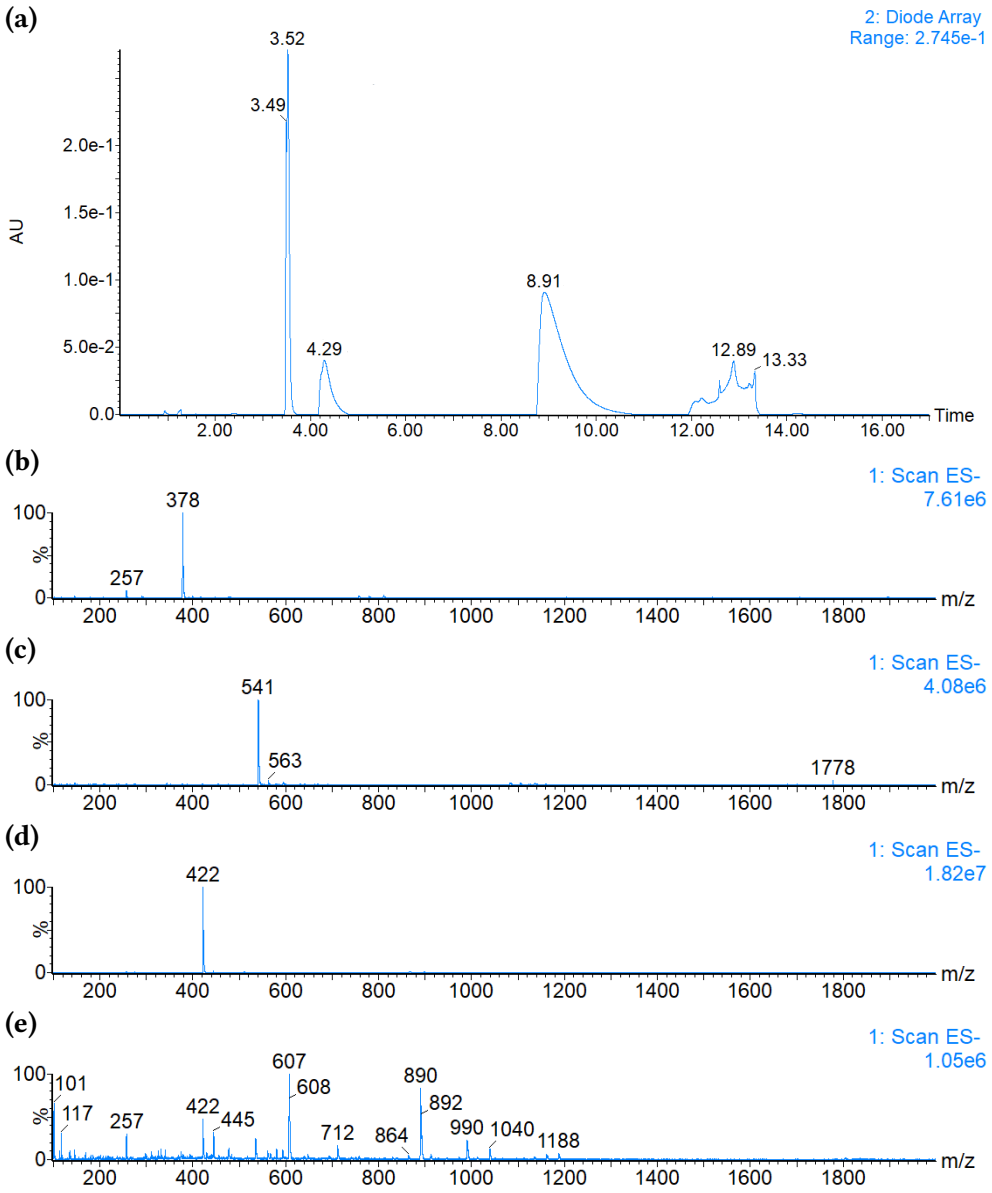

Figure 62: UPLC/ESI-MS in negative mode of Smoc-N-cysteine. The mass spectra are from the peaks at **(b)** 3.56 min **(c)** 4.33 min **(d)** 8.64 min **(e)** wash.

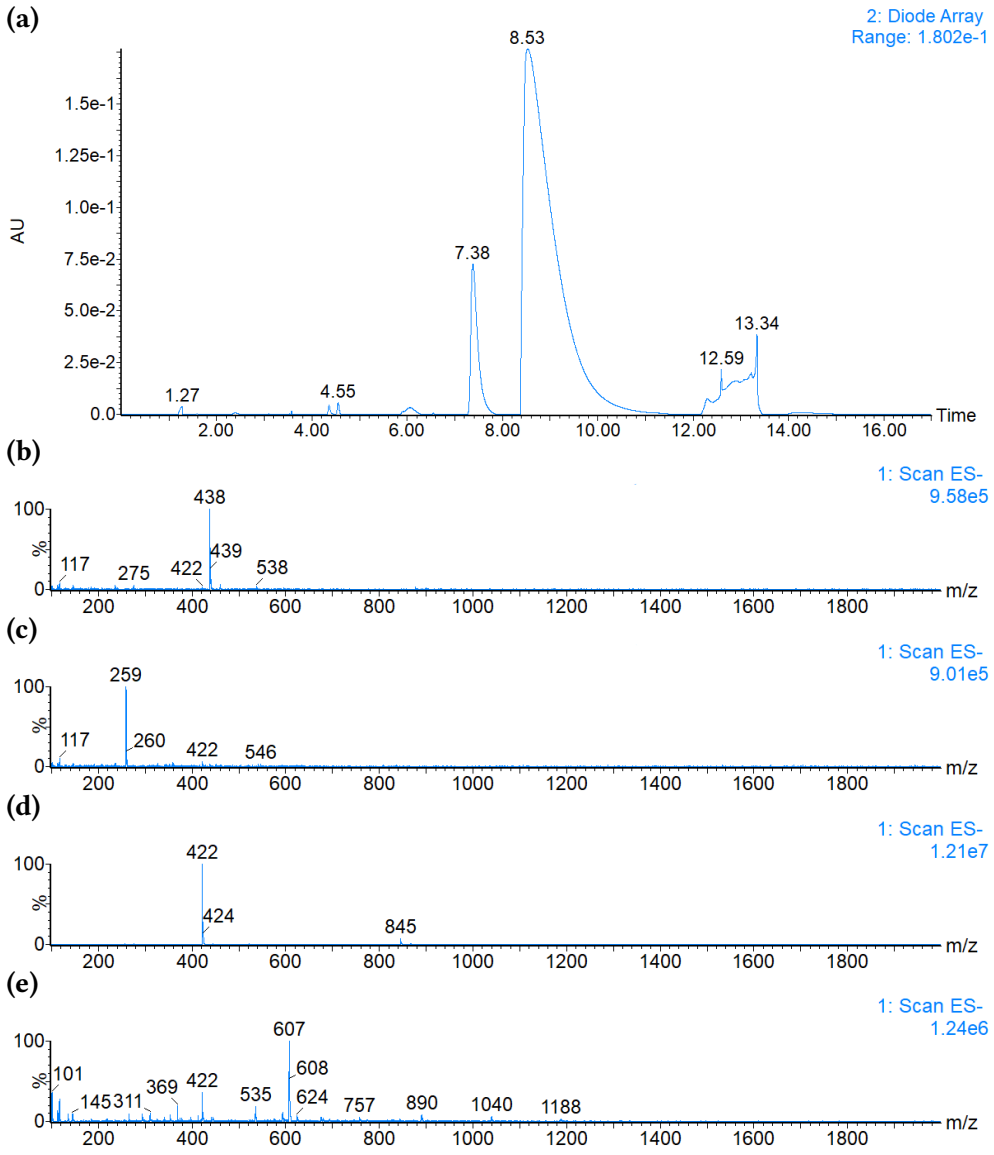

Figure 63: UPLC/ESI-MS in negative mode of Smoc-S-cysteine. The mass spectra are from the peaks at **(b)** 6.08 min **(c)** 7.46 min **(d)** 8.66 min **(e)** wash.

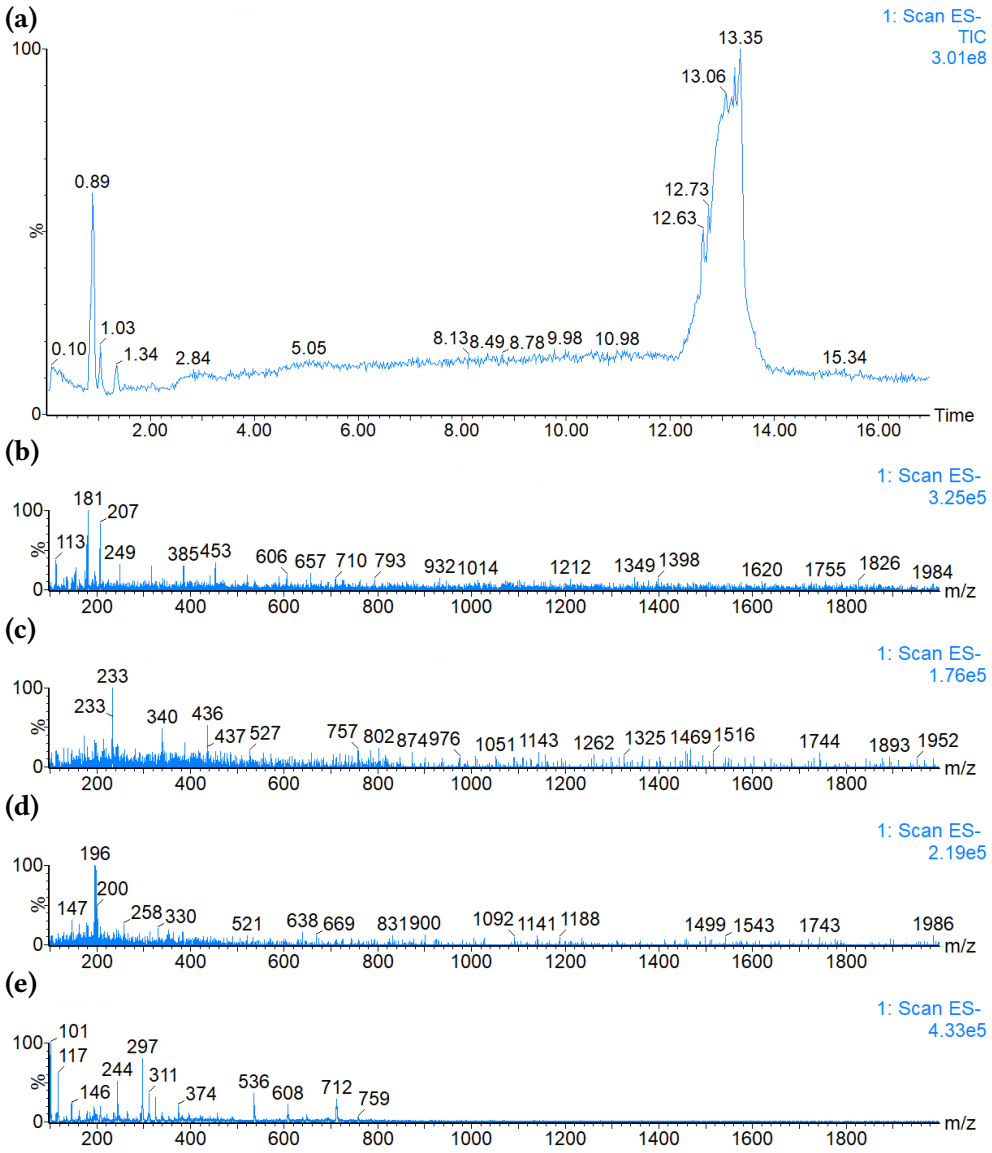

Figure 64: UPLC/ESI-MS in negative mode of the aldol reaction between 2-pentanone and pyridine-2-carbaldehyde catalyzed by pyrrolidine in water. The mass spectra are from the peaks at **(b)** 0.89 min **(c)** 1.03 min **(d)** 1.34 min **(e)** wash.

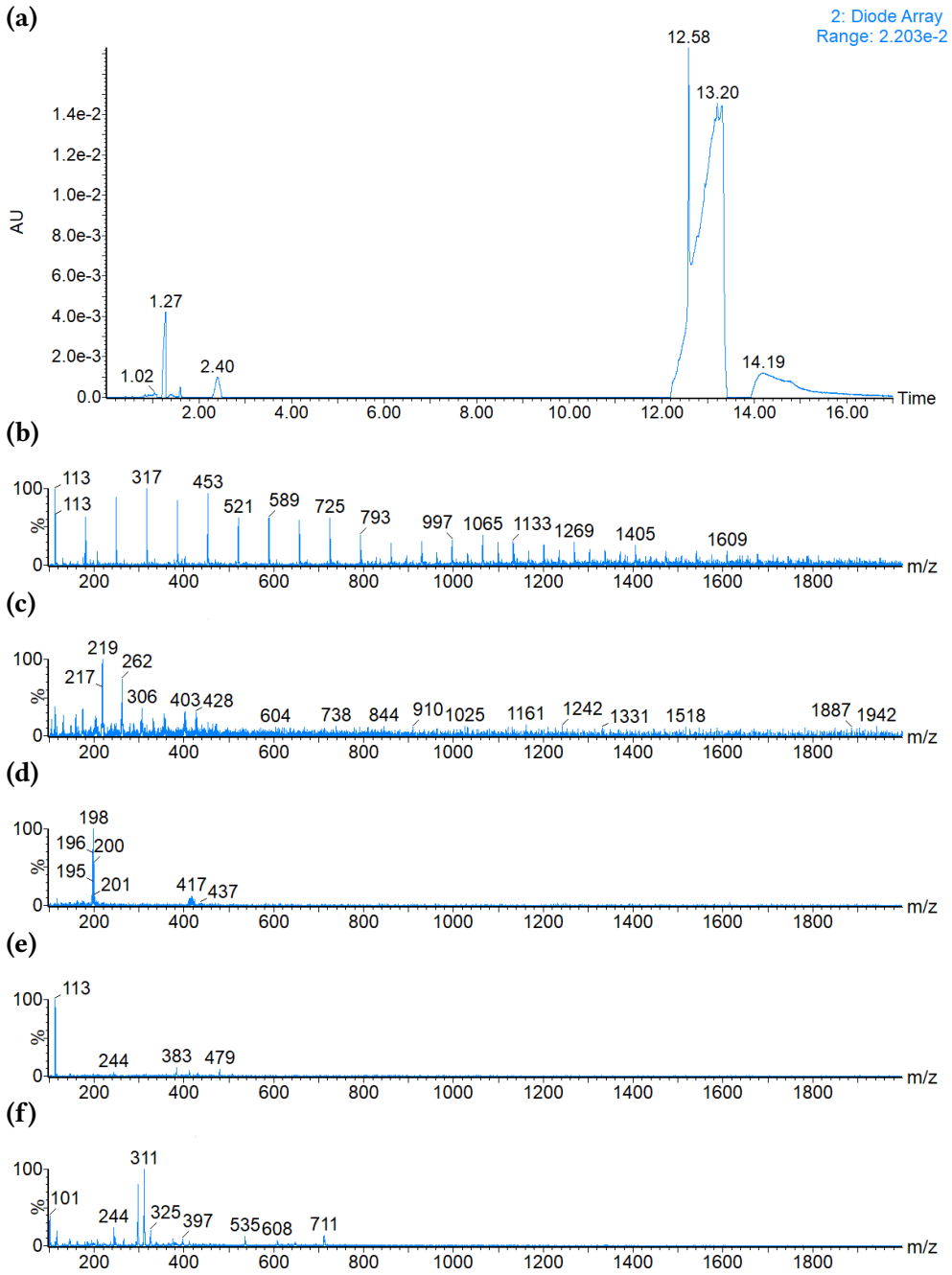

Figure 65: UPLC/ESI-MS in negative mode of the aldol reaction between 2-pentanone and pyridine-2-carbaldehyde potentially catalyzed by the self-replicator in water. The mass spectra are from the peaks at **(b)** 0.93 min **(c)** 1.07 min **(d)** 1.27 min **(e)** 2.75 min **(d)** wash.

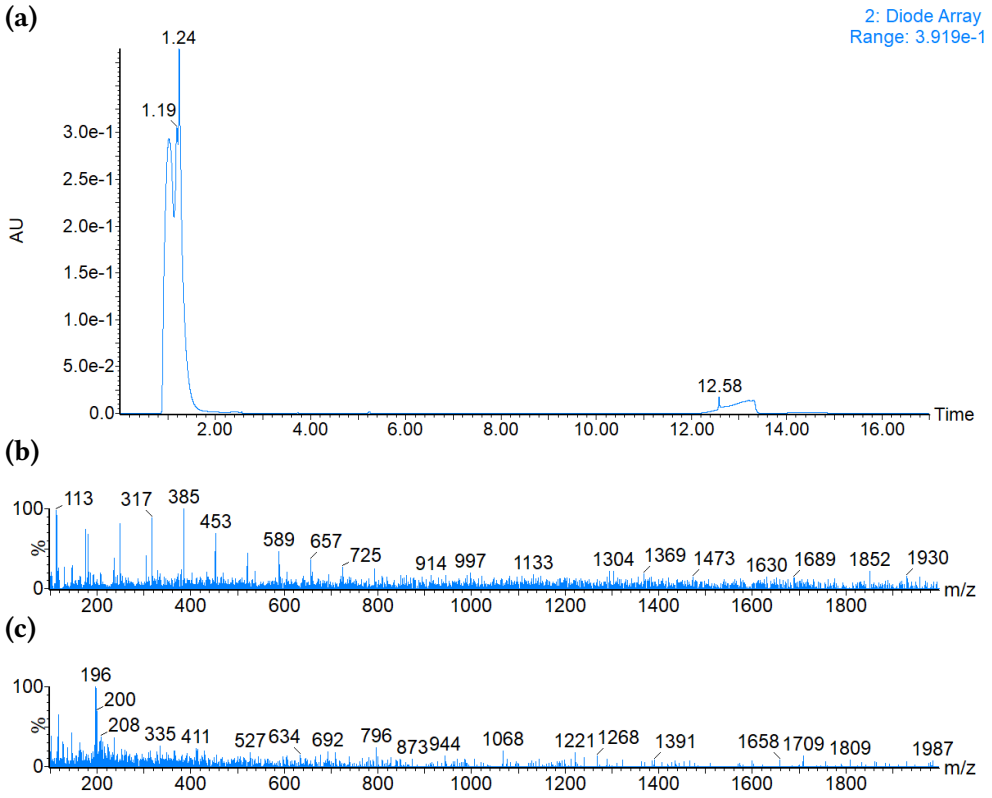

Figure 66: UPLC/ESI-MS in negative mode of the aldol reaction between 2-pentanone and pyridine-2-carbaldehyde without any additional catalyst in water. The mass spectra are from the peaks at **(b)** 0.98 min **(c)** 1.27 min **(d)** wash.

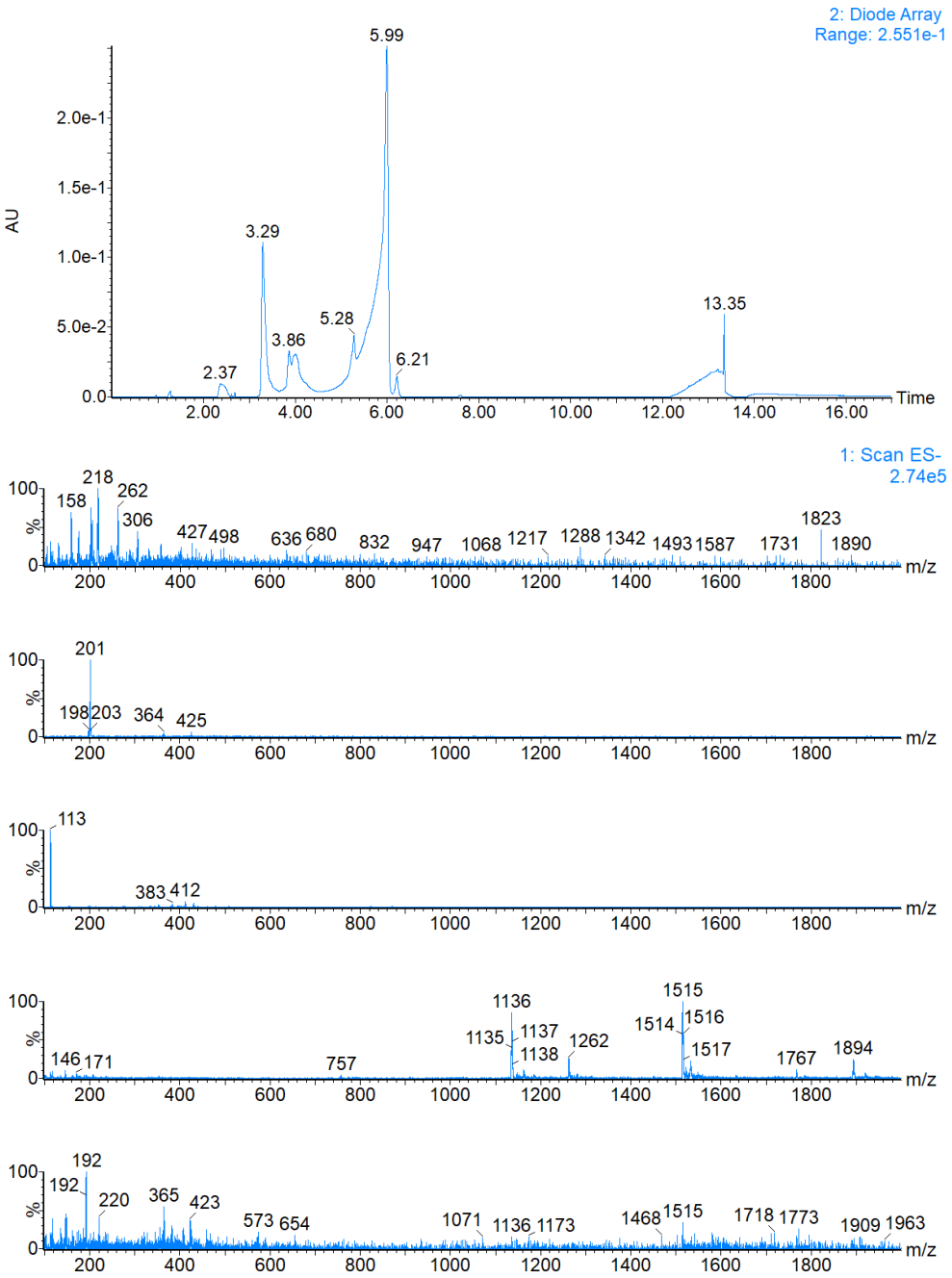

Figure 67: UPLC/ESI-MS in negative mode of the Knoevenagel reaction between diethylmalonate and p-nitrobenzaldehyde potentially catalyzed by the self-replicator in water. The mass spectra are from the peaks at **(b)** 1.07 min **(c)** 2.47 min **(d)** 2.77 min **(e)** 3.90 min **(d)** 5.31 min.

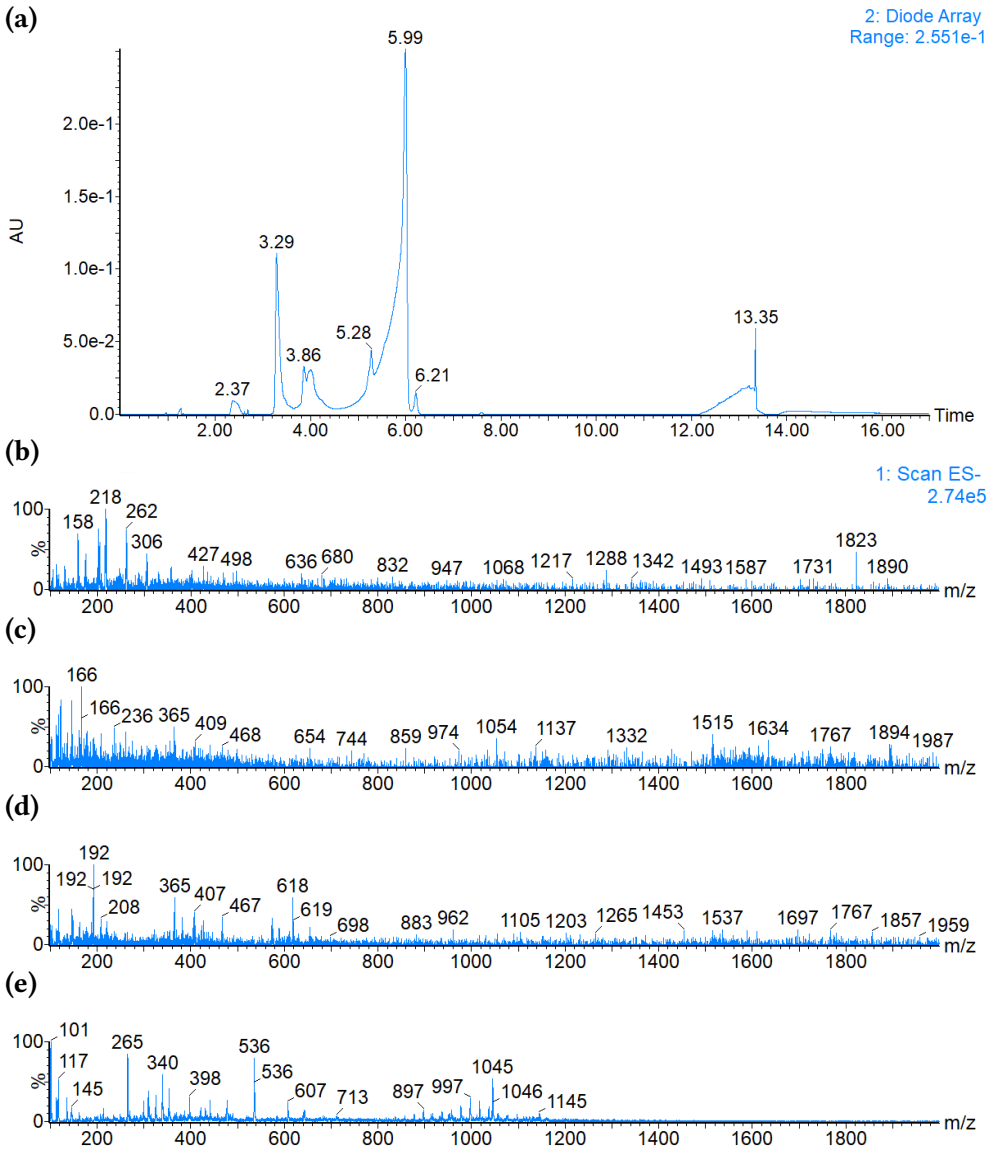

Figure 68: UPLC/ESI-MS in negative mode of the Knoevenagel reaction between diethylmalonate and p-nitrobenzaldehyde potentially catalyzed by the self-replicator in water. The mass spectra are from the peaks at **(b)** 1.07 min **(c)** 5.99 min **(d)** 6.21 min **(e)** wash.

[1] A. Eschenmoser. The search for the chemistry of life's origin. *Tetrahedron*, 63(52):12821–12844, 2007.

[2] H. Duim and S. Otto. Towards open-ended evolution in self-replicating molecular systems. *Beilstein journal of organic chemistry*, 13(1):1189–1203, 2017.

[3] A. Moreno and K. Ruiz-Mirazo. The problem of the emergence of functional diversity in prebiotic evolution. *Biology & Philosophy*, 24(5):585–605, 2009.

[4] A. Dzieciol and S. Mann. Designs for life: protocell models in the laboratory. *Chemical Society Reviews*, 41(1):79–85, 2012.

[5] R. Ludlow and S. Otto. Systems chemistry. *Chemical Society Reviews*, 37(1):101–108, 2008.

[6] V. Patzke and G. von Kiedrowski. Self replicating systems. *Arkivoc*, 5:293–310, 2007.

[7] A. Vidonne and D. Philp. Making molecules make themselves–the chemistry of artificial replicators. *European Journal of Organic Chemistry*, 2009(5):593–610, 2009.

[8] P. Frederix, J. Idé, Y. Altay, G. Schaeffer, M. Surin, D. Beljonne, A. Bondarenko, T. Jansen, S. Otto, and S. Marrink. Structural and spectroscopic properties of assemblies of self-replicating peptide macrocycles. *ACS nano*, 11(8):7858–7868, 2017.

[9] Y. Altay, M. Tezcan, and S. Otto. Emergence of a new self-replicator from a dynamic combinatorial library requires a specific pre-existing replicator. *Journal of the American Chemical Society*, 139(39):13612–13615, 2017.

[10] J. Reek and S. Otto. *Dynamic combinatorial chemistry*. John Wiley & Sons, 2010.

[11] D. Komáromy, M. Stuart, G. Monreal Santiago, M. Tezcan, V. Krasnikov, and S. Otto. Self-assembly can direct dynamic covalent bond formation toward diversity or specificity. *Journal of the American Chemical Society*, 139(17):6234–6241, 2017.

[12] S. Yao, I. Ghosh, R. Zutshi, and J. Chmielewski. Selective amplification by auto-and cross-catalysis in a replicating peptide system. *Nature*, 396(6710):447, 1998.

[13] Y. Ura, J. Beierle, L. Leman, L. Orgel, and M. Ghadiri. Self-assembling sequence-adaptive peptide nucleic acids. *science*, 325(5936):73–77, 2009.

[14] B. Rubinov, N. Wagner, M. Matmor, O. Regev, N. Ashkenasy, and G. Ashkenasy. Transient fibril structures facilitating nonenzymatic self-replication. *ACS nano*, 6(9):7893–7901, 2012.

[15] P. Nowak, M. Colomb-Delsuc, S. Otto, and J. Li. Template-triggered emergence of a self-replicator from a dynamic combinatorial library. *Journal of the American Chemical Society*, 137(34):10965–10969, 2015.

[16] G. Leonetti and S. Otto. Solvent composition dictates emergence in dynamic molecular networks containing competing replicators. *Journal of the American Chemical Society*, 137(5):2067–2072, 2015.

[17] M. Colomb-Delsuc, E. Mattia, J. Sadownik, and S. Otto. Exponential self-replication enabled through a fibre elongation/breakage mechanism. *Nature communications*, 6:7427, 2015.

[18] M. Malakoutikhah, J. Peyralans, M. Colomb-Delsuc, H. Fanlo-Virgós, M. Stuart, and S. Otto. Uncovering the selection criteria for the emergence of multi-building-block replicators from dynamic combinatorial libraries. *Journal of the American Chemical Society*, 135(49):18406–18417, 2013.

[19] J. Carnall, C. Waudby, A. Belenguer, M. Stuart, J. Peyralans, and S. Otto. Mechanosensitive self-replication driven by self-organization. *Science*, 327(5972):1502–1506, 2010.

[20] The scheme was adapted from Jim Ottelé, MSc.

[21] Y. Krishnan-Ghosh and S. Balasubramanian. Dynamic covalent chemistry on self-templating peptides: Formation of a disulfide-linked β-hairpin mimic. *Angewandte Chemie International Edition*, 42(19):2171–2173, 2003.

[22] B. Grzybowski and W. Huck. The nanotechnology of life-inspired systems. *Nature nanotechnology*, 11(7):585, 2016.

[23] J. Clayden, N. Greeves, and S. Warren. *Organic Chemistry*. OUP Oxford, 2012.

[24] J. Ottelé, A. Hussain, S. Otto, et al. Chance emergence of catalytic activity and promiscuity in a self-replicator. 2019.

[25] R. Merrifield and A. Bach. 9-(2-sulfo) fluorenylmethyloxycarbonyl chloride, a new reagent for the purification of synthetic peptides. *The Journal of Organic Chemistry*, 43(25):4808–4816, 1978.

[26] K. van Esterik. Master thesis kayleigh.

[27] A. Seoane, R. Brea, A. Fuertes, K. Podolsky, and N. Devaraj. Biomimetic generation and remodeling of phospholipid membranes by dynamic imine chemistry. *Journal of the American Chemical Society*, 140(27):8388–8391, 2018.

[28] S. Šegota et al. Spontaneous formation of vesicles. *Advances in colloid and interface science*, 121(1-3):51–75, 2006.

[29] J. Atwood and J. Steed. *Encyclopedia of supramolecular chemistry*, volume 1. CRC press, 2004.

[30] L. Sheng and K. Kurihara. Transformation of oil droplets into giant vesicles. *Chemical Communications*, 52(50):7786–7789, 2016.

[31] H. Espinosa-Andrews, J. Báez-González, F. Cruz-Sosa, and E. Vernon-Carter. Gum arabic- chitosan complex coacervation. *Biomacromolecules*, 8(4):1313–1318, 2007.

[32] G. Monreal Santiago. Phd thesis, guille.

[33] A. Kiani. Master thesis, armin.

[34] Z. Jiang, Z. Liang, X. Wu, and Y. Lu. Asymmetric aldol reactions catalyzed by tryptophan in water. *Chemical Communications*, (26):2801–2803, 2006.

[35] M. Gomes, C. de Oliveira, C. Garrote, V. de Oliveira, and R. Menegatti. Condensation of ethyl cyanoacetate with aromatic aldehydes in water, catalyzed by morpholine. *Synthetic Communications®*, 41(1):52–57, 2010.

[36] B. Gomperts, P. Tatham, et al. *Signal transduction*. Academic Press, 2009.

[37] S. Shah, B. Naseem, W. Rehman, and N. Bashir. Investigation of 1-alkanols in organised solutions. *Bulletin of the Chemical Society of Ethiopia*, 25(3), 2011.

[38] S. Hait and S. Moulik. Determination of critical micelle concentration (cmc) of nonionic surfactants by donor-acceptor interaction with Iodine and correlation of cmc with hydrophile-lipophile balance and other parameters of the surfactants. *Journal of Surfactants and Detergents*, 4(3):303–309, 2001.

[39] J. Neugebauer. [18] detergents: An overview. In *Methods in enzymology*, volume 182, pages 239–253. Elsevier, 1990.

[40] N. El Kadi, F. Martins, D. Clausse, and P. Schulz. Critical micelle concentrations of aqueous hexadecytrimethylammonium bromide-sodium oleate mixtures. *Colloid and Polymer Science*, 281(4):353–362, 2003.

[41] P. Mukerjee and K. Mysels. Critical micelle concentrations of aqueous surfactant systems. Technical report, National Standard reference data system, 1971.

[42] S. Knauer, T. Roese, O. Avrutina, H. Kolmar, and U. Christina. Method for peptide synthesis and apparatus for carrying out a method for solid phase synthesis of peptides, August 3 2017. US Patent App. 15/514,833.

[43] A. Córdova, W. Zou, I. Ibrahem, E. Reyes, M. Engqvist, and W. Liao. Acyclic amino acid-catalyzed direct asymmetric aldol reactions: alanine, the simplest stereoselective organocatalyst. *Chemical Communications*, (28):3586–3588, 2005.

[44] K. Sakthivel, W. Notz, T. Bui, and C. Barbas. Amino acid catalyzed direct asymmetric aldol reactions: a bioorganic approach to catalytic asymmetric carbon- carbon bond-forming reactions. *Journal of the American Chemical Society*, 123(22):5260–5267, 2001.

[45] A. Córdova, W. Notz, and C. Barbas III. Direct organocatalytic aldol reactions in buffered aqueous media. *Chemical Communications*, (24):3024–3025, 2002.

[46] R. Menegatti. Green chemistry–aspects for the knoevenagel reaction. In *Green chemistry-environmentally benign approaches*. IntechOpen, 2012.

[47] S. Shafqat, A. Khan, M. Khan, S. Salleh, M. Jamaludin, and P. Cem. Green synthesis and characterization of 3-carboxycoumarin and ethylcoumarin-3-carboxylate via knoevenagel condensation. *Asian Journal of Chemistry*, 29(2), 2017.

[48] Z. Ren, W. Cao, W. Tong, and X. Jing. Knoevenagel condensation of aldehydes with cyclic active methylene compounds in water. *Synthetic communications*, 32(13):1947–1952, 2002.

[49] M. Plater, P. Barnes, L. McDonald, S. Wallace, N. Archer, T. Gelbrich, P. Horton, and M. Hursthouse. Hidden signatures: new reagents for developing latent fingerprints. *Organic & Biomolecular Chemistry*, 7(8):1633–1641, 2009.

[50] S. Chimni and D. Mahajan. Electron deficiency of aldehydes controls the pyrrolidine catalyzed direct cross-aldol reaction of aromatic/heterocyclic aldehydes and ketones in water. *Tetrahedron*, 61(21):5019–5025, 2005.

[51] AWC Lau, A. Prasad, and Z. Dogic. Condensation of isolated semi-flexible filaments driven by depletion interactions. *EPL (Europhysics Letters)*, 87(4):48006, 2009.

ACKNOWLEDGEMENTS

After entering my Master studies, studying hard for exams and doing research in a foreign country, it is time to say thank you in my final Master thesis to the people who supported me and with whom this would not have been possible.

First of all, I want to thank you, *Prof. Sijbren Otto*, for offering me not only the chance to do my Master thesis in your group but also for giving me the freedom to plan and carry out my ideas with a great support. The way I was allowed to work in your research group taught me so many important things such as to deal with the fact that great scientific ideas do not always turn out to work in the lab but for sure lead to new knowledge. The way my creativity explored and developed in this time will help me to deal with (scientific) problems in a better way.

I would like to acknowledge *Prof. Johannes Fröhlich* and *Dr. Hannes Mikula* for the supervision of my thesis at the Technical University of Vienna.

Guillermo Monreal Santiago - Guille, believing in your students from the first day on and supporting while letting them to try out scientific ideas are properties, which I did not take for granted! Not only supporting but also teaching students important lessons, like that at some point a project needs to be closured before fighting against a dead end, is what makes a great supervisor. I am very thankful for your awesome day-to-day supervision! You do not only have passion for science but also for group activities - I'm especially talking about *Bang!*, which I enjoyed so much to play at the Borrels. I often try to portray your passion when explaining the rules of *Bang!* to my friends but it will never be as good as the original Guille.

Kayleigh, whenever I found myself too deep in a scientific direction, you simply dropped by to get me some distance from the mountain of projects that I wanted to try in the lab. And yes, life can depend on a single NMR! Thanks for the great collaboration - I enjoyed the midnight Colas in Groningen so much and wish we would have done this more often - and by the way, thanks for teaching me how to carry someone on the back of a bike in my last night in Groningen!

Jim, always a smile when crossing in the hallway and open to answer my questions. *Marcel*, many thanks for all the mass spectra that you have done for me and also, I think I will never forget the sound of your laughter! Huge thanks go to you *Falk*, for making sure I am supplied with coffee by our symbiotic deal card-against-tea. Also for the scientific discussions that we had in our office and even more the talks about the differences between Austria and Germany. Many acknowledgments to you *Paul*, for sharing amazing life hacks in organic synthesis. *Jasper*, thanks for making me addicted to *Pindakaas*! And also, together with *Babis*: Albert Heijn is the best! *Ivana*, I never knew, what you mean as a joke and what in serious way and this actually gave me huge laughs. Also, you made me feel super useful when asking me for help to find glassware in the perfect organized lab. *Armin*, *Ankush*, *Bin* and *Kai* thank you for completing this working group so that it became awesome!

I also would like to acknowledge the Erasmus$^+$ scholarship and TU Vienna KuWi scholarship for the financial support.

Great thanks go to my family for supporting me at any time in any situation. Speaking of what, moving to another apartment in a foreign country or getting loving nutrition and wine from Austria would have been *a bit* more exhausting and difficult without the help of my family. To my parents *Katharina* und *Gerhard* for all

of the support and dealing with my moods when I had to study hard for my exams (sorry for that!). Loving thanks to my sister *Katharina* for always being there for me and grandmother *Ingeborg* for making sure that I am fine with her energy providing "drug", the best Pasta Asciutta in the world! Great thanks to my uncle *Michael* and his wife *Tamara* for always cheering up, visiting me in Groningen and providing me live saving nutrition from Austria.

Finally, I want to express my thanks to all of my friends, especially to *Lukas* for all our meetings where you, as an external, made me see things clearly when I was too focused on my (scientific) problems and also for helping me with your technical and informatics skills - all of that even in Groningen with a bad Skype connection! Big thanks to *Anja* and *Kati*, for always being there when I needed someone for escaping of my studies. You guys give me a great time no matter how long we failed to meet!

Everything started when I was lying in my cradle, having my mother around reading good night stories out of science books for me – *Oh how I loved the stories out of the astronomy book!* - almost 25 years later here I am now, looking back on my path so far. I am stunned by the way I developed myself only in these few amazing months abroad - not only in a scientific way but also personally. During my stay in Groningen, I became so much more lighthearted, more *gezellig* and more easy going. *Der Mensch braucht ein Ziel*, as my grandpa said and *voor niets komt de zon op* (thanks Kayleigh and Jasper for teaching me some dutch sayings) - however, I also learned the important lesson about not always being so hard on myself while pursuing my goals. Jumping into the cold water and going abroad was one of my best decisions so far in my life and with whom my path will cross in future, be aware that I'm gonna talk *a lot* about these few months in Groningen!
Hartelijk bedankt et eet smakelijk,

Patricia